

# Classifying Order-Two Spatial Symmetries in Non-Hermitian Hamiltonians: Point-gapped AZ and $AZ^\dagger$ Classes

Yifan Wang\*

*Department of Physics, Emory University, Atlanta, GA 30322, USA*

Crystalline topological insulators and superconductors have been a prominent topic in the field of condensed matter physics. These systems obey certain crystalline (spatial) symmetries that depend on the geometry of the lattice. The presence of spatial symmetries can lead to shift in the classification of ten-fold Altland–Zirnbauer class, given rise to new symmetry-protected topological phases. If the constraint of Hermiticity is broken, the classification expand into 38-fold. In this paper, following procedures in Hermitian systems, we classify all possible types of order-two spatial symmetries for point-gapped non-Hermitian systems within 16 out of 38 non-Hermitian topological classes. These 16 classes are denoted by AZ and  $AZ^\dagger$  classes. We show that, similar to the Hermitian case, spatial symmetries will also lead to a shift in the classification of AZ and  $AZ^\dagger$  classes. There also exist novel symmetry-protected topological phases exclusive to point-gapped non-Hermitian Hamiltonians. Toy models are also given based on our classifications.

## CONTENTS

I. Introduction	1	A. Dimensional Hierarchy of AZ and $AZ^\dagger$ without spatial symmetries	19
II. Classification of order-two spatial symmetry for Hermitian Hamiltonians	2	1. CS to non-CS classes	19
A. Review of topological defects and $K$ group classification of stable equivalent Hermitian Hamiltonians	2	2. Non-CS to CS classes	21
B. Classification under order-two spatial symmetry	3	B. Dimensional Hierarchy of AZ and $AZ^\dagger$ with order-two spatial symmetries	23
III. Structure of 38-fold classification of NH Hamiltonian	4	1. Complex AZ with order-two unitary symmetries	23
IV. Order-two spatial symmetries in AZ and $AZ^\dagger$	6	2. Complex AZ with order-two anti-unitary symmetries	24
A. Complex classes A and AIII with order-two unitary symmetry	6	3. Real AZ and $AZ^\dagger$ with order-two symmetries	24
B. Complex classes A and AIII with order-two antiunitary symmetry	7	C. Properties of Clifford Algebra	25
C. Real AZ classes with order-two symmetry	8	D. Classifying space of AZ and $AZ^\dagger$ with spatial symmetries from Clifford algebra	25
D. Real $AZ^\dagger$ classes with order-two symmetry	10	1. Complex AZ classes	25
V. Periodic table of spatial symmetries for point-gapped Hamiltonian	10	2. Real AZ and $AZ^\dagger$ classes	27
VI. Examples	10	References	28
A. Point defect in $AI^\dagger$ protected by reflection symmetry ${}^cU_-^+$	12		
B. Point defect in C protected by reflection symmetry ${}^cU_-^+$	15		
C. Point defect in $D^\dagger$ with reflection symmetry ${}^cU_-^+$	16		
D. Point defect in $DIII$ protected by reflection symmetry ${}^cU_{-+}^+$	17		
VII. Discussions and Conclusions	18		

## I. INTRODUCTION

Topological insulators (TI) and superconductors (TSC) are some of the most intriguing discovery in condensed matter physics [1–4]. Ref. [5] proposed a systematic way of classifying TI and TSC based on three internal symmetries: time-reversal symmetry (TRS), particle-hole symmetry (PHS), and chiral symmetry (CS). Together, they composed 10 different classes which are called periodic table of TI and TSC or Altland–Zirnbauer (AZ) symmetry class [6]. AZ classes give a complete classification of gapped phases of non-interacting fermionic systems with respect to internal symmetries. Different AZ classes are distinct from each other by some topological invariants that could exist in the presence or absence of certain internal symmetries. A phase transition between systems that have different topological invariants

\* Ivan.wang@emory.edu

is achieved through the gap-closing of energy bands. For example, Chern insulator, which breaks TRS, can exist in 2D of class A [5, 7]. It has a  $\mathbb{Z}$  invariant called the Chern number. When a system with a non-trivial Chern number is in contact with the vacuum (which has Chern number 0), a gap closing of energy bands at the interface (or boundary) must happen. The states that localized at the boundary that closed the energy gap are the chiral edge states of Chern insulators. Similarly, quantum spin hall effect, which requires the existence of spinful TRS, can exist in class AII. It has a  $\mathbb{Z}_2$  invariant called Kane-Mele  $\mathbb{Z}_2$  invariant [8, 9]. When a non-trivial quantum spin hall system is in contact with the vacuum, helical edge states appear at the interface. These edge modes show that topological numbers can predict the phenomena of quantum systems.

The boundary of a system can be more generally understand in the context of topological defects [10–12]. Topological defects are defined to be lattice dislocation and disclination that cannot be gapped out by continuous deformation. Under the protection of symmetries, defects may also host gapless topological modes. Therefore, under this view, boundary of a system is just another form of defects.

Meanwhile, Ref. [13, 14] discovered TIs that are based on inversion and crystalline symmetries, which are non-local spatial symmetries that depends on the geometry of the lattice. And, as shown in Ref. [13, 14], non-trivial TIs exist under the protection of spatial symmetries which are outside the classification of AZ symmetry classes. Therefore, a complete classification that includes spatial symmetries is called for. Works that classifies AZ symmetry class in addition to spatial symmetries are Ref. [12, 15–20].

Another intriguing topics discovered in recent years is non-Hermitian (NH) TIs and TSCs. These systems break the conventional condition that the Hamiltonian describing the system must be Hermitian. A Hermitian Hamiltonian means the energy of the system is conserved. NH Hamiltonians counts in the exchange of energy between the original system and the environment, resulting in an exotic phenomenon called non-Hermitian skin effect (NHSE) [21–24]. NHSE is protected by a  $\mathbb{Z}$  invariant called winding number. When a system with non-trivial winding number is in contact with the vacuum, *all* states will localize at the boundary. This phenomenon is unique to NH systems which received vast attention in the recent years [25–36]. Another interesting aspect of non-Hermiticity is that every internal symmetries would split into two (See Sec. III): TRS splits into TRS and TRS<sup>†</sup>; PHS splits into PHS and PHS<sup>†</sup>; CS splits into CS and sub-lattice symmetry (SLS). A complete classification of NH Hamiltonian is made in Ref. [24, 37] shortly after the  $\mathbb{Z}$  topological invariant of NHSE is discovered. The bifurcation of internal symmetries results in 38 different classes, which greatly enriched the phenomenon of TIs and TSCs. Although much attention has been put into NH systems, little progress has been made to include

spatial symmetries in the 38-fold classification. In this paper, following Ref.[12] which classify all order-two spatial symmetries for Hermitian Hamiltonians, we aim to incorporate order-two spatial symmetries into the classification of 16 out of 38 classes of NH Hamiltonians.

This paper is organized as the following: in Sec. II, we review the topological classification of Hermitian Hamiltonian without and with order-two spatial symmetries. In Sec. III, we review the classification of point-gapped NH Hamiltonians without order-two spatial symmetries. In Sec. IV, we introduce the classification scheme for point-gapped Hamiltonians of 16 out of 38 classes with spatial symmetries. Periodic tables for spatial symmetries are introduced in Sec. V. Finally, in Sec. VI, we introduce several examples to illustrate our classification. We conclude the paper with several remarks in Sec. VII. Mathematical details are provided in Appendix.

## II. CLASSIFICATION OF ORDER-TWO SPATIAL SYMMETRY FOR HERMITIAN HAMILTONIANS

To understand the process of classification of spatial symmetries in NH systems, we first review the classification of stable equivalent Hermitian Hamiltonian and spatial symmetries of Hermitian systems.

### A. Review of topological defects and $K$ group classification of stable equivalent Hermitian Hamiltonians

First, we briefly review the process of including topological defects into the classification. In the absence of defects, we consider Hamiltonians that are defined on  $d$ -dimensional Brillouin zone (BZ) which is a  $d$ -Torus  $T^d$ . In general, we may consider BZ as a simpler space  $S^d$  which is a  $d$ -sphere. This substitution will not affect the strong topological invariants [12].

Topological defects are defined to be discontinuity or distortion in lattices that cannot be removed. This discontinuity may be a point, a line, or a surface. In real space, we let a  $D$ -dimensional sphere  $S^D$  surrounds the defects. Combining with the  $d$ -dimensional BZ, the total space of classification is given by  $S^{d+D}$ .  $K$  group classification is a common method for classifying topological invariants for topological insulators and superconductors in different dimensions [7, 10, 12, 15]. The classification of stable equivalent Hamiltonian is then equivalent to the classification of maps from base space  $(\mathbf{k}, \mathbf{r}) \in S^{d+D}$  of a  $d + D$  dimensional sphere to the classifying space of Hamiltonian  $H(\mathbf{k}, \mathbf{r})$ . This belongs to the problem of homotopy classification. As we will see, this classification can be simplified by considering the  $K$  group  $K = \pi_0$ , which is the zeroth homotopy group of classifying space. As we will see, the  $K$  group in fact has an Abelian group structure, which allows us to classify Hamiltonians that

are topologically distinct from each other.

We consider Hamiltonians that are gapped in the bulk i.e. far away from defects. This gap is often chosen to be the Fermi level. Two Hamiltonians are considered topologically equivalent if they can be continuously deformed into each other without closing the band gap. This means the two Hamiltonians have the same topological invariants. This allows us to deform a given Hamiltonian into two flat bands without closing the band gap: all the  $n$  ( $m$ ) bands below (above) the Fermi level are deformed into the same energy  $-1$  (1). Then, according to the symmetries that the Hamiltonian has, we can find the classifying space of this Hamiltonian. Then by computing  $\pi_0$  of the classifying space, we can derive the topological invariant of the corresponding Hamiltonian in 0 dimension. Topological invariants in higher dimension can be found by using the *dimensional hierarchy*, which we will introduce later in Eqs. (2) and (3).

Throughout the paper, we consider Hamiltonians that are stable equivalent: Hamiltonian  $H_1$  and  $H_2$  are stable equivalent  $H_1 \sim H_2$  if they can be continuously deformed into each other by adding trivial bands. This ensures that the dimension of the Hamiltonian will not affect the classification. In other words, the addition of trivial bands will not affect the topology of the Hamiltonian (Hamiltonians that violate this condition are called Fragile insulators or Hopf insulators which we will not discuss in this paper [38–43]). This allows us to identify a set of Hamiltonian  $[H]$  that includes all Hamiltonians that are stable equivalent to  $H$ . We define the addition of two sets to be  $[H_1] \oplus [H_2] = [H_1 \oplus H_2]$ , where  $\oplus$  is the direct sum. Then the inverse of  $[H]$  is given by  $[H] \oplus [-H] = [0]$ , where  $[0]$  is the set of trivial Hamiltonians. Since we are discussing stable equivalent Hamiltonians, the addition of  $[0]$  to any Hamiltonians will not change the set it belongs to i.e.  $[H] \oplus [0] = [H]$ . We see that  $[0]$  acts as the identity in this operation. The direct sum  $\oplus$  is associative and commutative. Therefore, different classes of Hamiltonians  $[H]$  form an Abelian group, which is called  $K$  group.

Now we consider symmetries that separate these classes. The internal symmetries that govern Hermitian Hamiltonians are

$$\begin{aligned} \text{TRS} : \quad \mathcal{T}H(\mathbf{k}, \mathbf{r})\mathcal{T}^{-1} &= H(-\mathbf{k}, \mathbf{r}), \mathcal{T}^2 = \pm 1 \\ \text{PHS} : \quad \mathcal{C}H(\mathbf{k}, \mathbf{r})\mathcal{C}^{-1} &= -H(-\mathbf{k}, \mathbf{r}), \mathcal{C}^2 = \pm 1 \\ \text{CS} : \quad \Gamma H(\mathbf{k}, \mathbf{r})\Gamma^{-1} &= -H(\mathbf{k}, \mathbf{r}), \Gamma^2 = 1, \end{aligned} \quad (1)$$

which are called Time-Reversal Symmetry (TRS), Particle-hole symmetry (PHS), and Chiral Symmetry (CS), respectively. Specifically,  $\mathcal{T}$  and  $\mathcal{C}$  are antiunitary operators, meaning they can be written in the form of a unitary matrix times complex conjugate operator  $\mathcal{K}$ . And  $\Gamma$  is a unitary operator. The combination of these symmetries will result in 10 classes. If no antiunitary symmetries (TRS and PHS) are present, the symmetry classes are called the complex AZ class. Since in the absence of complex conjugate operator  $\mathcal{K}$ , the Clifford gen-

erators that generate the classifying space of each class is defined up to a phase. So these generators are in general complex. Hence the name complex AZ class is given to classes without antiunitary symmetries. If one or both antiunitary symmetries are present, the symmetry classes are called real AZ class. In this case, generators of each class can only be real or imaginary. Hence the name real AZ class.

Having discussed  $K$  group and symmetries that govern each class, we now show the  $K$  group relationship of each class. The AZ symmetry classes may summarized as [10]

$$\begin{aligned} K_{\mathbb{C}}(s; d, D) &= K_{\mathbb{C}}(s - d + D; 0, 0) = \pi_0(\mathcal{C}_{s-d+D}) \\ s &= 0, 1 \pmod{2} \end{aligned} \quad (2)$$

for complex AZ classes (A and AIII), and

$$\begin{aligned} K_{\mathbb{R}}(s; d, D) &= K_{\mathbb{R}}(s - d + D; 0, 0) = \pi_0(\mathcal{R}_{s-d+D}) \\ s &= 0, \dots, 7 \pmod{8}, \end{aligned} \quad (3)$$

for real AZ classes (the rest of the eight classes). The  $\mathcal{C}_{s-d+D}$  and  $\mathcal{R}_{s-d+D}$  are classifying space of the Hamiltonians. Their exact expressions can be found in Ref. [5]. The number  $s$  labels the symmetry classes. Notice that complex AZ class has periodicity 2 i.e. the classifying space obeys  $\mathcal{C}_s \simeq \mathcal{C}_{s-2}$ . Hence  $s$  is defined mod 2 in Eq. (2). This periodicity is the origin of two complex AZ classes. Similarly, for real AZ class, the classifying space obeys  $\mathcal{R}_s \simeq \mathcal{R}_{s-8}$ . Hence  $s$  is defined mod 8 in Eq. (3). This periodicity gives eight real AZ classes. Periodicity of Eqs. (2) and (3) are called Bott periodicity, which is an essential mathematical property of  $K$  group in the classification of TIs and TSCs. The resulting table from Eqs. (2) and (3) is the AZ symmetry class, which we do not repeat it here.

Finally, we remark that Eqs. (2) and (3) are referred to as dimensional hierarchy of AZ symmetry class, which is first proved in Ref. [10]. A neat way to visualize Eq. (3) is by putting real AZ classes on a coordinate where  $x$  ( $y$ ) axis indicates the value of  $\mathcal{C}^2$  ( $\mathcal{T}^2$ ). We plot this visualization in Fig. 1 (a). In this way, eight real AZ classes would form a "clock". In Sec. III, we also provide a similar relation and visualization for point-gapped Hamiltonians.

## B. Classification under order-two spatial symmetry

The spatial symmetries (or crystalline symmetries) are symmetries that are dependent on the geometry of the lattice [12, 15, 17, 18]. In the paper, we consider spatial symmetries that are of order two, meaning apply them twice on the Hamiltonian will keep the Hamiltonian unchanged. These spatial symmetries can be unitary ( $U$ ) or antiunitary ( $A$ ). Furthermore, they can commute or anti-commute with the Hamiltonians. For the later, a bar is placed on top of the spatial operator. To sum up, possible order-two spatial symmetries for Hermitian systems

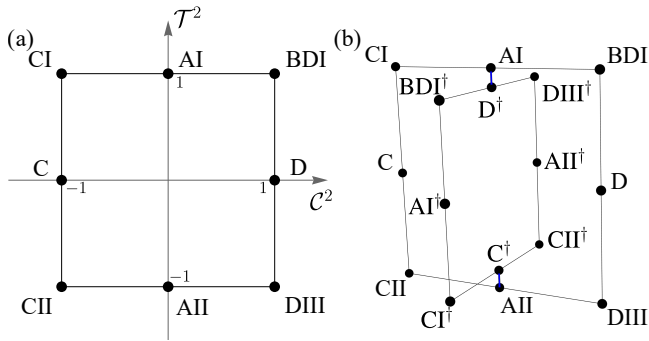


FIG. 1: Visualization of dimensional hierarchy of real Hermitian AZ class and point-gapped NH AZ/AZ<sup>†</sup>. (a) real Hermitian AZ class can be considered as a "clock" where eight classes are "hours" on the "clock". Two axes indicate the squared value of  $\mathcal{T}^2$  and  $\mathcal{C}^2$ . (b) For NH class, we may consider two "clocks" such that one of them indicates AZ the other indicates AZ<sup>†</sup>. Two "clocks" are connected by the mapping Eq. (6), indicated by two blue lines.

are

$$\begin{aligned}
 UH(\mathbf{k}, \mathbf{r})U^{-1} &= H(-\mathbf{k}_{\parallel}, \mathbf{k}_{\perp}, -\mathbf{r}_{\parallel}, \mathbf{r}_{\perp}) \\
 \bar{U}H(\mathbf{k})\bar{U}^{-1} &= -H(-\mathbf{k}_{\parallel}, \mathbf{k}_{\perp}, -\mathbf{r}_{\parallel}, \mathbf{r}_{\perp}) \\
 AH(\mathbf{k})A^{-1} &= H(\mathbf{k}_{\parallel}, -\mathbf{k}_{\perp}, -\mathbf{r}_{\parallel}, \mathbf{r}_{\perp}) \\
 \bar{A}H(\mathbf{k})\bar{A}^{-1} &= -H(\mathbf{k}_{\parallel}, -\mathbf{k}_{\perp}, -\mathbf{r}_{\parallel}, \mathbf{r}_{\perp}), \quad (4)
 \end{aligned}$$

where  $\mathbf{k}_{\parallel}$  ( $\mathbf{k}_{\perp}$ ) denotes  $\mathbf{k}$  that are flipped (unchanged) under unitary symmetries. Similar notation also applies to  $\mathbf{r}$ . Pioneer works that classify order-two spatial symmetries as an *addition* to internal symmetries are Ref. [12, 15]. These additional spatial symmetries will add a finer structure to the dimensional hierarchy Eqs. (2), (3) that may add or remove certain topological invariants.

In the following sections, we will repeat this process for point-gapped NH Hamiltonians. Before that, we first introduce the 38-fold classification of NH Hamiltonians in the next sections.

### III. STRUCTURE OF 38-FOLD CLASSIFICATION OF NH HAMILTONIAN

We consider internal symmetries of NH Hamiltonians. Due to non-Hermiticity,  $H$  will bifurcate into  $H$  and  $H^{\dagger}$ . Following notations in Ref. [24], internal symmetries for

NH Hamiltonians bifurcate into

$$\begin{aligned}
 \text{TRS} : \quad & \mathcal{T}_+ H(\mathbf{k}, \mathbf{r}) \mathcal{T}_+^{-1} = H(-\mathbf{k}, \mathbf{r}) \\
 \text{PHS} : \quad & \mathcal{C}_- H(\mathbf{k}, \mathbf{r}) \mathcal{C}_-^{-1} = -H^{\dagger}(-\mathbf{k}, \mathbf{r}) \\
 \text{TRS}^{\dagger} : \quad & \mathcal{C}_+ H(\mathbf{k}, \mathbf{r}) \mathcal{C}_+^{-1} = H^{\dagger}(-\mathbf{k}, \mathbf{r}) \\
 \text{PHS}^{\dagger} : \quad & \mathcal{T}_- H(\mathbf{k}, \mathbf{r}) \mathcal{T}_-^{-1} = -H(-\mathbf{k}, \mathbf{r}) \\
 \text{CS} : \quad & \Gamma H(\mathbf{k}, \mathbf{r}) \Gamma^{-1} = -H(\mathbf{k}, \mathbf{r})^{\dagger} \\
 \text{SLS} : \quad & S H(\mathbf{k}, \mathbf{r}) S^{-1} = -H(\mathbf{k}, \mathbf{r}), \quad (5)
 \end{aligned}$$

where SLS denotes sub-lattice symmetry. The combination of these symmetries will result in 38 independent classes. In this paper, we consider classes without SLS. As we will see, combinations of other symmetries will result in two sets of classes that are similar to Hermitian AZ symmetry classes.

We now comment on the structure of classes without SLS. The combination of TRS, PHS, and CS will result in 10 symmetry classes that are similar to AZ symmetry class for Hermitian Hamiltonians (See Table I). These 10 classes are called as AZ class for NH Hamiltonians. From now on, by AZ class, we mean AZ class for NH Hamiltonians from Table I. Next, consider the combination of TRS<sup>†</sup> and PHS<sup>†</sup>. Symmetry classes formed by these symmetries are called AZ<sup>†</sup> classes. They constitute 8 classes in total. Furthermore, if *only* PHS<sup>†</sup> is present (class D<sup>†</sup> and C<sup>†</sup> in Table I), PHS<sup>†</sup> can be transformed into TRS (class AI and AII) and vice versa [44]. To see this, consider a Hamiltonian  $H(\mathbf{k}, \mathbf{r})$  that obeys PHS<sup>†</sup> ( $\mathcal{T}_-$ ). Then  $iH(\mathbf{k}, \mathbf{r})$  obeys TRS with operator  $\mathcal{T}_-$ :

$$\mathcal{T}_- iH(\mathbf{k}, \mathbf{r}) \mathcal{T}_-^{-1} = iH(-\mathbf{k}, \mathbf{r}). \quad (6)$$

The mapping  $H(\mathbf{k}, \mathbf{r}) \rightarrow iH(\mathbf{k}, \mathbf{r})$  can be understood as a 90 degree rotation of energy spectrum on the complex plane. This operation does not change the topology of Hamiltonian  $H$ . Therefore, we see that class D<sup>†</sup> (C<sup>†</sup>) is unified with AI (AII). As we will see in Appendix. A, this unification will have some consequences on the dimensional hierarchy of AZ and AZ<sup>†</sup> classes. Therefore, there are 6 independent symmetry classes in AZ<sup>†</sup>. Similar to Hermitian classification, class A and AIII are complex classes, meaning they can be represented by complex Clifford algebra, while the rest of the classes are real (due to the existence of complex conjugate operator  $\mathcal{K}$  in  $\mathcal{T}_{\pm}$  and  $\mathcal{C}_{\pm}$ ), meaning they can be represented by real Clifford algebra. In Table I, we label AZ (AZ<sup>†</sup>) class by  $s$  ( $s^{\dagger}$ ).

The addition of SLS to AZ classes will result in additional 22 symmetry classes. So there are  $10 + 6 + 22 = 38$  symmetry classes in total. The 22-fold SLS classes can be further divided into five sub-classes (See Ref. [24] for details). However, since the SLS classes are rarely explored in current literature, we do not consider them in this paper.

As we are interested in point gap in this paper, we also briefly review the classification schemes for point gapped Hamiltonians. For a given point-gapped Hamiltonian  $H(\mathbf{k}, \mathbf{r})$ , we can continuously deform it into a unitary

TABLE I: AZ and  $AZ^\dagger$  symmetry classes for non-Hermitian Hamiltonians from Ref. [24]. Notice that class  $D^\dagger$  and  $C^\dagger$  are also in AZ class, so they do not enter the 38-fold classification classes [24].

Symmetry class	$s/s^\dagger$	$\mathcal{T}_+$	$\mathcal{C}_-$	$\mathcal{C}_+$	$\mathcal{T}_-$	$\Gamma$	C.L.	$\delta = 0$	1	2	3	4	5	6	7	
Complex AZ	A	1	0	0	0	0	0	$\mathcal{C}_1$	0	$\mathbb{Z}$	0	$\mathbb{Z}$	0	$\mathbb{Z}$	0	$\mathbb{Z}$
	AIII	0	0	0	0	0	1	$\mathcal{C}_0$	$\mathbb{Z}$	0	$\mathbb{Z}$	0	$\mathbb{Z}$	0	$\mathbb{Z}$	0
Real AZ	AI	1	+1	0	0	0	0	$\mathcal{R}_1$	$\mathbb{Z}_2$	$\mathbb{Z}$	0	0	0	$2\mathbb{Z}$	0	$\mathbb{Z}_2$
	BDI	2	+1	+1	0	0	1	$\mathcal{R}_2$	$\mathbb{Z}_2$	$\mathbb{Z}_2$	$\mathbb{Z}$	0	0	0	$2\mathbb{Z}$	0
	D	3	0	+1	0	0	0	$\mathcal{R}_3$	0	$\mathbb{Z}_2$	$\mathbb{Z}_2$	$\mathbb{Z}$	0	0	0	$2\mathbb{Z}$
	DIII	4	-1	+1	0	0	1	$\mathcal{R}_4$	$2\mathbb{Z}$	0	$\mathbb{Z}_2$	$\mathbb{Z}_2$	$\mathbb{Z}$	0	0	0
	AII	5	-1	0	0	0	0	$\mathcal{R}_5$	0	$2\mathbb{Z}$	0	$\mathbb{Z}_2$	$\mathbb{Z}_2$	$\mathbb{Z}$	0	0
	CII	6	-1	-1	0	0	1	$\mathcal{R}_6$	0	0	$2\mathbb{Z}$	0	$\mathbb{Z}_2$	$\mathbb{Z}_2$	$\mathbb{Z}$	0
	C	7	0	-1	0	0	0	$\mathcal{R}_7$	0	0	0	$2\mathbb{Z}$	0	$\mathbb{Z}_2$	$\mathbb{Z}_2$	$\mathbb{Z}$
	CI	0	+1	-1	0	0	1	$\mathcal{R}_0$	$\mathbb{Z}$	0	0	0	$2\mathbb{Z}$	0	$\mathbb{Z}_2$	$\mathbb{Z}_2$
Real $AZ^\dagger$	$AI^\dagger$	7	0	0	+1	0	0	$\mathcal{R}_7$	0	0	0	$2\mathbb{Z}$	0	$\mathbb{Z}_2$	$\mathbb{Z}_2$	$\mathbb{Z}$
	$BDI^\dagger$	0	0	0	+1	+1	1	$\mathcal{R}_0$	$\mathbb{Z}$	0	0	0	$2\mathbb{Z}$	0	$\mathbb{Z}_2$	$\mathbb{Z}_2$
	$D^\dagger$	1	0	0	0	+1	0	$\mathcal{R}_1$	$\mathbb{Z}_2$	$\mathbb{Z}$	0	0	0	$2\mathbb{Z}$	0	$\mathbb{Z}_2$
	$DIII^\dagger$	2	0	0	-1	+1	1	$\mathcal{R}_2$	$\mathbb{Z}_2$	$\mathbb{Z}_2$	$\mathbb{Z}$	0	0	0	$2\mathbb{Z}$	0
	$AII^\dagger$	3	0	0	-1	0	0	$\mathcal{R}_3$	0	$\mathbb{Z}_2$	$\mathbb{Z}_2$	$\mathbb{Z}$	0	0	0	$2\mathbb{Z}$
	$CII^\dagger$	4	0	0	-1	-1	1	$\mathcal{R}_4$	$2\mathbb{Z}$	0	$\mathbb{Z}_2$	$\mathbb{Z}_2$	$\mathbb{Z}$	0	0	0
	$C^\dagger$	5	0	0	0	-1	0	$\mathcal{R}_5$	0	$2\mathbb{Z}$	0	$\mathbb{Z}_2$	$\mathbb{Z}_2$	$\mathbb{Z}$	0	0
	$CI^\dagger$	6	0	0	+1	-1	1	$\mathcal{R}_6$	0	0	$2\mathbb{Z}$	0	$\mathbb{Z}_2$	$\mathbb{Z}_2$	$\mathbb{Z}$	0

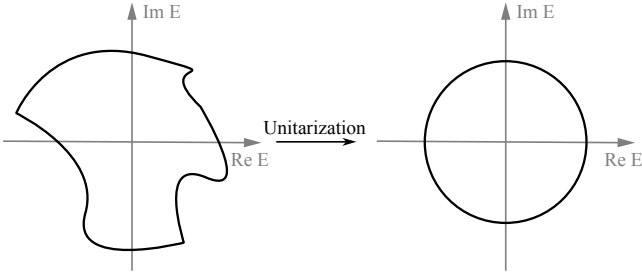


FIG. 2: Effect of unitarization of a point-gapped Hamiltonian on energy spectrum.

matrix  $\mathcal{U}(\mathbf{k}, \mathbf{r})$  without closing the point gap. This process is called unitary flattening [24, 45], which we show in Fig. 2. We may then consider the extended Hermitian Hamiltonian

$$\tilde{H}(\mathbf{k}, \mathbf{r}) = \begin{pmatrix} 0 & \mathcal{U}(\mathbf{k}, \mathbf{r}) \\ \mathcal{U}^\dagger(\mathbf{k}, \mathbf{r}) & 0 \end{pmatrix}. \quad (7)$$

If original Hamiltonian  $H(\mathbf{k}, \mathbf{r})$  obeys symmetries in Eq. (5), the extended Hamiltonian  $\tilde{H}(\mathbf{k}, \mathbf{r})$  then obeys

$$\begin{aligned} \tilde{\mathcal{T}}_\pm \tilde{H}(\mathbf{k}, \mathbf{r}) \tilde{\mathcal{T}}_\pm^{-1} &= \pm \tilde{H}(-\mathbf{k}, \mathbf{r}), \tilde{\mathcal{T}}_\pm = \begin{pmatrix} \mathcal{T}_\pm & 0 \\ 0 & \mathcal{T}_\pm \end{pmatrix} \\ \tilde{\mathcal{C}}_\pm \tilde{H}(\mathbf{k}, \mathbf{r}) \tilde{\mathcal{C}}_\pm^{-1} &= \pm \tilde{H}(-\mathbf{k}, \mathbf{r}), \tilde{\mathcal{C}}_\pm = \begin{pmatrix} 0 & \mathcal{C}_\pm \\ \mathcal{C}_\pm & 0 \end{pmatrix} \\ \tilde{\Gamma} \tilde{H}(\mathbf{k}, \mathbf{r}) \tilde{\Gamma}^{-1} &= -\tilde{H}(\mathbf{k}, \mathbf{r}), \tilde{\Gamma} = \begin{pmatrix} 0 & \Gamma \\ \Gamma & 0 \end{pmatrix} \\ \tilde{\mathcal{S}} \tilde{H}(\mathbf{k}, \mathbf{r}) \tilde{\mathcal{S}}^{-1} &= -\tilde{H}(\mathbf{k}, \mathbf{r}), \tilde{\mathcal{S}} = \begin{pmatrix} \mathcal{S} & 0 \\ 0 & \mathcal{S} \end{pmatrix}. \end{aligned} \quad (8)$$

Furthermore, Eq. (7) also obeys an additional CS

$$\Sigma \tilde{H}(\mathbf{k}, \mathbf{r}) \Sigma^{-1} = -\tilde{H}(\mathbf{k}, \mathbf{r}), \Sigma = \begin{pmatrix} 1 & 0 \\ 0 & -1 \end{pmatrix}. \quad (9)$$

For clearance, Eq. (9) will be called  $\Sigma$  symmetry in the rest of the paper. Notably,  $\Sigma$  symmetry arise since we are using extended Hamiltonian for the classification. In fact, the existence of  $\Sigma$  is the biggest difference between classifying a Hermitian Hamiltonian and a point-gapped NH Hamiltonian. Now, the classification of point-gapped Hamiltonian  $H(\mathbf{k}, \mathbf{r})$  is mapped to the classification of extended Hermitian Hamiltonian (7) with symmetries (8) and (9). This allows us to use the classification process on  $\tilde{H}$  for Hermitian Hamiltonians discussed in Sec. II. The  $K$  group relationships are given by

$$\begin{aligned} K_{\mathbb{C}}(s; d, D) &= K_{\mathbb{C}}(s - d + D; 0, 0) = \pi_0(\mathcal{C}_{s-d+D}), \\ s &= 0, 1 \pmod{2} \end{aligned} \quad (10)$$

for complex AZ classes and

$$\begin{aligned} K_{\mathbb{R}}(s; d, D) &= K_{\mathbb{R}}(s - d + D; 0, 0) = \pi_0(\mathcal{R}_{s-d+D}), \\ s &= 0, \dots, 7 \pmod{8} \end{aligned} \quad (11)$$

for real AZ classes and finally

$$\begin{aligned} K_{\mathbb{R}}^\dagger(s^\dagger; d, D) &= K_{\mathbb{R}}^\dagger(s^\dagger - d + D; 0, 0) = \pi_0(\mathcal{R}_{s^\dagger-d+D}), \\ s^\dagger &= 0, \dots, 7 \pmod{8} \end{aligned} \quad (12)$$

for  $AZ^\dagger$  classes; The superscript  $\dagger$  is put to distinguish  $K$  group of  $AZ^\dagger$  class from that of AZ class. The unification of AI and  $D^\dagger$ , AII and  $C^\dagger$  also gives

$$\begin{aligned} K_{\mathbb{R}}(1; d, D) &= K_{\mathbb{R}}^\dagger(1; d, D) \\ K_{\mathbb{R}}(5; d, D) &= K_{\mathbb{R}}^\dagger(5; d, D). \end{aligned} \quad (13)$$

We proof these relationships rigorously in Appendix A.

The dimensional hierarchy of AZ and AZ<sup>†</sup> class for point-gapped Hamiltonian can be understood as two "clocks": one for AZ and the other for AZ<sup>†</sup>. Two clocks are connected by the mapping Eq. (6). We draw these two clocks in Fig. 1.

In order to include spatial symmetries in the classification, we also need to consider the extension of spatial symmetries. In the following, we focus on order-two spatial symmetries as an additional symmetry to 16-fold AZ and AZ<sup>†</sup> classes in Table I.

#### IV. ORDER-TWO SPATIAL SYMMETRIES IN AZ AND AZ<sup>†</sup>

Similar to the bifurcation of internal symmetries, each type of spatial symmetry Eqs. (4) will also bifurcate into two. We label them according to

$$\begin{aligned}
{}^cUH(\mathbf{k}, \mathbf{r}) {}^cU^{-1} &= H(-\mathbf{k}_{\parallel}, \mathbf{k}_{\perp}, -\mathbf{r}_{\parallel}, \mathbf{r}_{\perp}) \\
{}^gUH(\mathbf{k}, \mathbf{r}) {}^gU^{-1} &= H^{\dagger}(-\mathbf{k}_{\parallel}, \mathbf{k}_{\perp}, -\mathbf{r}_{\parallel}, \mathbf{r}_{\perp}) \\
{}^c\bar{U}H(\mathbf{k}, \mathbf{r}) {}^c\bar{U}^{-1} &= -H(-\mathbf{k}_{\parallel}, \mathbf{k}_{\perp}, -\mathbf{r}_{\parallel}, \mathbf{r}_{\perp}) \\
{}^g\bar{U}H(\mathbf{k}, \mathbf{r}) {}^g\bar{U}^{-1} &= -H^{\dagger}(-\mathbf{k}_{\parallel}, \mathbf{k}_{\perp}, -\mathbf{r}_{\parallel}, \mathbf{r}_{\perp}) \\
{}^cAH(\mathbf{k}, \mathbf{r}) {}^cA^{-1} &= H(\mathbf{k}_{\parallel}, -\mathbf{k}_{\perp}, -\mathbf{r}_{\parallel}, \mathbf{r}_{\perp}) \\
{}^gAH(\mathbf{k}, \mathbf{r}) {}^gA^{-1} &= H^{\dagger}(\mathbf{k}_{\parallel}, -\mathbf{k}_{\perp}, -\mathbf{r}_{\parallel}, \mathbf{r}_{\perp}) \\
{}^c\bar{A}H(\mathbf{k}, \mathbf{r}) {}^c\bar{A}^{-1} &= -H(\mathbf{k}_{\parallel}, -\mathbf{k}_{\perp}, -\mathbf{r}_{\parallel}, \mathbf{r}_{\perp}) \\
{}^g\bar{A}H(\mathbf{k}, \mathbf{r}) {}^g\bar{A}^{-1} &= -H^{\dagger}(\mathbf{k}_{\parallel}, -\mathbf{k}_{\perp}, -\mathbf{r}_{\parallel}, \mathbf{r}_{\perp}), \quad (14)
\end{aligned}$$

where  $c$  and  $g$  refer to conventional and generalized spatial symmetries, respectively;  $\mathbf{k}_{\parallel}$  ( $\mathbf{k}_{\perp}$ ) denotes  $\mathbf{k}$  that are flipped (unchanged) under unitary symmetries. Similar notation also applies to  $\mathbf{r}$ . Similar to the extension of internal symmetries for point-gapped Hamiltonians in Eq. (8), to include spatial symmetries in the classification, we also consider the extension of Eq. (14). For the conventional spatial symmetries (those with  $c$  at the front), their extensions are given by

$${}^c\tilde{L} = \begin{pmatrix} {}^cL & 0 \\ 0 & {}^cL \end{pmatrix}, \quad (15)$$

where  $L = {}^cU, {}^c\bar{U}, {}^cA$ , or  ${}^c\bar{A}$ . For generalized spatial symmetries (those with  $g$  at the front), their extensions are given by

$${}^g\tilde{L} = \begin{pmatrix} 0 & {}^gL \\ {}^gL & 0 \end{pmatrix}, \quad (16)$$

where  $L = {}^gU, {}^g\bar{U}, {}^gA$ , or  ${}^g\bar{A}$ . These extended spatial symmetries would have the same effect on  $\tilde{H}$  in Eq. (7) as original spatial symmetries on original  $H$ . Therefore, we again mapped the classification problem of point gapped Hamiltonian to that of extended Hamiltonian (7).

Before continuing, we would like to comment on an important effect of the  $\Sigma$  symmetry [Eq. (9)] that would "unify" certain spatial symmetries. As an example, consider spatial symmetry  ${}^cU$  and its extension  ${}^c\tilde{U}$ , which operate on extended Hermitian Hamiltonian

$${}^c\tilde{U}\tilde{H}(\mathbf{k}, \mathbf{r}) {}^c\tilde{U}^{-1} = \tilde{H}(-\mathbf{k}_{\parallel}, \mathbf{k}_{\perp}, -\mathbf{r}_{\parallel}, \mathbf{r}_{\perp}). \quad (17)$$

Combining with  $\Sigma$  symmetry, which is always present for point gap Hamiltonians,  ${}^c\tilde{U}$  will result in the following symmetry:

$$\Sigma {}^c\tilde{U}\tilde{H}(\mathbf{k}, \mathbf{r})(\Sigma {}^c\tilde{U})^{-1} = -\tilde{H}(-\mathbf{k}_{\parallel}, \mathbf{k}_{\perp}, -\mathbf{r}_{\parallel}, \mathbf{r}_{\perp}). \quad (18)$$

Therefore, we see that  $\Sigma {}^c\tilde{U}$  has the exact same expression as  ${}^c\tilde{U}$  on Hamiltonian. Hence  $\Sigma$  symmetry would map a spatial symmetry that commutes with extended Hamiltonian to its anti-commuting counterpart and vice versa. In this sense,  $\Sigma$  symmetry "unifies" commuting and anti-commuting symmetries. However, this unification is not physical. We can understand this fact in two ways: First,  $\Sigma$  symmetry is only present for extended Hamiltonians instead of the original Hamiltonians. Therefore, this unification is only a by-product of adopting extended Hamiltonian formalism. Second, if we write  $\Sigma {}^c\tilde{U}$  explicitly, we would find

$$\Sigma {}^c\tilde{U} = \begin{pmatrix} {}^cU & 0 \\ 0 & -{}^cU \end{pmatrix} \quad (19)$$

which does not follow the form of Eq. (15). Hence, even if commuting symmetries will always have the same classification as anti-commuting symmetries, we should bear in mind that such unification is only a mathematical coincidence, which *does not* implies that both symmetries exist in the original system. However, since the classification problem is mapped to  $\tilde{H}$ ,  $\Sigma$  symmetry *will* cause the same classification for  ${}^cU$  and  ${}^c\tilde{U}$ , as they have the same effect on  $\tilde{H}$  up to a multiplication of  $\Sigma$ . In the following sections, we will discuss the effects of  $\Sigma$  symmetry in more detail.

In the present of internal symmetries Eqs. 5, not all these spatial symmetries are independent. Following the process of Ref. [12], we first find equivalent spatial symmetries under the presenting internal symmetries for a certain symmetry class, then we give a finer classification of the corresponding symmetry classes due to spatial symmetries.

##### A. Complex classes A and AIII with order-two unitary symmetry

We first consider classes A and AIII in the present of order-two unitary symmetry ( ${}^{c/g}U$  and  ${}^{c/g}\bar{U}$  in Eqs. (14)). Due to the absent of antiunitary symmetries, symmetries  ${}^{c/g}U$  and  ${}^{c/g}\bar{U}$  are defined up to a phase that

does not affect the classification. Therefore, we may set  $({}^{c/g}U)^2 = ({}^{c/g}\bar{U})^2 = 1$ .

For class A in which no internal symmetries are present, all  ${}^{c/g}U$  and  ${}^{c/g}\bar{U}$  are independent of each other.

Now consider class AIII where only CS in Eq. (5) is present. The CS operator  $\Gamma$  might commute or anti-commute with spatial symmetry operators. For example,

$$\Gamma {}^gU = \eta_\Gamma {}^gU\Gamma, \quad (20)$$

where  $\eta_\Gamma \in \{0, 1\}$ . To indicate this commutation relation between operators, we put a subscript  $\eta_\Gamma$  to spatial operator such that  $\Gamma {}^gU_{\eta_\Gamma} = \eta_\Gamma {}^gU_{\eta_\Gamma}\Gamma$ . Next, we investigate the combination of CS operator and spatial symmetry operators. Based on the effect of CS in Eq. (5), CS would flip spatial symmetries  $g/c$  to  $c/g$  and add another minus sign. Therefore, we see that  $\Gamma {}^{c/g}U = {}^{g/c}\bar{U}$  and  $\Gamma {}^{c/g}\bar{U} = {}^{g/c}U$ . We summarize all possible order-two unitary symmetries for A and AIII in Table II.

Notice that all the conclusions up until now are applicable to all kinds of energy gaps. Following the discussion at the beginning of Sec. IV, by considering the effect of  $\Sigma$  symmetry, we limit our scope to point gap. As an example, consider  ${}^gU$  in class A. Then  $\Sigma {}^g\tilde{U}$  will have the same effect on extended Hamiltonian as  ${}^{g\tilde{}}$ . As another example, consider  ${}^gU_+$  in class AIII. Notice that  $\Sigma$  anti-commute with extended CS operator  $\tilde{\Gamma}$ . Therefore,  $\Sigma {}^g\tilde{U}_+$  will have the same effect on the extended Hamiltonian as  ${}^{g\tilde{}}\bar{U}_-$ . By going over all possible order-two unitary symmetries for A and AIII in similar process, we can find all symmetries that are independent or related to each other through  $\Sigma$  symmetry. We label those symmetries that are independent by  $t = 0$  and  $t = 1$ , where  $t$  is defined mod2. For simplicity, we abbreviate them into  $t_0$  and  $t_1$  in Table II. We emphasize again that such connection is a purely mathematical coincidence which does not imply both symmetries exist in the system.

In Appendix B, we show the following dimensional hierarchy of complex AZ classes with unitary spatial symmetries

$$\begin{aligned} K_C^U(s, t; d + D, d_\parallel + D_\parallel, 0, 0) \\ = K_C^U(s - d + D, t - d_\parallel + D_\parallel; 0, 0, 0, 0), \end{aligned} \quad (21)$$

where the superscript  $U$  indicates this relationship works for unitary spatial symmetries. Recall that  $d$  is the dimension of the system and  $D$  is the dimension of the sphere surrounds the defect. Here,  $d_\parallel(D_\parallel)$  is the dimension of the system(sphere) that is being flipped under the spatial symmetry. Furthermore,

$$\begin{aligned} K_C^U(s, t = 0; 0, 0, 0, 0) &= \pi_0(\mathcal{C}_s) \times \pi_0(\mathcal{C}_s) \\ K_C^U(s, t = 1; 0, 0, 0, 0) &= \pi_0(\mathcal{C}_{s-1}), \end{aligned} \quad (22)$$

which we show in Appendix D using Clifford Algebra. We record some properties of Clifford Algebra in Appendix C. For both Eqs,  $s$  and  $t$  are defined mod2.

TABLE II: Possible types of order-two unitary symmetry for complex classes A and AIII. The symmetries in brackets indicate that they are related by  $\Gamma$  operators. The subscript  $\eta_\Gamma$  indicates commutation relation  $\Gamma U_{\eta_\Gamma} = \eta_\Gamma U_{\eta_\Gamma}\Gamma$ . Symmetries that are related by  $\Sigma$  symmetry Eq. (9) are labeled by identical  $t_n, n \in \{0, 1\}$  at the end.

Class		
A	${}^gU_{t_1}$	${}^{g\tilde{}}\bar{U}_{t_1}$
A	${}^cU_{t_0}$	${}^{c\tilde{}}\bar{U}_{t_0}$
AIII	$({}^gU_+, {}^{c\tilde{}}\bar{U}_+)_{t_1}$	$({}^gU_-, {}^{c\tilde{}}\bar{U}_-)_{t_0}$
AIII	$({}^cU_+, {}^g\bar{U}_+)_{t_0}$	$({}^cU_-, {}^g\bar{U}_-)_{t_1}$

Eqs. 21 and 22 allow us to conclude periodic table for complex AZ class with unitary spatial symmetries, which we will introduce in Sec. V.

### B. Complex classes A and AIII with order-two antiunitary symmetry

Now we consider the presence of antiunitary spatial symmetries [ ${}^{c/g}A$  and  ${}^{c/g}\bar{A}$  in Eqs. (14)].

For both  $g$  and  $c$  types of antiunitary symmetry, we use superscript  $\epsilon_A$  to denote their squared value i.e.  $(A^{\epsilon_A})^2 = \epsilon_A$ ,  $(\bar{A}^{\epsilon_A})^2 = \epsilon_A$ ; The subscript  $\eta_\Gamma$  (if present) denote their commutation relationship between CS operator  $\Gamma$  i.e.  $A_{\eta_\Gamma}^{\epsilon_A}\Gamma = \eta_\Gamma\Gamma A_{\eta_\Gamma}^{\epsilon_A}$ . Furthermore, in the present of CS, CS would flip  $g/c$  to  $c/g$  and add another minus sign. Therefore, the following relationship hold  ${}^{g/c}A_{\eta_\Gamma}^{\epsilon_A} = \Gamma {}^{c/g}\bar{A}_{\eta_\Gamma}^{\epsilon_A}$ .

Similar to the antiunitary spatial symmetry with Hermitian Hamiltonians (See Ref. [12]), the presence of antiunitary spatial symmetries will map complex classes A and AIII into one of real AZ and  $AZ^\dagger$  classes. To see this, one may consider antiunitary symmetries as effective TRS<sup>(†)</sup> or PHS<sup>(†)</sup> symmetries.

As an example, consider the addition of  ${}^cA^+$  to class A (First row of Table III), which add the symmetry

$${}^cA^+H(\mathbf{k}, \mathbf{r})[{}^cA^+]^{-1} = H(\mathbf{k}_\parallel, -\mathbf{k}_\perp, -\mathbf{r}_\parallel, \mathbf{r}_\perp), ({}^cA^+)^2 = 1 \quad (23)$$

to class A. If we treat  $(\mathbf{k}_\perp, \mathbf{r}_\parallel)$  as "momentum" and  $(\mathbf{k}_\parallel, \mathbf{r}_\perp)$  as "positions", we see that Eq. (23) has exactly the same form as TRS  $\mathcal{T}_+$  with  $\mathcal{T}_+^2 = 1$ . Now, the dimension of the BZ is given by the combined dimension of  $\mathbf{k}_\perp$  and  $\mathbf{r}_\parallel$ , which is  $d - d_\parallel + D_\parallel$ . The dimension of the sphere that surrounds the defect is given by the combined dimension of  $\mathbf{k}_\parallel$  and  $\mathbf{r}_\perp$ , which is  $D - D_\parallel + d_\parallel$ . Therefore, with the addition of  ${}^cA^+$ , class A is mapped to class AI.

As another example, consider the addition of  ${}^g\bar{A}_+^\dagger$  to class AIII (Second row of Table III). By considering  $(\mathbf{k}_\perp, \mathbf{r}_\parallel)$  as "momentum", the antiunitary symmetry  ${}^g\bar{A}_+^\dagger$  has the same form as PHS with  $({}^g\bar{A}_+^\dagger)^2 = 1$ .

Next, consider  $\Gamma^g \bar{A}_+^\dagger$ . The CS symmetry  $\Gamma$  takes Hermitian conjugate of the Hamiltonian again and give another minus sign i.e.  $\Gamma^g \bar{A}_+^\dagger H(\mathbf{k}, \mathbf{r}) [\Gamma^g \bar{A}_+^\dagger]^{-1} = H(\mathbf{k}_\parallel, -\mathbf{k}_\perp, -\mathbf{r}_\parallel, \mathbf{r}_\perp)$ . Finally, since  $\Gamma$  and  ${}^g \bar{A}_+^\dagger$  commute, we have  $(\Gamma^g \bar{A}_+^\dagger)^2 = 1$ . This suggest we can define  ${}^c A_+^\dagger = \Gamma^g \bar{A}_+^\dagger$  which has the same form as TRS. We see that the addition of  ${}^g \bar{A}_+^\dagger$  will map AIII to BDI.

Following similar process, we enumerate all possible types of order-two antiunitary symmetries in class A and AIII and their mapped classes in Table III.

Finally, we comment on the effect of  $\Sigma$  symmetry. As an example, we consider again  ${}^c A^+$  in class AI. Due to the  $\Sigma$  symmetry, the operator  $\Sigma^c A^+$  has the same effect on extended Hamiltonian as  ${}^c \bar{A}^+$ . According to Table III,  $\Sigma$  symmetry would unify class AI and  $D^\dagger$  i.e. these two classes would have the same topological invariants and classification. Indeed, in the 38-fold classification, AI and  $D^\dagger$  have the same classification under point gap. We mark symmetry classes that are equivalent under  $\Sigma$  symmetry by identical symbols at the end of the symmetry operator in Table III. Notice that our results are consistent with 38-fold classification in Ref. [24] i.e. the mapped classes marked with same symbol in Table III have the same topological classification under point gap.

The dimensional hierarchy of complex AZ class with antiunitary spatial symmetry is thus given by

$$\begin{aligned} K_{\mathbb{C}}^A(s; d, d_\parallel, D, D_\parallel) &= K_{\mathbb{R}}(s; d - d_\parallel + D_\parallel, D + d_\parallel - D_\parallel) \\ &= K_{\mathbb{R}}(s - d + D + 2(d_\parallel - D_\parallel); 0, 0) \\ &= \pi_0(\mathcal{R}_{s-d+D+2(d_\parallel-D_\parallel)}) \end{aligned} \quad (24)$$

where  $K_{\mathbb{R}}$  is given in Eq. (11).

### C. Real AZ classes with order-two symmetry

In this section, we consider the classification of real AZ classes with order-two spatial symmetries. Throughout this section, all Eqs. are also valid upon exchange  $g \leftrightarrow c$ ; The superscripts denote the squared value of the spatial operators, and the subscripts denote the commutation relationship between spatial operators and  $\mathcal{T}_+$  and  $\mathcal{C}_-$ . Throughout this paper, we take the convention that  $[\mathcal{T}_+, \mathcal{C}_-] = 0$ .

For class A and AII, we have the following equivalence symmetries

*AI and AII* ( $\mathcal{T}_+$ ):

$$\begin{aligned} {}^g U_{\eta_T}^{\epsilon_U} &= i {}^g U_{-\eta_T}^{-\epsilon_U} = \mathcal{T}_+ {}^g A_{\eta_T}^{\eta_T \epsilon_T \epsilon_U} = i \mathcal{T}_+ {}^g A_{-\eta_T}^{\eta_T \epsilon_T \epsilon_U} \\ {}^g \bar{U}_{\eta_T}^{\epsilon_U} &= i {}^g \bar{U}_{-\eta_T}^{-\epsilon_U} = \mathcal{T}_+ {}^g \bar{A}_{\eta_T}^{\eta_T \epsilon_T \epsilon_U} = i \mathcal{T}_+ {}^g \bar{A}_{-\eta_T}^{\eta_T \epsilon_T \epsilon_U}, \end{aligned} \quad (25)$$

where the subscript  $\eta_T$  denotes the commutation relationship between the operator and  $\mathcal{T}_+$ .

For class D and C, we have the following equivalence symmetries

TABLE III: Possible types of order-two antiunitary symmetry for complex classes A and AIII. The superscript  $A^{\epsilon_A}$  denote the sign of  $(A^{\epsilon_A})^2 = \epsilon_A$ , and subscript  $A_{\eta_T}^{\epsilon_A}$  (if present) denotes commutation relationship between  $A$  and CS  $\Gamma$ :  $A_{\eta_T}^{\epsilon_A} \Gamma = \eta_T \Gamma A_{\eta_T}^{\epsilon_A}$ . Symmetries in the brackets are equivalent upon being multiplied by CS operator  $\Gamma$ . Symmetries that are related by  $\Sigma$  symmetry Eq. (9) are labeled by identical symbols at the end.

Class	Symmetry	Map to class
A	${}^c A^+ \square$	AI
AIII	$({}^g \bar{A}_+^\dagger, {}^c A_+^\dagger) \heartsuit$	BDI
A	${}^g \bar{A}^+ \triangle$	D
AIII	$({}^g \bar{A}_-^\dagger, {}^c A_-^\dagger) \spadesuit$	DIII
A	${}^c A^- \diamond$	AII
AIII	$({}^g \bar{A}_+^\dagger, {}^c A_+^\dagger) \blacklozenge$	CII
A	${}^g \bar{A}^- \circ$	C
AIII	$({}^g \bar{A}_-^\dagger, {}^c A_-^\dagger) \bullet$	CI
A	${}^g A^+ \circ$	AI $^\dagger$
AIII	$({}^g A_+^\dagger, {}^c \bar{A}_+^\dagger) \bullet$	BDI $^\dagger$
A	${}^c \bar{A}^+ \square$	D $^\dagger$
AIII	$({}^g A_-^\dagger, {}^c \bar{A}_-^\dagger) \heartsuit$	DIII $^\dagger$
A	${}^g A^- \triangle$	AII $^\dagger$
AIII	$({}^g A_+^\dagger, {}^c \bar{A}_+^\dagger) \spadesuit$	CII $^\dagger$
A	${}^c \bar{A}^- \diamond$	C $^\dagger$
AIII	$({}^g A_-^\dagger, {}^c \bar{A}_-^\dagger) \blacklozenge$	CI $^\dagger$

*D and C* ( $\mathcal{C}_-$ ):

$$\begin{aligned} {}^g U_{\eta_C}^{\epsilon_U} &= i {}^g U_{-\eta_C}^{-\epsilon_U} = \mathcal{C}_- {}^c \bar{A}_{\eta_C}^{\eta_C \epsilon_C \epsilon_U} = i \mathcal{C}_- {}^c \bar{A}_{-\eta_C}^{\eta_C \epsilon_C \epsilon_U} \\ {}^g \bar{U}_{\eta_C}^{\epsilon_U} &= i {}^g \bar{U}_{-\eta_C}^{-\epsilon_U} = \mathcal{C}_- {}^c A_{\eta_C}^{\eta_C \epsilon_C \epsilon_U} = i \mathcal{C}_- {}^c A_{-\eta_C}^{\eta_C \epsilon_C \epsilon_U}, \end{aligned} \quad (26)$$

where the subscript  $\eta_C$  denotes the commutation relationship between the operator and  $\mathcal{C}_-$ .

Finally, for class BDI, DIII, CII, and CI, we have *BDI, DIII, CII, and CI* ( $\mathcal{C}_-$  and  $\mathcal{T}_+$ ):

$$\begin{aligned} {}^g U_{\eta_T, \eta_C}^{\epsilon_U} &= i {}^g U_{-\eta_T, -\eta_C}^{-\epsilon_U} = \mathcal{T}_+ {}^g A_{\eta_T, \eta_C}^{\eta_T \epsilon_T \epsilon_U} = i \mathcal{T}_+ {}^g A_{-\eta_T, -\eta_C}^{\eta_T \epsilon_T \epsilon_U} \\ &= \mathcal{C}_- {}^c \bar{A}_{\eta_T, \eta_C}^{\eta_C \epsilon_C \epsilon_U} = i \mathcal{C}_- {}^c \bar{A}_{-\eta_T, -\eta_C}^{\eta_C \epsilon_C \epsilon_U} \end{aligned}$$

$$\begin{aligned} {}^g \bar{U}_{\eta_T, \eta_C}^{\epsilon_U} &= i {}^g \bar{U}_{-\eta_T, -\eta_C}^{-\epsilon_U} = \mathcal{T}_+ {}^g \bar{A}_{\eta_T, \eta_C}^{\eta_T \epsilon_T \epsilon_U} = i \mathcal{T}_+ {}^g \bar{A}_{-\eta_T, -\eta_C}^{\eta_T \epsilon_T \epsilon_U} \\ &= \mathcal{C}_- {}^c A_{\eta_T, \eta_C}^{\eta_C \epsilon_C \epsilon_U} = i \mathcal{C}_- {}^c A_{-\eta_T, -\eta_C}^{\eta_C \epsilon_C \epsilon_U}, \end{aligned} \quad (27)$$

where the first (second) subscript  $\eta_T$  ( $\eta_C$ ) indicates the commutation relationship between the operator and  $\mathcal{T}_+$  ( $\mathcal{C}_-$ ).

By going over all possible combinations of  $\epsilon_U, \eta_T, \eta_C$ , we summarize possible order-two spatial symmetries for real AZ classes in Table IV.

Next, we discuss the effect of  $\Sigma$  symmetry. Similar to the previous case for complex AZ classes,  $\Sigma$  symmetry would "unify" some spatial symmetries in Table IV. As an example, consider class AI with spatial symmetry  ${}^g U_+^\dagger$ . Recall that the  $\Sigma$  operator in Eq. (9) anti-commutes with generalized spatial symmetries Eq. (16).



TABLE IV: Possible order-two spatial symmetries for real AZ classes. The superscript of the operators indicates sign the squared value of the operator ; The subscript indicates the commutation relationship between the spatial symmetry operators and TRS  $\mathcal{T}_+$  or PHS  $\mathcal{C}_-$ : + for commutation and - for anti-commutation. If both TRS and PHS are present, the first (second) subscript indicates the commutation relationship between the spatial symmetry operator and TRS (PHS). Symmetries inside the same circular bracket are equivalent. For each AZ class, spatial symmetries that are related by  $\Sigma$  symmetry (9) are labeled by the same  $t_n, n \in \{0, 1, 2, 3\}$  at the end of the circular bracket.

$s$ AZ class					
1	AI	$({}^g U_+^+, {}^g U_-^-)t_1$	$({}^g \bar{U}_+^+, {}^g \bar{U}_-^-)t_1$	$({}^g U_+^+, {}^g U_-^-)t_3$	$({}^g \bar{U}_+^+, {}^g \bar{U}_-^-)t_3$
		$({}^g A_+^+, {}^g A_-^-)$	$({}^g \bar{A}_+^+, {}^g \bar{A}_-^-)$	$({}^g A_+^+, {}^g A_-^-)$	$({}^g \bar{A}_+^+, {}^g \bar{A}_-^-)$
		$({}^c U_+^+, {}^c U_-^-)t_0$	$({}^c \bar{U}_+^+, {}^c \bar{U}_-^-)t_2$	$({}^c U_+^+, {}^c U_-^-)t_2$	$({}^c \bar{U}_+^+, {}^c \bar{U}_-^-)t_0$
		$({}^c A_+^+, {}^c A_-^-)$	$({}^c \bar{A}_+^+, {}^c \bar{A}_-^-)$	$({}^c A_+^+, {}^c A_-^-)$	$({}^c \bar{A}_+^+, {}^c \bar{A}_-^-)$
2	BDI	$({}^g U_{++}^+, {}^g U_{--}^-, {}^c \bar{U}_{++}^+, {}^c \bar{U}_{--}^-)t_1$	$({}^g U_{+-}^+, {}^g U_{-+}^-, {}^c \bar{U}_{+-}^+, {}^c \bar{U}_{-+}^-)t_2$	$({}^g U_{+-}^+, {}^g U_{-+}^-, {}^c \bar{U}_{--}^-, {}^c \bar{U}_{++}^+)t_3$	$({}^g U_{+-}^+, {}^g U_{-+}^-, {}^c \bar{U}_{++}^+, {}^c \bar{U}_{--}^-)t_0$
		$({}^g A_{++}^+, {}^g A_{--}^-, {}^c \bar{A}_{++}^+, {}^c \bar{A}_{--}^-)$	$({}^g A_{+-}^+, {}^g A_{-+}^-, {}^c \bar{A}_{+-}^+, {}^c \bar{A}_{-+}^-)$	$({}^g A_{--}^-, {}^g A_{++}^+, {}^c \bar{A}_{--}^-, {}^c \bar{A}_{++}^+)$	$({}^g A_{+-}^+, {}^g A_{-+}^-, {}^c \bar{A}_{++}^+, {}^c \bar{A}_{--}^-)$
		$({}^c U_{++}^+, {}^c U_{--}^-, {}^g \bar{U}_{++}^+, {}^g \bar{U}_{--}^-)t_0$	$({}^c U_{+-}^+, {}^c U_{-+}^-, {}^g \bar{U}_{+-}^+, {}^g \bar{U}_{-+}^-)t_1$	$({}^c U_{+-}^+, {}^c U_{-+}^-, {}^g \bar{U}_{--}^-, {}^g \bar{U}_{++}^+)t_2$	$({}^c U_{+-}^+, {}^c U_{-+}^-, {}^g \bar{U}_{++}^+, {}^g \bar{U}_{--}^-)t_3$
		$({}^c A_{++}^+, {}^c A_{--}^-, {}^g \bar{A}_{++}^+, {}^g \bar{A}_{--}^-)$	$({}^c A_{+-}^+, {}^c A_{-+}^-, {}^g \bar{A}_{+-}^+, {}^g \bar{A}_{-+}^-)$	$({}^c A_{--}^-, {}^c A_{++}^+, {}^g \bar{A}_{--}^-, {}^g \bar{A}_{++}^+)$	$({}^c A_{+-}^+, {}^c A_{-+}^-, {}^g \bar{A}_{++}^+, {}^g \bar{A}_{--}^-)$
3	D	$({}^g U_+^+, {}^g U_-^-)t_1$	$({}^g \bar{U}_+^+, {}^g \bar{U}_-^-)t_1$	$({}^g U_+^+, {}^g U_-^-)t_3$	$({}^g \bar{U}_+^+, {}^g \bar{U}_-^-)t_3$
		$({}^g A_+^+, {}^g A_-^-)$	$({}^g \bar{A}_+^+, {}^g \bar{A}_-^-)$	$({}^g A_+^+, {}^g A_-^-)$	$({}^g \bar{A}_+^+, {}^g \bar{A}_-^-)$
		$({}^c U_+^+, {}^c U_-^-)t_0$	$({}^c \bar{U}_+^+, {}^c \bar{U}_-^-)t_2$	$({}^c U_+^+, {}^c U_-^-)t_2$	$({}^c \bar{U}_+^+, {}^c \bar{U}_-^-)t_0$
		$({}^g A_+^+, {}^g A_-^-)$	$({}^g \bar{A}_+^+, {}^g \bar{A}_-^-)$	$({}^g A_+^+, {}^g A_-^-)$	$({}^g \bar{A}_+^+, {}^g \bar{A}_-^-)$
4	DIII	$({}^g U_{++}^+, {}^g U_{--}^-, {}^c \bar{U}_{++}^+, {}^c \bar{U}_{--}^-)t_1$	$({}^g U_{+-}^+, {}^g U_{-+}^-, {}^c \bar{U}_{+-}^+, {}^c \bar{U}_{-+}^-)t_2$	$({}^g U_{+-}^+, {}^g U_{-+}^-, {}^c \bar{U}_{--}^-, {}^c \bar{U}_{++}^+)t_3$	$({}^g U_{+-}^+, {}^g U_{-+}^-, {}^c \bar{U}_{++}^+, {}^c \bar{U}_{--}^-)t_0$
		$({}^g A_{++}^+, {}^g A_{--}^-, {}^c \bar{A}_{++}^+, {}^c \bar{A}_{--}^-)$	$({}^g A_{+-}^+, {}^g A_{-+}^-, {}^c \bar{A}_{+-}^+, {}^c \bar{A}_{-+}^-)$	$({}^g A_{--}^-, {}^g A_{++}^+, {}^c \bar{A}_{--}^-, {}^c \bar{A}_{++}^+)$	$({}^g A_{+-}^+, {}^g A_{-+}^-, {}^c \bar{A}_{++}^+, {}^c \bar{A}_{--}^-)$
		$({}^c U_{++}^+, {}^c U_{--}^-, {}^g \bar{U}_{++}^+, {}^g \bar{U}_{--}^-)t_0$	$({}^c U_{+-}^+, {}^c U_{-+}^-, {}^g \bar{U}_{+-}^+, {}^g \bar{U}_{-+}^-)t_1$	$({}^c U_{+-}^+, {}^c U_{-+}^-, {}^g \bar{U}_{--}^-, {}^g \bar{U}_{++}^+)t_2$	$({}^c U_{+-}^+, {}^c U_{-+}^-, {}^g \bar{U}_{++}^+, {}^g \bar{U}_{--}^-)t_3$
		$({}^c A_{++}^+, {}^c A_{--}^-, {}^g \bar{A}_{++}^+, {}^g \bar{A}_{--}^-)$	$({}^c A_{+-}^+, {}^c A_{-+}^-, {}^g \bar{A}_{+-}^+, {}^g \bar{A}_{-+}^-)$	$({}^c A_{--}^-, {}^c A_{++}^+, {}^g \bar{A}_{--}^-, {}^g \bar{A}_{++}^+)$	$({}^c A_{+-}^+, {}^c A_{-+}^-, {}^g \bar{A}_{++}^+, {}^g \bar{A}_{--}^-)$
5	AII	$({}^g U_+^+, {}^g U_-^-)t_1$	$({}^g \bar{U}_+^+, {}^g \bar{U}_-^-)t_1$	$({}^g U_+^+, {}^g U_-^-)t_3$	$({}^g \bar{U}_+^+, {}^g \bar{U}_-^-)t_3$
		$({}^g A_+^+, {}^g A_-^-)$	$({}^g \bar{A}_+^+, {}^g \bar{A}_-^-)$	$({}^g A_+^+, {}^g A_-^-)$	$({}^g \bar{A}_+^+, {}^g \bar{A}_-^-)$
		$({}^c U_+^+, {}^c U_-^-)t_0$	$({}^c \bar{U}_+^+, {}^c \bar{U}_-^-)t_2$	$({}^c U_+^+, {}^c U_-^-)t_2$	$({}^c \bar{U}_+^+, {}^c \bar{U}_-^-)t_0$
		$({}^g A_+^+, {}^g A_-^-)$	$({}^g \bar{A}_+^+, {}^g \bar{A}_-^-)$	$({}^g A_+^+, {}^g A_-^-)$	$({}^g \bar{A}_+^+, {}^g \bar{A}_-^-)$
6	CII	$({}^g U_{++}^+, {}^g U_{--}^-, {}^c \bar{U}_{++}^+, {}^c \bar{U}_{--}^-)t_1$	$({}^g U_{+-}^+, {}^g U_{-+}^-, {}^c \bar{U}_{+-}^+, {}^c \bar{U}_{-+}^-)t_2$	$({}^g U_{+-}^+, {}^g U_{-+}^-, {}^c \bar{U}_{--}^-, {}^c \bar{U}_{++}^+)t_3$	$({}^g U_{+-}^+, {}^g U_{-+}^-, {}^c \bar{U}_{++}^+, {}^c \bar{U}_{--}^-)t_0$
		$({}^g A_{++}^+, {}^g A_{--}^-, {}^c \bar{A}_{++}^+, {}^c \bar{A}_{--}^-)$	$({}^g A_{+-}^+, {}^g A_{-+}^-, {}^c \bar{A}_{+-}^+, {}^c \bar{A}_{-+}^-)$	$({}^g A_{--}^-, {}^g A_{++}^+, {}^c \bar{A}_{--}^-, {}^c \bar{A}_{++}^+)$	$({}^g A_{+-}^+, {}^g A_{-+}^-, {}^c \bar{A}_{++}^+, {}^c \bar{A}_{--}^-)$
		$({}^c U_{++}^+, {}^c U_{--}^-, {}^g \bar{U}_{++}^+, {}^g \bar{U}_{--}^-)t_0$	$({}^c U_{+-}^+, {}^c U_{-+}^-, {}^g \bar{U}_{+-}^+, {}^g \bar{U}_{-+}^-)t_1$	$({}^c U_{+-}^+, {}^c U_{-+}^-, {}^g \bar{U}_{--}^-, {}^g \bar{U}_{++}^+)t_2$	$({}^c U_{+-}^+, {}^c U_{-+}^-, {}^g \bar{U}_{++}^+, {}^g \bar{U}_{--}^-)t_3$
		$({}^c A_{++}^+, {}^c A_{--}^-, {}^g \bar{A}_{++}^+, {}^g \bar{A}_{--}^-)$	$({}^c A_{+-}^+, {}^c A_{-+}^-, {}^g \bar{A}_{+-}^+, {}^g \bar{A}_{-+}^-)$	$({}^c A_{--}^-, {}^c A_{++}^+, {}^g \bar{A}_{--}^-, {}^g \bar{A}_{++}^+)$	$({}^c A_{+-}^+, {}^c A_{-+}^-, {}^g \bar{A}_{++}^+, {}^g \bar{A}_{--}^-)$
7	C	$({}^g U_+^+, {}^g U_-^-)t_1$	$({}^g \bar{U}_+^+, {}^g \bar{U}_-^-)t_1$	$({}^g U_+^+, {}^g U_-^-)t_3$	$({}^g \bar{U}_+^+, {}^g \bar{U}_-^-)t_3$
		$({}^g A_+^+, {}^g A_-^-)$	$({}^g \bar{A}_+^+, {}^g \bar{A}_-^-)$	$({}^g A_+^+, {}^g A_-^-)$	$({}^g \bar{A}_+^+, {}^g \bar{A}_-^-)$
		$({}^c U_+^+, {}^c U_-^-)t_0$	$({}^c \bar{U}_+^+, {}^c \bar{U}_-^-)t_2$	$({}^c U_+^+, {}^c U_-^-)t_2$	$({}^c \bar{U}_+^+, {}^c \bar{U}_-^-)t_0$
		$({}^g A_+^+, {}^g A_-^-)$	$({}^g \bar{A}_+^+, {}^g \bar{A}_-^-)$	$({}^g A_+^+, {}^g A_-^-)$	$({}^g \bar{A}_+^+, {}^g \bar{A}_-^-)$
0	CI	$({}^g U_{++}^+, {}^g U_{--}^-, {}^c \bar{U}_{++}^+, {}^c \bar{U}_{--}^-)t_1$	$({}^g U_{+-}^+, {}^g U_{-+}^-, {}^c \bar{U}_{+-}^+, {}^c \bar{U}_{-+}^-)t_2$	$({}^g U_{+-}^+, {}^g U_{-+}^-, {}^c \bar{U}_{--}^-, {}^c \bar{U}_{++}^+)t_3$	$({}^g U_{+-}^+, {}^g U_{-+}^-, {}^c \bar{U}_{++}^+, {}^c \bar{U}_{--}^-)t_0$
		$({}^g A_{++}^+, {}^g A_{--}^-, {}^c \bar{A}_{++}^+, {}^c \bar{A}_{--}^-)$	$({}^g A_{+-}^+, {}^g A_{-+}^-, {}^c \bar{A}_{+-}^+, {}^c \bar{A}_{-+}^-)$	$({}^g A_{--}^-, {}^g A_{++}^+, {}^c \bar{A}_{--}^-, {}^c \bar{A}_{++}^+)$	$({}^g A_{+-}^+, {}^g A_{-+}^-, {}^c \bar{A}_{++}^+, {}^c \bar{A}_{--}^-)$
		$({}^c U_{++}^+, {}^c U_{--}^-, {}^g \bar{U}_{++}^+, {}^g \bar{U}_{--}^-)t_0$	$({}^c U_{+-}^+, {}^c U_{-+}^-, {}^g \bar{U}_{+-}^+, {}^g \bar{U}_{-+}^-)t_1$	$({}^c U_{+-}^+, {}^c U_{-+}^-, {}^g \bar{U}_{--}^-, {}^g \bar{U}_{++}^+)t_2$	$({}^c U_{+-}^+, {}^c U_{-+}^-, {}^g \bar{U}_{++}^+, {}^g \bar{U}_{--}^-)t_3$
		$({}^c A_{++}^+, {}^c A_{--}^-, {}^g \bar{A}_{++}^+, {}^g \bar{A}_{--}^-)$	$({}^c A_{+-}^+, {}^c A_{-+}^-, {}^g \bar{A}_{+-}^+, {}^g \bar{A}_{-+}^-)$	$({}^c A_{--}^-, {}^c A_{++}^+, {}^g \bar{A}_{--}^-, {}^g \bar{A}_{++}^+)$	$({}^c A_{+-}^+, {}^c A_{-+}^-, {}^g \bar{A}_{++}^+, {}^g \bar{A}_{--}^-)$

Therefore,  $\Sigma {}^g U_+^+$  has the same classification as  ${}^g \bar{U}_+^+$ . We may repeat this process for all classes in Table IV. For each class, we label symmetries that are independent by  $t = 0, 1, 2, 3$ , where  $t$  is defined mod4. We abbreviate these symbols into  $t_0, t_1, t_2, t_3$  and label them at the end of the circular bracket in Table IV.

In Appendix B, we show that the  $K$  group for real AZ classes with spatial symmetries obey the following relationship

$$K_{\mathbb{R}}^{U/A}(s, t; d, d_{\parallel}, D, D_{\parallel}) = K_{\mathbb{R}}^{U/A}(s - d + D, t - d_{\parallel} + D_{\parallel}; 0, 0, 0, 0), \quad (28)$$

where the superscript  $U/A$  indicates this relationship works for both unitary and anti-unitary spatial symmetries. Furthermore,

$$\begin{aligned} K_{\mathbb{R}}^{U/A}(s, t = 0; 0, 0, 0, 0) &= \pi_0(\mathcal{R}_s) \times \pi_0(\mathcal{R}_s) \\ K_{\mathbb{R}}^{U/A}(s, t = 1; 0, 0, 0, 0) &= \pi_0(\mathcal{R}_{s-1}) \\ K_{\mathbb{R}}^{U/A}(s, t = 2; 0, 0, 0, 0) &= \pi_0(\mathcal{C}_s) \\ K_{\mathbb{R}}^{U/A}(s, t = 3; 0, 0, 0, 0) &= \pi_0(\mathcal{R}_{s+1}), \end{aligned} \quad (29)$$

which we show in Appendix D using Clifford Algebra. For both Eqs.  $s$  is defined mod8 while  $t$  is defined mod4.

#### D. Real $AZ^\dagger$ classes with order-two symmetry

Following similar steps as previous section, we derive equivalent symmetries for real  $AZ^\dagger$  classes in this section. All Eqs. in this section are also valid upon exchange  $g \leftrightarrow c$ . Throughout this paper, we take the convention that  $\text{TRS}^\dagger$  operator  $\mathcal{C}_+$  and  $\text{PHS}^\dagger$  operator  $\mathcal{T}_-$  commute:  $[\mathcal{C}_+, \mathcal{T}_-] = 0$ .

For class  $AI^\dagger$  and  $AIII^\dagger$ , we have the following equivalent symmetries

$AI^\dagger$  and  $AIII^\dagger$  ( $\mathcal{C}_+$ ):

$$\begin{aligned} {}^g U_{\eta_C}^{\epsilon_U} &= i {}^g U_{-\eta_C}^{-\epsilon_U} = \mathcal{C}_+ {}^c A_{\eta_C}^{\eta_C \epsilon_C \epsilon_U} = i \mathcal{C}_+ {}^c A_{-\eta_C}^{\eta_C \epsilon_C \epsilon_U} \\ {}^g \bar{U}_{\eta_C}^{\epsilon_U} &= i {}^g \bar{U}_{-\eta_C}^{-\epsilon_U} = \mathcal{C}_+ {}^c \bar{A}_{\eta_C}^{\eta_C \epsilon_C \epsilon_U} = i \mathcal{C}_+ {}^c \bar{A}_{-\eta_C}^{\eta_C \epsilon_C \epsilon_U}, \end{aligned} \quad (30)$$

where the subscript indicates the commutation relationship between spatial symmetries and  $\text{TRS}^\dagger$  operator  $\mathcal{C}_+$ .

For class  $D^\dagger$  and  $C^\dagger$ , we have

$D^\dagger$  and  $C^\dagger$  ( $\mathcal{T}_-$ ):

$$\begin{aligned} {}^g U_{\eta_T}^{\epsilon_U} &= i {}^g U_{-\eta_T}^{-\epsilon_U} = \mathcal{T}_- {}^g \bar{A}_{\eta_T}^{\eta_T \epsilon_T \epsilon_U} = i \mathcal{T}_- {}^g \bar{A}_{-\eta_T}^{\eta_T \epsilon_T \epsilon_U} \\ {}^g \bar{U}_{\eta_T}^{\epsilon_U} &= i {}^g \bar{U}_{-\eta_T}^{-\epsilon_U} = \mathcal{T}_- {}^g A_{\eta_T}^{\eta_T \epsilon_T \epsilon_U} = i \mathcal{T}_- {}^g A_{-\eta_T}^{\eta_T \epsilon_T \epsilon_U}, \end{aligned} \quad (31)$$

where the subscript indicates the commutation relationship of  $\text{PHS}^\dagger$  operator  $\mathcal{T}_-$ .

Finally, for class  $BDI^\dagger$ ,  $DIII^\dagger$ ,  $CII^\dagger$ , and  $CI^\dagger$ , we have  $BDI^\dagger$ ,  $DIII^\dagger$ ,  $CII^\dagger$ , and  $CI^\dagger$ :

$$\begin{aligned} {}^g U_{\eta_C, \eta_T}^{\epsilon_U} &= i {}^g U_{-\eta_C, -\eta_T}^{-\epsilon_U} = \mathcal{C}_+ {}^c A_{\eta_C, \eta_T}^{\eta_C \epsilon_C \epsilon_U} = i \mathcal{C}_+ {}^c A_{-\eta_C, -\eta_T}^{\eta_C \epsilon_C \epsilon_U} \\ &= \mathcal{T}_- {}^g \bar{A}_{\eta_C, \eta_T}^{\eta_T \epsilon_T \epsilon_U} = i \mathcal{T}_- {}^g \bar{A}_{-\eta_C, -\eta_T}^{\eta_T \epsilon_T \epsilon_U} \\ {}^g \bar{U}_{\eta_C, \eta_T}^{\epsilon_U} &= i {}^g \bar{U}_{-\eta_C, -\eta_T}^{-\epsilon_U} = \mathcal{C}_+ {}^c \bar{A}_{\eta_C, \eta_T}^{\eta_C \epsilon_C \epsilon_U} = i \mathcal{C}_+ {}^c \bar{A}_{-\eta_C, -\eta_T}^{\eta_C \epsilon_C \epsilon_U} \\ &= \mathcal{T}_- {}^g A_{\eta_C, \eta_T}^{\eta_T \epsilon_T \epsilon_U} = i \mathcal{T}_- {}^g A_{-\eta_C, -\eta_T}^{\eta_T \epsilon_T \epsilon_U}, \end{aligned} \quad (32)$$

where the first (second) subscript indicates the commutation relationship between spatial symmetries and  $\text{TRS}^\dagger$  ( $\text{PHS}^\dagger$ ).

By going over all possible combinations of  $\epsilon_U, \eta_T, \eta_C$ , we summarize the equivalent symmetries in Table V. Similar to real  $AZ$  classes,  $\Sigma$  would unify certain spatial symmetries for  $AZ^\dagger$  class. The procedure to classify them is the same as  $AZ$  class. We label them by  $t_0, t_1, t_2, t_3$  at the end of circular bracket in Table V.

In Appendix B, we show the following  $K$  group relationship for  $AZ^\dagger$  classes with spatial symmetries

$$\begin{aligned} K_{\mathbb{R}}^{\dagger U/A}(s^\dagger, t; d, d_{\parallel}, D, D_{\parallel}) \\ = K_{\mathbb{R}}^{\dagger U/A}(s^\dagger - d + D, t + d_{\parallel} - D_{\parallel}; 0, 0, 0, 0), \end{aligned} \quad (33)$$

where the superscript  $U/A$  indicates this relationship works for both unitary and antiunitary spatial symmetries. Furthermore,

$$\begin{aligned} K_{\mathbb{R}}^{\dagger U/A}(s^\dagger, t=0) &= \pi_0(\mathcal{R}_{s^\dagger}) \times \pi_0(\mathcal{R}_{s^\dagger}) \\ K_{\mathbb{R}}^{\dagger U/A}(s^\dagger, t=1) &= \pi_0(\mathcal{R}_{s^\dagger-1}) \\ K_{\mathbb{R}}^{\dagger U/A}(s^\dagger, t=2) &= \pi_0(\mathcal{C}_{s^\dagger}) \\ K_{\mathbb{R}}^{\dagger U/A}(s^\dagger, t=3) &= \pi_0(\mathcal{R}_{s^\dagger+1}), \end{aligned} \quad (34)$$

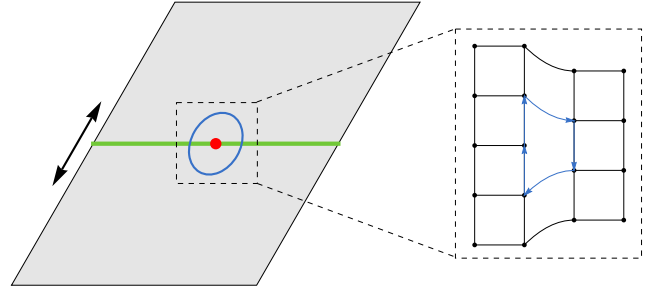


FIG. 3: Point defect with reflection symmetry in  $y$  direction. Red dot indicates the location of the defect. Blue circle is the  $S^1$  sphere that surrounds the defect. Green line is the reflection symmetry line i.e. the lattice is reflection symmetric with respect to the green line. In this case, Burgers vector  $\mathbf{B} = \hat{y}$  which is shown by an additional upwards arrow after completing a loop surround the defect.

which we show in Appendix D using Clifford Algebra. For both Eqs,  $s^\dagger$  is defined mod8 while  $t$  is defined mod4

#### V. PERIODIC TABLE OF SPATIAL SYMMETRIES FOR POINT-GAPPED HAMILTONIAN

Having introduced the  $K$  group of  $AZ$  and  $AZ^\dagger$  class in the presence of spatial symmetries, we are now ready to present their periodic table under spatial symmetries.

Each  $AZ$  ( $AZ^\dagger$ ) class is labeled by  $s$  ( $s^\dagger$ ). The dimensional hierarchy for these parameters is controlled by the difference between spatial dimensions  $d$  and the dimension  $D$  of the  $D$ -sphere that surrounds the defects:  $\delta = d - D$ . The periodic table is given by ranging  $\delta$  from 0 to 7 for each class (See Table I). In the previous section, for each class, we give them a finer labeling  $t$  in the presence of spatial symmetries, where  $t$  is defined mod 2 for A and AIII or mod 4 for the rest of the classes. As we can see from  $K$  group relationship we introduce at the end of each sub-section [Eqs. (21), (28), and (33)], the dimensional hierarchy for  $t$  is controlled by  $\delta_{\parallel} = d_{\parallel} - D_{\parallel}$ , where  $d_{\parallel}$  ( $D_{\parallel}$ ) is the number of spatial dimension (dimension of  $D$ -sphere that surrounds the defect) that is being flipped under spatial symmetry. In the following, we introduce periodic tables by ranging  $\delta_{\parallel}$  from 0 to 3. This would give us four distinct tables. We summarize the result in table VI, VII, VIII, and IX for  $\delta_{\parallel} = 0, 1, 2, 3$ , respectively. In the following sections, we use specific examples to illustrate these topological invariants.

#### VI. EXAMPLES

In this section, we give several concrete examples of toy models that demonstrate how to use our periodic table introduced in the previous section. Before introducing

TABLE V: Possible order-two spatial symmetries for real  $AZ^\dagger$  classes. The superscript of the operators indicates sign the squared value of the operator ; The subscript indicates the commutation relationship between the spatial symmetry operators and  $\text{TRS}^\dagger \mathcal{C}_+$  or  $\text{PHS}^\dagger \mathcal{T}_-$ : + for commutation and - for anti-commutation. If both  $\text{TRS}^\dagger$  and  $\text{PHS}^\dagger$  are present, the first (second) subscript indicates the commutation relationship between the spatial symmetry operator and  $\text{TRS}^\dagger$  ( $\text{PHS}^\dagger$ ). Symmetries inside the same circular bracket are equivalent. For each  $AZ^\dagger$  class, spatial symmetries that are related by  $\Sigma$  symmetry (9) are labeled by the  $t_n, n \in \{0, 1, 2, 3\}$  at the end of the circular bracket.

$s^\dagger AZ^\dagger$ class					
7	AI $^\dagger$	$({}^g U_+^+, {}^g U_-^-)t_1$	$({}^g \bar{U}_+^-, {}^g \bar{U}_-^+)t_3$	$({}^g U_-^+, {}^g U_+^-)t_3$	$({}^g \bar{U}_+^+, {}^g \bar{U}_-^-)t_1$
		$({}^c A_+^+, {}^c A_-^-)$	$({}^c \bar{A}_+^-, {}^c \bar{A}_-^+)$	$({}^c A_-^+, {}^c A_+^-)$	$({}^c \bar{A}_+^+, {}^c \bar{A}_-^-)$
0	BDI $^\dagger$	$({}^g U_{++}^+, {}^g U_{--}^-, {}^g \bar{U}_{++}^+, {}^g \bar{U}_{--}^-)t_1$	$({}^g U_{+-}^+, {}^g U_{-+}^-, {}^g \bar{U}_{+-}^+, {}^g \bar{U}_{-+}^-)t_0$	$({}^g U_{+-}^+, {}^g U_{++}^-, {}^g \bar{U}_{--}^+, {}^g \bar{U}_{++}^-)t_3$	$({}^g U_{++}^+, {}^g U_{+-}^-, {}^g \bar{U}_{+-}^+, {}^g \bar{U}_{++}^-)t_2$
		$({}^c A_{++}^+, {}^c A_{--}^-, {}^c \bar{A}_{++}^+, {}^c \bar{A}_{--}^-)$	$({}^c A_{+-}^+, {}^c A_{-+}^-, {}^c \bar{A}_{+-}^+, {}^c \bar{A}_{-+}^-)$	$({}^c A_{+-}^+, {}^c A_{++}^-, {}^c \bar{A}_{--}^+, {}^c \bar{A}_{++}^-)$	$({}^c A_{++}^+, {}^c A_{+-}^-, {}^c \bar{A}_{+-}^+, {}^c \bar{A}_{++}^-)$
1	D $^\dagger$	$({}^g U_+^+, {}^g U_-^-)t_1$	$({}^g \bar{U}_+^+, {}^g \bar{U}_-^-)t_3$	$({}^g U_-^+, {}^g U_+^-)t_3$	$({}^g \bar{U}_+^+, {}^g \bar{U}_-^-)t_1$
		$({}^c U_+^+, {}^c U_-^-)t_0$	$({}^c \bar{U}_+^+, {}^c \bar{U}_-^-)t_0$	$({}^c U_-^+, {}^c U_+^-)t_2$	$({}^c \bar{U}_+^+, {}^c \bar{U}_-^-)t_2$
2	DIII $^\dagger$	$({}^g U_{++}^+, {}^g U_{--}^-, {}^g \bar{U}_{++}^+, {}^g \bar{U}_{--}^-)t_1$	$({}^g U_{+-}^+, {}^g U_{-+}^-, {}^g \bar{U}_{+-}^+, {}^g \bar{U}_{-+}^-)t_0$	$({}^g U_{+-}^+, {}^g U_{++}^-, {}^g \bar{U}_{--}^+, {}^g \bar{U}_{++}^-)t_3$	$({}^g U_{++}^+, {}^g U_{+-}^-, {}^g \bar{U}_{+-}^+, {}^g \bar{U}_{++}^-)t_2$
		$({}^c A_{++}^+, {}^c A_{--}^-, {}^c \bar{A}_{++}^+, {}^c \bar{A}_{--}^-)$	$({}^c A_{+-}^+, {}^c A_{-+}^-, {}^c \bar{A}_{+-}^+, {}^c \bar{A}_{-+}^-)$	$({}^c A_{+-}^+, {}^c A_{++}^-, {}^c \bar{A}_{--}^+, {}^c \bar{A}_{++}^-)$	$({}^c A_{++}^+, {}^c A_{+-}^-, {}^c \bar{A}_{+-}^+, {}^c \bar{A}_{++}^-)$
3	AII $^\dagger$	$({}^g U_+^+, {}^g U_-^-)t_1$	$({}^g \bar{U}_+^+, {}^g \bar{U}_-^-)t_3$	$({}^g U_-^+, {}^g U_+^-)t_3$	$({}^g \bar{U}_+^+, {}^g \bar{U}_-^-)t_1$
		$({}^c U_+^+, {}^c U_-^-)t_0$	$({}^c \bar{U}_+^+, {}^c \bar{U}_-^-)t_0$	$({}^c U_-^+, {}^c U_+^-)t_2$	$({}^c \bar{U}_+^+, {}^c \bar{U}_-^-)t_2$
4	CIII $^\dagger$	$({}^g U_{++}^+, {}^g U_{--}^-, {}^g \bar{U}_{++}^+, {}^g \bar{U}_{--}^-)t_1$	$({}^g U_{+-}^+, {}^g U_{-+}^-, {}^g \bar{U}_{+-}^+, {}^g \bar{U}_{-+}^-)t_0$	$({}^g U_{+-}^+, {}^g U_{++}^-, {}^g \bar{U}_{--}^+, {}^g \bar{U}_{++}^-)t_3$	$({}^g U_{++}^+, {}^g U_{+-}^-, {}^g \bar{U}_{+-}^+, {}^g \bar{U}_{++}^-)t_2$
		$({}^c A_{++}^+, {}^c A_{--}^-, {}^c \bar{A}_{++}^+, {}^c \bar{A}_{--}^-)$	$({}^c A_{+-}^+, {}^c A_{-+}^-, {}^c \bar{A}_{+-}^+, {}^c \bar{A}_{-+}^-)$	$({}^c A_{+-}^+, {}^c A_{++}^-, {}^c \bar{A}_{--}^+, {}^c \bar{A}_{++}^-)$	$({}^c A_{++}^+, {}^c A_{+-}^-, {}^c \bar{A}_{+-}^+, {}^c \bar{A}_{++}^-)$
5	CI $^\dagger$	$({}^g U_+^+, {}^g U_-^-)t_1$	$({}^g \bar{U}_+^+, {}^g \bar{U}_-^-)t_3$	$({}^g U_-^+, {}^g U_+^-)t_3$	$({}^g \bar{U}_+^+, {}^g \bar{U}_-^-)t_1$
		$({}^c U_+^+, {}^c U_-^-)t_0$	$({}^c \bar{U}_+^+, {}^c \bar{U}_-^-)t_0$	$({}^c U_-^+, {}^c U_+^-)t_2$	$({}^c \bar{U}_+^+, {}^c \bar{U}_-^-)t_2$
6	CII $^\dagger$	$({}^g U_{++}^+, {}^g U_{--}^-, {}^g \bar{U}_{++}^+, {}^g \bar{U}_{--}^-)t_1$	$({}^g U_{+-}^+, {}^g U_{-+}^-, {}^g \bar{U}_{+-}^+, {}^g \bar{U}_{-+}^-)t_0$	$({}^g U_{+-}^+, {}^g U_{++}^-, {}^g \bar{U}_{--}^+, {}^g \bar{U}_{++}^-)t_3$	$({}^g U_{++}^+, {}^g U_{+-}^-, {}^g \bar{U}_{+-}^+, {}^g \bar{U}_{++}^-)t_2$
		$({}^c A_{++}^+, {}^c A_{--}^-, {}^c \bar{A}_{++}^+, {}^c \bar{A}_{--}^-)$	$({}^c A_{+-}^+, {}^c A_{-+}^-, {}^c \bar{A}_{+-}^+, {}^c \bar{A}_{-+}^-)$	$({}^c A_{+-}^+, {}^c A_{++}^-, {}^c \bar{A}_{--}^+, {}^c \bar{A}_{++}^-)$	$({}^c A_{++}^+, {}^c A_{+-}^-, {}^c \bar{A}_{+-}^+, {}^c \bar{A}_{++}^-)$

concrete models, we first discuss several preliminary considerations.

To simplify our discussion and also to be aligned with current interest within the field of non-Hermitian defects, we focus on the case of point defect in 2D [Fig. 3 (a)] protected by reflection symmetry. In this case,  $\delta_{\parallel} = 0$  and the periodic table is table VI. Without loss of generality, we assume the model obeys reflection symmetry in  $y$  direction. For a complete enumeration of defects for different  $\delta_{\parallel} = 0$ , see Ref. [12].

Physically, a point defect on lattice is obtained by removing a site and reintroducing hopping for sites after the defect (Fig. 3 (b)). For a point-gapped non-Hermitian system in 2D, point defect is known to gener-

ate skin effects, which is referred to as dislocation non-Hermitian skin effect in previous works [33–35]. We see that, by this construction of point defects, the circle surrounds the point would give us a Burgers vector  $\mathbf{B} = \hat{y}$ . In order to preserve periodic boundary condition (PBC), another defect with burgers vector pointing in the opposite direction must be introduced at the other end hoppings chains that are reintroduced. Since the defect is probing the topological property of sub-manifold  $\mathbf{B} \cdot \mathbf{k} \bmod 2\pi = \pi$ , we see that for  $\mathbf{B} = \hat{y}$ , the topological property of the defect is given by the sub-manifold  $k_y = \pi$ .

Finally, to give a sharp contrast between models with and without reflection symmetries, we are investigating the reflection-symmetry-protected phases. By comparing

TABLE VI: Periodic table for  $\delta_{||} = 0$ .

Symmetry	Class	Classifying space	$\delta = 0$	1	2	3	4	5	6	7
$t_1$	A	$\mathcal{C}_1 \times \mathcal{C}_1$	0	$\mathbb{Z} \oplus \mathbb{Z}$	0	$\mathbb{Z} \oplus \mathbb{Z}$	0	$\mathbb{Z} \oplus \mathbb{Z}$	0	$\mathbb{Z} \oplus \mathbb{Z}$
	AIII	$\mathcal{C}_0 \times \mathcal{C}_0$	$\mathbb{Z} \oplus \mathbb{Z}$	0	$\mathbb{Z} \oplus \mathbb{Z}$	0	$\mathbb{Z} \oplus \mathbb{Z}$	0	$\mathbb{Z} \oplus \mathbb{Z}$	0
$t_1$	A	$\mathcal{C}_0$	$\mathbb{Z}$	0	$\mathbb{Z}$	0	$\mathbb{Z}$	0	$\mathbb{Z}$	0
	AIII	$\mathcal{C}_1$	0	$\mathbb{Z}$	0	$\mathbb{Z}$	0	$\mathbb{Z}$	0	$\mathbb{Z}$
$t_0$	AI, D $^\dagger$	$\mathcal{R}_1 \times \mathcal{R}_1$	$\mathbb{Z}_2 \oplus \mathbb{Z}_2$	$\mathbb{Z} \oplus \mathbb{Z}$	0	0	0	$2\mathbb{Z} \oplus 2\mathbb{Z}$	0	$\mathbb{Z}_2 \oplus \mathbb{Z}_2$
	BDI, DIII $^\dagger$	$\mathcal{R}_2 \times \mathcal{R}_2$	$\mathbb{Z}_2 \oplus \mathbb{Z}_2$	$\mathbb{Z}_2 \oplus \mathbb{Z}_2$	$\mathbb{Z} \oplus \mathbb{Z}$	0	0	0	$2\mathbb{Z} \oplus 2\mathbb{Z}$	0
	D, AII $^\dagger$	$\mathcal{R}_3 \times \mathcal{R}_3$	0	$\mathbb{Z}_2 \oplus \mathbb{Z}_2$	$\mathbb{Z}_2 \oplus \mathbb{Z}_2$	$\mathbb{Z} \oplus \mathbb{Z}$	0	0	0	$2\mathbb{Z} \oplus 2\mathbb{Z}$
	DIII, CII $^\dagger$	$\mathcal{R}_4 \times \mathcal{R}_4$	$2\mathbb{Z} \oplus 2\mathbb{Z}$	0	$\mathbb{Z}_2 \oplus \mathbb{Z}_2$	$\mathbb{Z}_2 \oplus \mathbb{Z}_2$	$\mathbb{Z} \oplus \mathbb{Z}$	0	0	0
	AII, C $^\dagger$	$\mathcal{R}_5 \times \mathcal{R}_5$	0	$2\mathbb{Z} \oplus 2\mathbb{Z}$	0	$\mathbb{Z}_2 \oplus \mathbb{Z}_2$	$\mathbb{Z}_2 \oplus \mathbb{Z}_2$	$\mathbb{Z} \oplus \mathbb{Z}$	0	0
	CII, CI $^\dagger$	$\mathcal{R}_6 \times \mathcal{R}_6$	0	0	$2\mathbb{Z} \oplus 2\mathbb{Z}$	0	$\mathbb{Z}_2 \oplus \mathbb{Z}_2$	$\mathbb{Z}_2 \oplus \mathbb{Z}_2$	$\mathbb{Z} \oplus \mathbb{Z}$	0
	C, AI $^\dagger$	$\mathcal{R}_7 \times \mathcal{R}_7$	0	0	0	$2\mathbb{Z} \oplus 2\mathbb{Z}$	0	$\mathbb{Z}_2 \oplus \mathbb{Z}_2$	$\mathbb{Z}_2 \oplus \mathbb{Z}_2$	$\mathbb{Z} \oplus \mathbb{Z}$
	CI, BDI $^\dagger$	$\mathcal{R}_0 \times \mathcal{R}_0$	$\mathbb{Z} \oplus \mathbb{Z}$	0	0	0	$2\mathbb{Z} \oplus 2\mathbb{Z}$	0	$\mathbb{Z}_2 \oplus \mathbb{Z}_2$	$\mathbb{Z}_2 \oplus \mathbb{Z}_2$
	$t_1$	AI, AI $^\dagger$	$\mathcal{R}_0$	$\mathbb{Z}$	0	0	0	$2\mathbb{Z}$	0	$\mathbb{Z}_2$
BDI, BDI $^\dagger$		$\mathcal{R}_1$	$\mathbb{Z}_2$	$\mathbb{Z}$	0	0	0	$2\mathbb{Z}$	0	$\mathbb{Z}_2$
D, D $^\dagger$		$\mathcal{R}_2$	$\mathbb{Z}_2$	$\mathbb{Z}_2$	$\mathbb{Z}$	0	0	0	$2\mathbb{Z}$	0
DIII, DIII $^\dagger$		$\mathcal{R}_3$	0	$\mathbb{Z}_2$	$\mathbb{Z}_2$	$\mathbb{Z}$	0	0	0	$2\mathbb{Z}$
AII, AII $^\dagger$		$\mathcal{R}_4$	$2\mathbb{Z}$	0	$\mathbb{Z}_2$	$\mathbb{Z}_2$	$\mathbb{Z}$	0	0	0
CII, CII $^\dagger$		$\mathcal{R}_5$	0	$2\mathbb{Z}$	0	$\mathbb{Z}_2$	$\mathbb{Z}_2$	$\mathbb{Z}$	0	0
C, C $^\dagger$		$\mathcal{R}_6$	0	0	$2\mathbb{Z}$	0	$\mathbb{Z}_2$	$\mathbb{Z}_2$	$\mathbb{Z}$	0
CI, CI $^\dagger$		$\mathcal{R}_7$	0	0	0	$2\mathbb{Z}$	0	$\mathbb{Z}_2$	$\mathbb{Z}_2$	$\mathbb{Z}$
$t_2$	AI, D, AII, C, AI $^\dagger$ , D $^\dagger$ , AII $^\dagger$ , C $^\dagger$	$\mathcal{C}_1$	0	$\mathbb{Z}$	0	$\mathbb{Z}$	0	$\mathbb{Z}$	0	$\mathbb{Z}$
	BDI, DIII, CII, CI, BDI $^\dagger$ , DIII $^\dagger$ , CII $^\dagger$ , CI $^\dagger$	$\mathcal{C}_0$	$\mathbb{Z}$	0	$\mathbb{Z}$	0	$\mathbb{Z}$	0	$\mathbb{Z}$	0
$t_3$	AI, AII $^\dagger$	$\mathcal{R}_2$	$\mathbb{Z}_2$	$\mathbb{Z}_2$	$\mathbb{Z}$	0	0	0	$2\mathbb{Z}$	0
	BDI, CII $^\dagger$	$\mathcal{R}_3$	0	$\mathbb{Z}_2$	$\mathbb{Z}_2$	$\mathbb{Z}$	0	0	0	$2\mathbb{Z}$
	D, C $^\dagger$	$\mathcal{R}_4$	$2\mathbb{Z}$	0	$\mathbb{Z}_2$	$\mathbb{Z}_2$	$\mathbb{Z}$	0	0	0
	DIII, CI $^\dagger$	$\mathcal{R}_5$	0	$2\mathbb{Z}$	0	$\mathbb{Z}_2$	$\mathbb{Z}_2$	$\mathbb{Z}$	0	0
	AII, AI $^\dagger$	$\mathcal{R}_6$	0	0	$2\mathbb{Z}$	0	$\mathbb{Z}_2$	$\mathbb{Z}_2$	$\mathbb{Z}$	0
	CII, BDI $^\dagger$	$\mathcal{R}_7$	0	0	0	$2\mathbb{Z}$	0	$\mathbb{Z}_2$	$\mathbb{Z}_2$	$\mathbb{Z}$
	C, D $^\dagger$	$\mathcal{R}_0$	$\mathbb{Z}$	0	0	0	$2\mathbb{Z}$	0	$\mathbb{Z}_2$	$\mathbb{Z}_2$
CI, DIII $^\dagger$	$\mathcal{R}_1$	$\mathbb{Z}_2$	$\mathbb{Z}$	0	0	0	$2\mathbb{Z}$	0	$\mathbb{Z}_2$	

table VI and I, we see that class AI $^\dagger$  with  $t_2$  class symmetry and class C with  $t_2$  class symmetry are protected by the extra spatial symmetry with invariant  $\mathbb{Z}$ ; Class DIII with  $t_1$  class symmetry is also protected by the extra spatial symmetry with a  $\mathbb{Z}_2$  invariant. If we break the relevant spatial symmetry (reflection in this case), the topological invariant will vanish since their original classification in Table I is trivial. By doing so, there are two possible ways the system will change: (i) the modes that are originally localized around the defect will be delocalized, or (ii) a line gap will open, in which case the topological property is governed by line gap instead of point gap. In this sense, the defects mode for point-gapped spectrum is protected by the reflection symmetry. On the other hand, for class D $^\dagger$  with  $t_2$  class symmetry, if the spatial symmetry is broken, we expect the defect mode and point gap remain the same since D $^\dagger$  has a  $\mathbb{Z}$  invariant for  $\delta = 1$  without spatial symmetry. In this case, the reflection symmetry does not protect the point gap or the defect modes.

In the following, we introduce four models in  $\delta_{||} = 0$  (Table VI) that would realize scenarios that we described above. They belong to class AI $^\dagger$ , C, and D $^\dagger$  with  $t_2$  class reflection symmetry, and class DIII with  $t_1$  class symmetry.

### A. Point defect in AI $^\dagger$ protected by reflection symmetry ${}^cU_-^\dagger$

We build a two-dimensional AI $^\dagger$  model that obeys reflection symmetry of the type  ${}^cU_-^\dagger$ . Following the construction of  $\mathbb{Z}_2$  NHSE model [23], we stack an HN model with its AI $^\dagger$  pair in  $x$  direction with symmetry-preserving coupling in  $y$  direction. The resulting model is

$$\begin{aligned}
h_{\text{AI}^\dagger}(k_x, k_y) &= \begin{pmatrix} h_{\text{HN}}(k_x) & \Delta_1(k_y) \\ \Delta_2(k_y) & h_{\text{HN}}^T(-k_x) \end{pmatrix} \\
&= t\sigma_0\tau_x \\
&+ \frac{1}{2}(\sigma_0\tau_x - i\sigma_z\tau_y)g_1 \cos k_x - \frac{i}{2}(\sigma_z\tau_x - i\sigma_0\tau_y)g_1 \sin k_x \\
&+ \frac{1}{2}(\sigma_0\tau_x + i\sigma_z\tau_y)g_2 \cos k_x + \frac{i}{2}(\sigma_z\tau_x + i\sigma_0\tau_y)g_2 \sin k_x \\
&- \frac{i}{2}(\sigma_x - i\sigma_y)\tau_y\mu_1 \sin k_y - \frac{i}{2}(\sigma_x + i\sigma_y)\tau_y\mu_2 \sin k_y,
\end{aligned} \tag{35}$$

where  $h_{\text{HN}}(k_x)$  is the two-band HN model

$$h_{\text{HN}}(k_x) = \begin{pmatrix} 0 & t + g_2 \exp(ik_x) \\ t + g_1 \exp(ik_x) & 0 \end{pmatrix}. \tag{36}$$

$\Delta_{1(2)}(k_y) = -\frac{i}{2}(\sigma_x \mp i\sigma_y)\tau_y\mu_{1(2)} \sin k_y$  is the symmetry-preserving coupling in  $y$  direction.  $t, g_1, g_2, \mu_1, \mu_2$  are all



TABLE IX: Periodic table for  $\delta_{||} = 3$ .

Symmetry	Class	Classifying space	$\delta = 0$	1	2	3	4	5	6	7
AZ: $t_0$ AZ $^\dagger$ : $t_0$	AI, $D^\dagger$	$\mathcal{R}_0$	$\mathbb{Z}$	0	0	0	$2\mathbb{Z}$	0	$\mathbb{Z}_2$	$\mathbb{Z}_2$
	BDI,DIII $^\dagger$	$\mathcal{R}_1$	$\mathbb{Z}_2$	$\mathbb{Z}$	0	0	0	$2\mathbb{Z}$	0	$\mathbb{Z}_2$
	D,AII $^\dagger$	$\mathcal{R}_2$	$\mathbb{Z}_2$	$\mathbb{Z}_2$	$\mathbb{Z}$	0	0	0	$2\mathbb{Z}$	0
	DIII,CI $^\dagger$	$\mathcal{R}_3$	0	$\mathbb{Z}_2$	$\mathbb{Z}_2$	$\mathbb{Z}$	0	0	0	$2\mathbb{Z}$
	AII, $C^\dagger$	$\mathcal{R}_4$	$2\mathbb{Z}$	0	$\mathbb{Z}_2$	$\mathbb{Z}_2$	$\mathbb{Z}$	0	0	0
	CII,CI $^\dagger$	$\mathcal{R}_5$	0	$2\mathbb{Z}$	0	$\mathbb{Z}_2$	$\mathbb{Z}_2$	$\mathbb{Z}$	0	0
	C,AI $^\dagger$	$\mathcal{R}_6$	0	0	$2\mathbb{Z}$	0	$\mathbb{Z}_2$	$\mathbb{Z}_2$	$\mathbb{Z}$	0
	CI,BDI $^\dagger$	$\mathcal{R}_7$	0	0	0	$2\mathbb{Z}$	0	$\mathbb{Z}_2$	$\mathbb{Z}_2$	$\mathbb{Z}$
AZ: $t_1$	AI,D,AII,C,AI $^\dagger$ , $D^\dagger$ ,AII $^\dagger$ , $C^\dagger$	$\mathcal{C}_1$	0	$\mathbb{Z}$	0	$\mathbb{Z}$	0	$\mathbb{Z}$	0	$\mathbb{Z}$
AZ $^\dagger$ : $t_3$	BDI,DIII,CII,CI,BDI $^\dagger$ ,DIII $^\dagger$ ,CI $^\dagger$ ,CI $^\dagger$	$\mathcal{C}_0$	$\mathbb{Z}$	0	$\mathbb{Z}$	0	$\mathbb{Z}$	0	$\mathbb{Z}$	0
AZ: $t_2$ AZ $^\dagger$ : $t_2$	AI, $D^\dagger$	$\mathcal{R}_2$	$\mathbb{Z}_2$	$\mathbb{Z}_2$	$\mathbb{Z}$	0	0	0	$2\mathbb{Z}$	0
	BDI,DIII $^\dagger$	$\mathcal{R}_3$	0	$\mathbb{Z}_2$	$\mathbb{Z}_2$	$\mathbb{Z}$	0	0	0	$2\mathbb{Z}$
	D,AII $^\dagger$	$\mathcal{R}_4$	$2\mathbb{Z}$	0	$\mathbb{Z}_2$	$\mathbb{Z}_2$	$\mathbb{Z}$	0	0	0
	DIII,CI $^\dagger$	$\mathcal{R}_5$	0	$2\mathbb{Z}$	0	$\mathbb{Z}_2$	$\mathbb{Z}_2$	$\mathbb{Z}$	0	0
	AII, $C^\dagger$	$\mathcal{R}_6$	0	0	$2\mathbb{Z}$	0	$\mathbb{Z}_2$	$\mathbb{Z}_2$	$\mathbb{Z}$	0
	CII,CI $^\dagger$	$\mathcal{R}_7$	0	0	0	$2\mathbb{Z}$	0	$\mathbb{Z}_2$	$\mathbb{Z}_2$	$\mathbb{Z}$
	C,AI $^\dagger$	$\mathcal{R}_0$	$\mathbb{Z}$	0	0	0	$2\mathbb{Z}$	0	$\mathbb{Z}_2$	$\mathbb{Z}_2$
	CI,BDI $^\dagger$	$\mathcal{R}_1$	$\mathbb{Z}_2$	$\mathbb{Z}$	0	0	0	$2\mathbb{Z}$	0	$\mathbb{Z}_2$
AZ: $t_3$ AZ $^\dagger$ : $t_1$	AI, $D^\dagger$	$\mathcal{R}_1 \times \mathcal{R}_1$	$\mathbb{Z}_2 \oplus \mathbb{Z}_2$	$\mathbb{Z} \oplus \mathbb{Z}$	0	0	0	$2\mathbb{Z} \oplus 2\mathbb{Z}$	0	$\mathbb{Z}_2 \oplus \mathbb{Z}_2$
	BDI,DIII $^\dagger$	$\mathcal{R}_2 \times \mathcal{R}_2$	$\mathbb{Z}_2 \oplus \mathbb{Z}_2$	$\mathbb{Z}_2 \oplus \mathbb{Z}_2$	$\mathbb{Z} \oplus \mathbb{Z}$	0	0	0	$2\mathbb{Z} \oplus 2\mathbb{Z}$	0
	D,AII $^\dagger$	$\mathcal{R}_3 \times \mathcal{R}_3$	0	$\mathbb{Z}_2 \oplus \mathbb{Z}_2$	$\mathbb{Z}_2 \oplus \mathbb{Z}_2$	$\mathbb{Z} \oplus \mathbb{Z}$	0	0	0	$2\mathbb{Z} \oplus 2\mathbb{Z}$
	DIII,CI $^\dagger$	$\mathcal{R}_4 \times \mathcal{R}_4$	$2\mathbb{Z} \oplus 2\mathbb{Z}$	0	$\mathbb{Z}_2 \oplus \mathbb{Z}_2$	$\mathbb{Z}_2 \oplus \mathbb{Z}_2$	$\mathbb{Z} \oplus \mathbb{Z}$	0	0	0
	AII, $C^\dagger$	$\mathcal{R}_5 \times \mathcal{R}_5$	0	$2\mathbb{Z} \oplus 2\mathbb{Z}$	0	$\mathbb{Z}_2 \oplus \mathbb{Z}_2$	$\mathbb{Z}_2 \oplus \mathbb{Z}_2$	$\mathbb{Z} \oplus \mathbb{Z}$	0	0
	CII,CI $^\dagger$	$\mathcal{R}_6 \times \mathcal{R}_6$	0	0	$2\mathbb{Z} \oplus 2\mathbb{Z}$	0	$\mathbb{Z}_2 \oplus \mathbb{Z}_2$	$\mathbb{Z}_2 \oplus \mathbb{Z}_2$	$\mathbb{Z} \oplus \mathbb{Z}$	0
	C,AI $^\dagger$	$\mathcal{R}_7 \times \mathcal{R}_7$	0	0	0	$2\mathbb{Z} \oplus 2\mathbb{Z}$	0	$\mathbb{Z}_2 \oplus \mathbb{Z}_2$	$\mathbb{Z}_2 \oplus \mathbb{Z}_2$	$\mathbb{Z} \oplus \mathbb{Z}$
	CI,BDI $^\dagger$	$\mathcal{R}_0 \times \mathcal{R}_0$	$\mathbb{Z} \oplus \mathbb{Z}$	0	0	0	$2\mathbb{Z} \oplus 2\mathbb{Z}$	0	$\mathbb{Z}_2 \oplus \mathbb{Z}_2$	$\mathbb{Z}_2 \oplus \mathbb{Z}_2$

real parameters. Model (35) obeys TRS $^\dagger$  with  $\mathcal{C}_+ = \sigma_x \tau_0 \mathcal{K}$ . It also obeys the reflection  ${}^c U_-^+ = \sigma_z \tau_0$  such that  ${}^c U_-^+ h_{\text{AI}^\dagger}(k_x, k_y) {}^c U_-^+ = h_{\text{AI}^\dagger}(k_x, -k_y)$ . According to the classification table V and VI, this model belongs to the subclass  $t_2$  of AI $^\dagger$ . In the case of 2D with a point defect such that  $\delta = 2 - 1 = 1$ , this topological phases has a  $\mathbb{Z}$  invariant which we will later show is given by the mirror winding number.

We plot the spectrum of model (35) in Fig. 4 (a) under full PBC. After introducing two defects for a HN chain in  $x$  direction, in-gap states that are localized at the defect appear [Fig. 4 (b) and (c)]. As mentioned at the beginning of the section, in this construction, the Burgers vector is given by  $\mathbf{B} = \pm \hat{y}$ , which is probing the topological property of the sub-manifold  $k_y = \pi$ . At  $k_y = \pi$ ,  $\Delta_1(\pi) = \Delta_2(\pi) = 0$ , Eq. (35) decoupled into two independent HN models with opposite winding numbers. We can diagonalize the resulting Hamiltonian into sectors that correspond to the eigenvalues  $\pm 1$  of  ${}^c U_-^+ = \sigma_z \tau_0$ . This was automatically done for model (35). We are now left with

$$h_{\text{AI}^\dagger}(k_x, \pi) = \begin{pmatrix} h_{\text{HN}}(k_x) & 0 \\ 0 & h_{\text{HN}}^T(-k_x) \end{pmatrix}. \quad (37)$$

For each sectors of the above Hamiltonian, we can define

a winding number

$$W_+ = \frac{1}{2\pi i} \int_{k_x=-\pi}^{k_x=\pi} dk_x \frac{d}{dk_x} \log \det h_{\text{HN}}(k_x)$$

$$W_- = \frac{1}{2\pi i} \int_{k_x=-\pi}^{k_x=\pi} dk_x \frac{d}{dk_x} \log \det h_{\text{HN}}^T(-k_x). \quad (38)$$

The  $\mathbb{Z}$  invariant is given by the *mirror winding number* [46]

$$W_m = \frac{W_+ - W_-}{2}. \quad (39)$$

For model (35), we have  $W_m = 1$  since  $W_\pm = \pm 1$ . In turn, this nontrivial mirror winding number gives rise to the localization of in-gap state around the defect. Notice that now the total winding number  $W_{\text{tot}} = W_+ + W_-$  vanishes. Since  $W_m$  is only well-defined under reflection symmetry while  $W_{\text{tot}}$  is always well-defined, we see that the topological phase of model (35) is protected by reflection symmetry. Mirror winding number is first proposed in Ref. [46] for NHSE protected by mirror symmetry (which is a different name of reflection symmetry). The mirror winding number is defined in a similar way as mirror Chern number [12].

The protection of reflection symmetry can also be seen by noticing that in the classification without reflection symmetry (Table I), class AI $^\dagger$  is trivial in the case  $\delta = 1$ . Therefore, by breaking reflection symmetry, we expect either the in-gap state to loss localization and become trivial or the system opens a line gap such that the

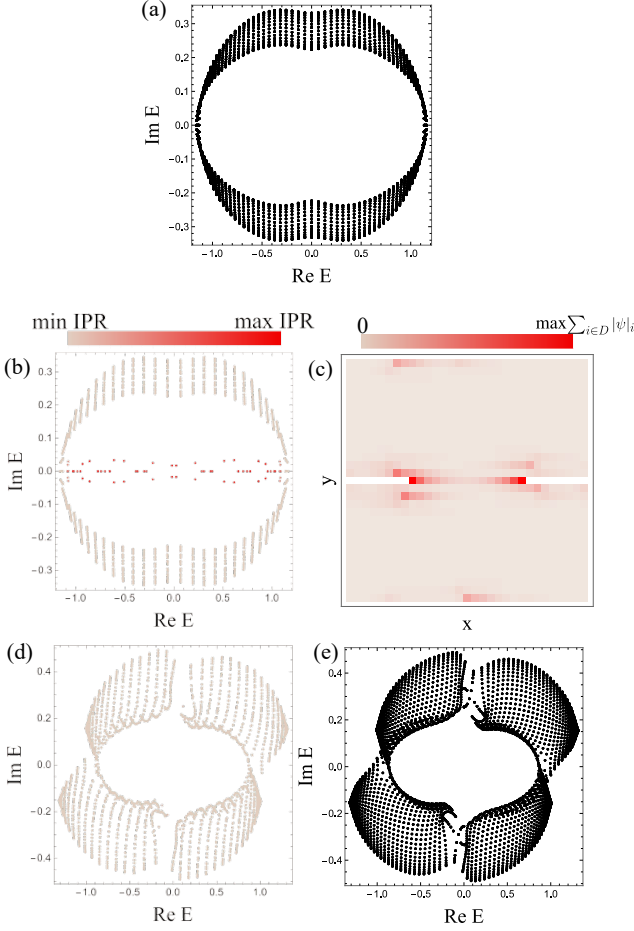


FIG. 4: Spectrum and eigenstates distribution of model (35). The parameters are set at  $t = 0.5$ ,  $g_1 = 0.4$ ,  $g_2 = 1$ ,  $\mu_1 = 0.3$ ,  $\mu_2 = 0.2$ . (a) Spectrum on complex plane plotted under full PBC. (b) Spectrum when two point defects are introduced in the  $x$  direction. In-gap states that are localized at the defect appear. (c) Distribution of in-gap in real space.  $D$  on the legend is referred to defect states inside the point gap [i.e. eigenstates of red dots in (b)]. White space indicates sites that are removed. (d), (e) Spectrum of (35) after introducing a reflection-symmetry-breaking perturbation  $0.15(1+i)\sigma_x\tau_0$  for (d) with two point defects, for which the in-gap states vanish, and (e) full PBC.

classification changes. To show this explicitly, we introduce a reflection-symmetry-breaking term  $\epsilon(1+i)\sigma_x\tau_0$ . As shown in Fig. 4 (d) and (e), the in-gap states vanish after the addition of a symmetry-breaking term for  $\epsilon = 0.15$ . Notice that for smaller  $\epsilon$ , the in-gap states still exist. However, by increasing the value of  $\epsilon$  the in-gap states would vanish *without* going through a phase transition. Thus, in-gap states after the addition of reflection-symmetry-breaking term are not topological and can be gapped out by continuous deformation.

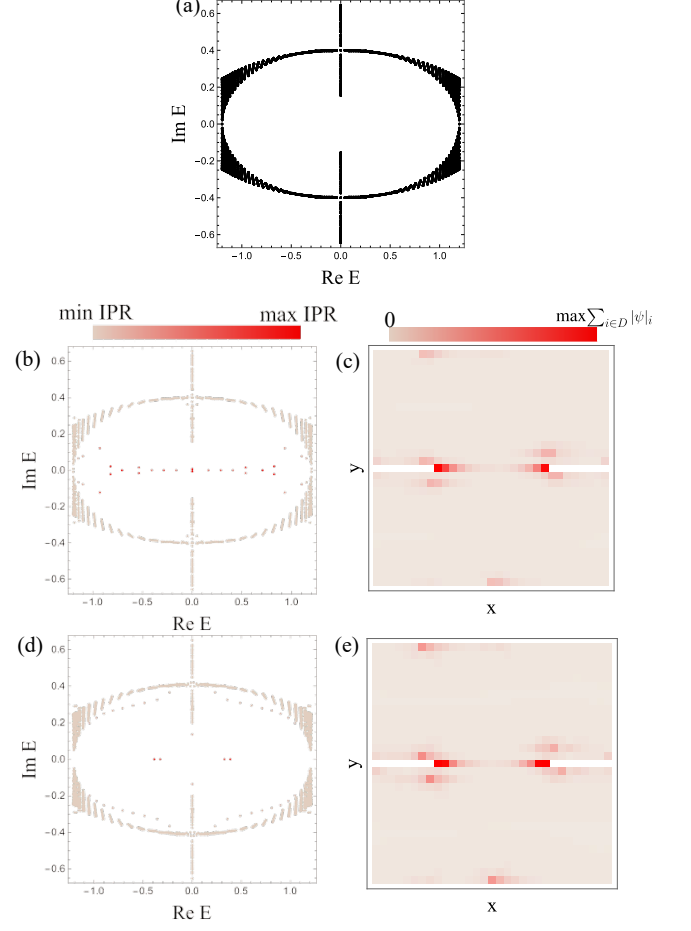


FIG. 5: Spectrum and eigenstates distribution of the model (40). Parameters are set at  $t = 0.5$ ,  $g_1 = 0.3$ ,  $g_2 = 1.3$ ,  $\mu_1 = 0.2$ ,  $\mu_2 = 0.3$ . (a)-(c) are the same contents as Fig. 4 but for model (40). (d) The spectrum of the model (40) after the addition of reflection-symmetry-breaking term  $0.12\sigma_y\tau_0$  with two point defects. (e) Distribution of in-gap states after the addition of reflection-symmetry-breaking term.

### B. Point defect in C protected by reflection symmetry ${}^cU_{-}^{+}$

To strengthen our findings, we now turn our attention to class C. Consider the model

$$\begin{aligned}
 h_C(k_x, k_y) &= \begin{pmatrix} h_{HN}(k_x) & \Delta_1(k_y) \\ \Delta_2(k_y) & -h_{HN}^T(-k_x) \end{pmatrix} \\
 &= -t\sigma_z\tau_X \\
 &+ \frac{1}{2}(\sigma_z\tau_x - i\sigma_0\tau_y)g_1 \cos k_x - \frac{i}{2}(\sigma_0\tau_x + i\sigma_z\tau_y)g_1 \sin k_x \\
 &+ \frac{1}{2}(\sigma_z\tau_x + i\sigma_0\tau_y)g_2 \cos k_x + \frac{i}{2}(\sigma_0\tau_x - i\sigma_z\tau_y)g_2 \sin k_x \\
 &- \frac{i}{2}(\sigma_x - i\sigma_y)\tau_y\mu_1 \sin k_y - \frac{i}{2}(\sigma_x + i\sigma_y)\tau_y\mu_2 \sin k_y,
 \end{aligned} \tag{40}$$

where  $h_{HN}$  is the two bands HN model defined in Eq. (36).  $\Delta_1$  and  $\Delta_2$  are the same as the previous section. This model obeys PHS with  $\mathcal{C}_- = i\sigma_y\tau_0\mathcal{K}$ . It also obeys reflection symmetry in  $y$  direction with  ${}^cU_-^+ = \sigma_z\tau_0$  such that  $\sigma_z h_C(k_x, k_y)\sigma_z = h_C(k_x, -k_y)$ . According to the classification Table IV and VI, this model belongs to class C with  $t_2$  symmetries, which possess a  $\mathbb{Z}$  invariant.

In the sub-manifold  $k_y = \pi$ , we have  $\Delta_1(\pi) = \Delta_2(\pi) = 0$ . Then we can define the winding number  $W_+$  ( $W_-$ ) for  $h_{HN}(k_x)$  ( $-h_{HN}^T(-k_x)$ ), which lives in the  $+1$  ( $-1$ ) sector of reflection symmetry operator  ${}^cU_-^+ = \sigma_z\tau_0$ . Notice that since  $h_{HN}$  is a 2 by 2 matrix,  $\det[-h_{HN}^T(-k_x)] = \det h_{HN}^T(-k_x)$ . Then we see that  $W_{\pm} = \pm 1$ . Hence, similar to model (35), mirror winding number (39)  $W_m = 1$  while the total winding number vanish. Thus, we see that the topological phase of model (40) is indeed protected by reflection symmetry.

We plot the spectrum of the model (40) in Fig. 5 (a) under full periodic boundary conditions (PBC). After the introduction of point defect, in-gap states that are localized around the defect begin to show (Fig. 5 (b) and (c)). Since the classification of class C without spatial symmetries is trivial in dimension  $\delta = 1$  (See Table I), model (40) is another example of reflection-symmetry protected topological phases. We now try to break reflection symmetry while preserving PHS by introducing an on-site perturbation  $0.12\sigma_y\tau_0$  to the Hamiltonian. The resulting spectrum and localization of in-gap states are shown in Fig. 5 (d) and (e). Notably, instead of vanishing defect-localized in-gap states like class  $AI^\dagger$ , an imaginary-line gap is now open. The classification is now given by line gaps instead of point gaps. In this sense, the reflection symmetry is protecting point gaps for model (40).

### C. Point defect in $D^\dagger$ with reflection symmetry ${}^cU_-^+$

Now we introduce a model that is not protected by reflection symmetry. First notice, for class  $D^\dagger$  in dimension  $\delta = 1$ , it has the same topological invariant  $\mathbb{Z}$  in the absence of spatial symmetry (Table I) and with spatial symmetry in  $t_2$  class (Table VI). We then consider the following model

$$\begin{aligned} h_{D^\dagger}(k_x, k_y) &= \begin{pmatrix} h_{HN}(k_x) & \Delta(k_y) \\ \Delta(k_y) & -h_{HN}^*(-k_x) \end{pmatrix} \\ &= t\sigma_z\tau_x \\ &+ \frac{1}{2}(\sigma_z\tau_x - i\sigma_z\tau_y)g_1 \cos k_x - \frac{i}{2}(\sigma_z\tau_x - i\sigma_z\tau_y)g_1 \sin k_x \\ &+ \frac{1}{2}(\sigma_z\tau_x + i\sigma_z\tau_y)g_2 \cos k_x + \frac{i}{2}(\sigma_z\tau_x + i\sigma_z\tau_y)g_2 \sin k_x \\ &- \frac{i}{2}(\sigma_x - i\sigma_y)\tau_y\mu \sin k_y - \frac{i}{2}(\sigma_x + i\sigma_y)\tau_y\mu \sin k_y, \end{aligned} \quad (41)$$

where  $h_{HN}$  is two-bands HN model defined in Eq. (36);  $\Delta(k_y) = -\frac{i}{2}\tau_y\mu \sin k_y$ . This model obeys PHS $^\dagger$  with  $\mathcal{T}_- = \sigma_x\tau_0\mathcal{K}$ . It also obeys the reflection symmetry in the  $y$  direction with operator  ${}^cU_-^+ = \sigma_z\tau_0$ .

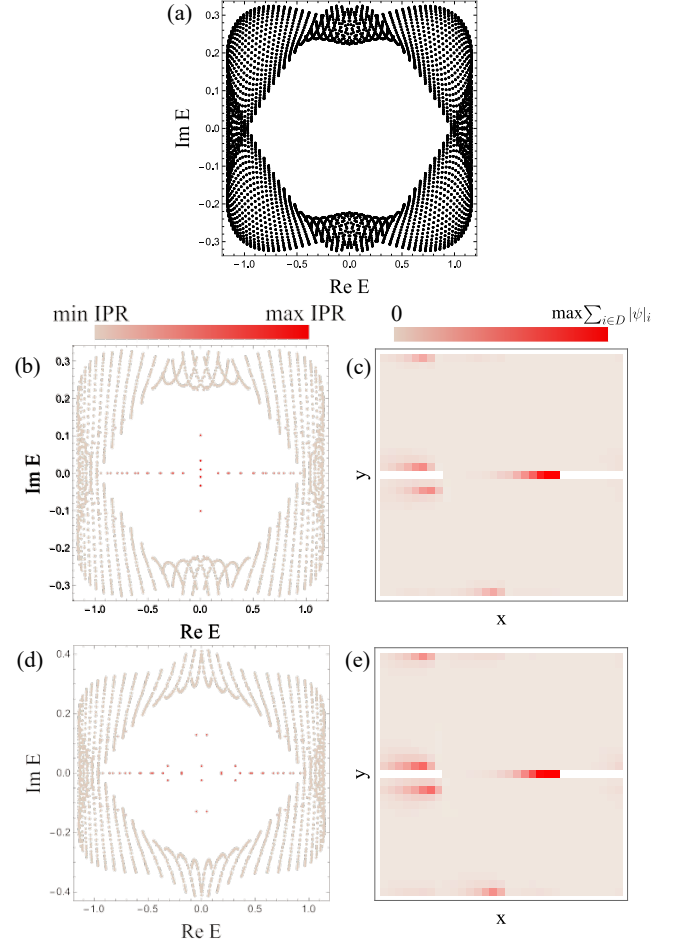


FIG. 6: Spectrum and eigenstates distribution of model (41). Parameters are set at  $t = 0.5$ ,  $g_1 = 0.4$ ,  $g_2 = 1$ ,  $\mu = 0.2$ . The contents of this plot are the same as Fig. 5.

Unlike previous models (35) and (40), for model (41),  $W_{\pm}$  defined on the sub-manifold  $k_y = \pi$  for  $h_{HN}(k_x)$  and  $-h_{HN}^*(-k_x)$  have the same sign. More specifically,  $W_+ = W_- = 1$ . Now, the mirror winding number (39) vanishes while the total winding number  $W_{\text{tot}} = W_+ + W_- = 2$  is nontrivial for  $k_y = \pi$ . This shows that the topological phase of model (41) is not protected by reflection symmetry.

We plot its spectrum under full PBC in Fig. 6 (a). Similar to the previous two models, we introduce defects with Burgers vector  $\mathbf{B} = \pm\hat{y}$ . After the introduction of defects, as shown in Fig. 6 (b) and (c), we see that in-gap states that are localized around the defect appears. We now consider a reflection-symmetry-breaking term  $0.2i\sigma_1\tau_0$  added to Hamiltonian. Since the topological invariant is not protected by reflection symmetry  ${}^cU_-^+ = \sigma_z\tau_0$ , we see that both point gap and localization of in-gap states are not affected by the introduction of additional term [Fig. 6 (d) and (e)].



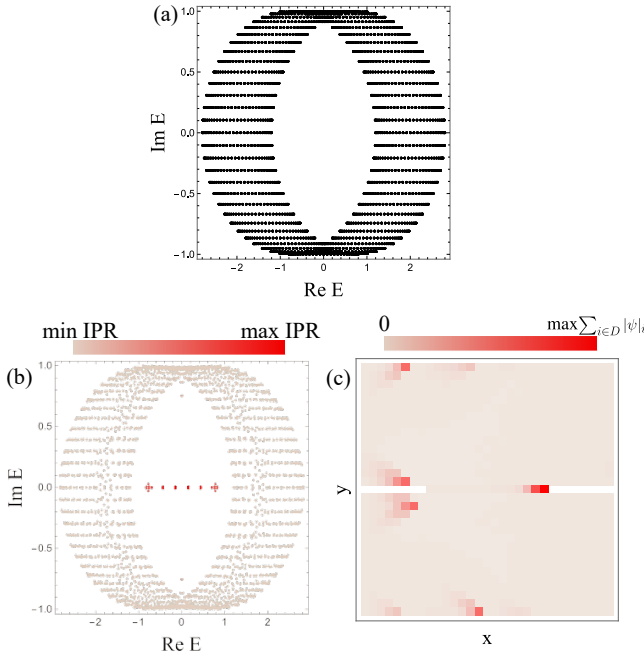


FIG. 7: Spectrum and eigenstates distribution of model (42) with point defects. Parameters are chosen at  $t = 0.5, g = 1.5, \mu_1 = 0.4, \mu_2 = 0.8$ . The contents of the plot are the same as Fig. 4-6 (a)-(c).

#### D. Point defect in DIII protected by reflection symmetry ${}^cU_{-+}^+$

Finally, we consider the following model

$$\begin{aligned}
 h_{DIII}(k_x, k_y) &= \begin{pmatrix} h_1(k_x) & \Delta(k_y) \\ \Delta(k_y) & h_1^*(-k_x) \end{pmatrix} \\
 &= \sigma_x \tau_0 \mu_2 \sin k_y + \frac{1}{2} \sigma_z (\tau_x + i\tau_y) \mu_1 \sin k_x \\
 &\quad + \sigma_0 \tau_z (g + t) \cos k_x + \sigma_0 \tau_0 i (g - t) \sin k_x, \quad (42)
 \end{aligned}$$

where  $\Delta(k_y) = \sigma_x \tau_0 \mu_2 \sin k_y$ ,  $h_1(k_x) = \frac{1}{2} (\tau_x + i\tau_y) \mu_1 \sin k_x + \tau_z (g + t) \cos k_x + \tau_0 i (g - t) \sin k_x$ . Model (42) obeys TRS with  $\mathcal{T}_+ = i\sigma_y \tau_0 \mathcal{K}$ , PHS with  $\mathcal{C}_- = \sigma_0 \tau_x \mathcal{K}$ , and reflection symmetry in  $y$  direction with  ${}^cU_{-+}^+ = \sigma_z \tau_0$ . Since  $\mathcal{T}_+^2 = -1$ ,  $\mathcal{C}_-^2 = 1$ , this places model (42) in class DIII with symmetry  $t_1$ . According to Table VI, the model (42) has a  $\mathbb{Z}_2$  invariant in the presence of a point defect. Furthermore, in the absence of spatial symmetries, class DIII has trivial classification for  $\delta = 1$  (Table I).

We plot its spectrum under full PBC in Fig. 7 (a). Upon the introduction of point defects, in-gap states localized at the defects begin to appear [Fig. 7 (b) and (c)]. In-gap states are protected by a  $\mathbb{Z}_2$  topological invariant. Notice that in the sub-manifold  $k_y = 0$ , reflection symmetry  ${}^cU_{-+}^+ = \sigma_z \tau_0$  ensures that the coupling term would vanish. To see this, we consider the most general 4 by 4

Hamiltonian

$$h_g(k_x, k_y) = \begin{pmatrix} h_+(k_x, k_y) & \Delta_1(k_x, k_y) \\ \Delta_2(k_x, k_y) & h_-(k_x, k_y) \end{pmatrix} \quad (43)$$

The reflection symmetry gives

$$\begin{aligned}
 \sigma_z \tau_0 h_g(k_x, k_y) \sigma_z \tau_0 &= \begin{pmatrix} h_+(k_x, k_y) & -\Delta_1(k_x, k_y) \\ -\Delta_2(k_x, k_y) & h_-(k_x, k_y) \end{pmatrix} \\
 &= \begin{pmatrix} h_+(k_x, -k_y) & \Delta_1(k_x, -k_y) \\ \Delta_2(k_x, -k_y) & h_-(k_x, -k_y) \end{pmatrix} = h_g(k_x, -k_y). \quad (44)
 \end{aligned}$$

Then we see that  $-\Delta_{1,2}(k_x, k_y) = \Delta_{1,2}(k_x, -k_y)$ , which ensures that they must vanish at  $k_y = \pi$ . In this sense, the reflection symmetry ensures that  $h_+$  and  $h_-$  are decoupled at  $k_y = \pi$ . Return to model (42), we can define the  $\mathbb{Z}_2$  topological invariant  $\nu \in \{0, 1\}$  for each  $\pm 1$  sector of  ${}^cU_{-+}^+ = \sigma_z \tau_0$  defined for sub-manifold  $k_y = \pi$ , where

$$\begin{aligned}
 (-1)^\nu &= \text{sgn} \left\{ \frac{\text{Pf}[h_1(\pi)U_C]}{\text{Pf}[h_1(0)U_C]} \right. \\
 &\quad \left. \times \exp \left[ -\frac{1}{2} \int_{k_x=0}^{k_x=\pi} dk_x \frac{d}{dk_x} \log \det(h_1(k_x)U_C) \right] \right\}, \quad (45)
 \end{aligned}$$

where we also defined  $\mathcal{C}_- = U_C \mathcal{K}$ . A similar invariant can also be defined for  $h_1^*(-k_x)$ . Since the diagonal Hamiltonian  $h_1$  and  $h_1^*(-k_x)$  are decoupled at  $k_y = \pi$ , even if they both have  $\nu = 1$ , the overall Hamiltonian is still topological.

To further confirm our claims that reflection symmetry protects  $\mathbb{Z}_2$  topological invariant, we check the following two things: (i) By breaking reflection symmetries, the model (42) would either lose localization of in-gap states or open a line gap; (ii) To demonstrate the  $\mathbb{Z}_2$  nature of this model, we stack two copies of (42) together with symmetry-preserving couplings. We expect the in-gap states would vanish in latter case. As we will see, these checkings are indeed valid.

To confirm (i), we consider the introduction of a reflection-symmetry-breaking term  $\epsilon \sigma_y \tau_y$ . We first tune  $\epsilon = 0.05$ . As shown in Fig. 8 (a), there still exist two in-gap states. However, these two states are not topological. Indeed, increasing the strength  $\epsilon$  of added term, we see that these two states shift into the bulk *without* closing the band gap of bulk bands [Fig. 8 (b)-(d)]. This means that these two states can be gaped out through continuous deformation. Hence, we see that the reflection symmetry is protecting the topological in-gap states.

To confirm (ii), we consider the stacked Hamiltonian

$$h_{\text{stacked}}(k_x, k_y) = \begin{pmatrix} h_{DIII}(k_x, k_y) & \alpha \sigma_0 \tau_0 \\ \alpha \sigma_0 \tau_0 & h_{DIII}(k_x, k_y) \end{pmatrix}, \quad (46)$$

where the coupling is controlled by the parameter  $\alpha$ . The stacked Hamiltonian has all the symmetries that  $h_{DIII}$  obeys. Although in-gap states exist for small value of  $\alpha$ , these states would merge into the bulk if we increase the value of  $\alpha$  *without* going through a phase transition (Fig. 9). Therefore, these states are not topological. Hence, we see that model (42) indeed has a  $\mathbb{Z}_2$  invariant.

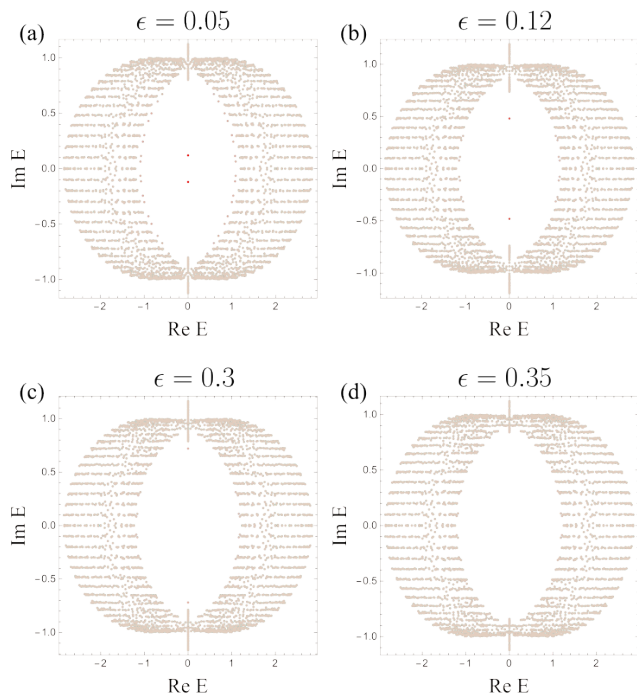


FIG. 8: Adding on-site perturbation term  $\epsilon\sigma_y\tau_y$  to Hamiltonian (42). The parameter  $\epsilon$  increases from (a)-(d) which causes the in-gap states vanish without going through a phase transition.

## VII. DISCUSSIONS AND CONCLUSIONS

In this paper, we give topological classification for all order-two spatial symmetries within AZ and  $AZ^\dagger$  class. The classification of crystalline symmetry for non-Hermitian system is a field that has been rarely studied. The classification table VI, VII, VIII, IX that we derived in the paper give a systematic way of understanding dislocation non-Hermitian skin effect proposed in [33–35]. In this paper, we generalized the classification results from Ref. [12] to non-Hermitian systems. Our classification is also more generalized than Ref. [47], which only considered reflection symmetry for non-Hermitian Hamiltonian without defects, and Ref. [48], which only considered defects with no spatial symmetries. Ref. [49] considered more generalized crystalline symmetries in non-Hermitian systems. However, Ref. [49] did not include internal symmetries in their classifications. In the grand scheme, our result paved the way for discovering novel symmetry-protected topological phases of non-Hermitian systems. As we have demonstrated in this paper, the existence of novel symmetry-protected topological phases also reveals that it is crucial to reexamine the effect of crystalline symmetries on non-Hermitian systems.

In this paper, we also demonstrate our findings through several toy models. Furthermore, we generalized the "clock" shaped dimensional hierarchy of Hermitian Hamiltonian proposed in Ref. [10] to NH Hamilto-

nian within AZ and  $AZ^\dagger$  class. However, since AZ and  $AZ^\dagger$  constitute only 16 out of 38-fold classification of NH matrices, it still remains a problem to find the classification for the rest of the 22 classes. Since the 22-fold SLS classes are rarely studied in current literature, their classifications are left for future works.

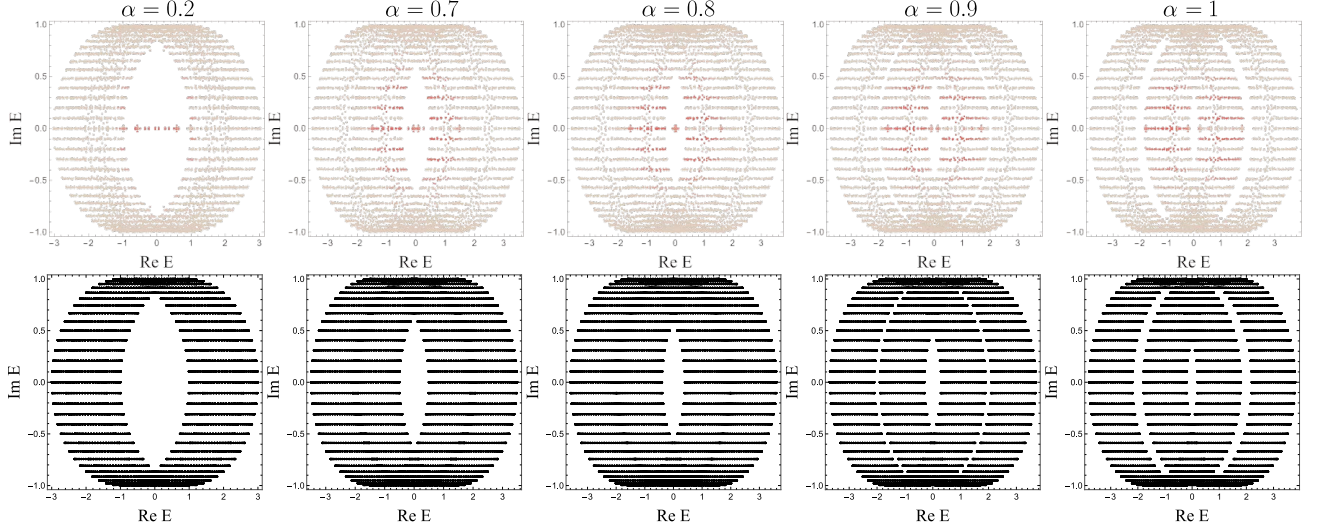


FIG. 9: The spectrum of stacked Hamiltonian (46) by increasing the value of coupling strength  $\alpha$ . The in-gap states merge into the bulk without going through a phase transition.

### Appendix A: Dimensional Hierarchy of AZ and AZ $^\dagger$ without spatial symmetries

Similar to Hermitian case, we wish to derive a dimensional hierarchy for AZ and AZ $^\dagger$  classes. In this section, we focus on the dimensional hierarchy for point-gapped Hamiltonian without any spatial symmetries. By dimensional hierarchy, we mean the following relationship (isomorphism)

$$\begin{aligned} K_{\mathbb{C}}(s; d, D) &= K_{\mathbb{C}}(s - d + D; 0, 0), \\ s &= 0, 1 \pmod{2} \end{aligned} \quad (\text{A1})$$

for complex AZ classes and

$$\begin{aligned} K_{\mathbb{R}}(s; d, D) &= K_{\mathbb{R}}(s - d + D; 0, 0), \\ s &= 0, \dots, 7 \pmod{8} \end{aligned} \quad (\text{A2})$$

for real AZ classes and finally

$$\begin{aligned} K_{\mathbb{R}}^\dagger(s^\dagger; d, D) &= K_{\mathbb{R}}^\dagger(s^\dagger - d + D; 0, 0), \\ s^\dagger &= 0, \dots, 7 \pmod{8} \end{aligned} \quad (\text{A3})$$

for AZ $^\dagger$  classes.

#### 1. CS to non-CS classes

First we consider AZ class. We first consider a mapping that send a chiral symmetry Hamiltonian  $H_c$  to a Hamiltonian without chiral symmetry  $H_{nc}$ .

Before discussing specific mappings, we specify the following requirements for the mappings. As mentioned in Sec. III, through continuous deformation, we can deform a point-gapped Hamiltonian into a unitary matrix

$U_c(\mathbf{k}, \mathbf{r})$ , which obeys  $U_c^\dagger U_c = 1$ . The classification problem then becomes the classification of extended Hermitian Hamiltonian  $\tilde{H}_c(\mathbf{k}, \mathbf{r})$ , which obeys  $\tilde{H}_c^2 = 1$  [See Eq. (7)]. We introduce an extra dimension  $\theta$  to  $\tilde{H}_c(\mathbf{k}, \mathbf{r})$  which allows us to map the extended Hamiltonian to different symmetry classes. Let us call the mapping  $\tilde{H}_{nc}(\mathbf{k}, \mathbf{r}, \theta)$ , which satisfy

$$\tilde{H}_{nc}(\mathbf{k}, \mathbf{r}, 0) = \text{const}, \tilde{H}_{nc}(\mathbf{k}, \mathbf{r}, \pi) = \text{const}'. \quad (\text{A4})$$

The parameter  $\theta$  can either be momentum-like or position-like. For a momentum-like (position-like)  $\theta$ , it transforms the same way as  $\mathbf{k}$  ( $\mathbf{r}$ ) under symmetries. In this case, the dimension  $\delta$  of the Hamiltonian will increase (decrease) by 1 [Recall that  $\delta = d - D$ ].

We may write the mapping as

$$\tilde{H}_{nc}(\mathbf{k}, \mathbf{r}, \theta) = \cos \theta \tilde{H}_c(\mathbf{k}, \mathbf{r}) + \sin \theta H_2, \quad (\text{A5})$$

where  $H_2$  is the term that would make the mapped Hamiltonian  $\tilde{H}_{nc}(\mathbf{k}, \mathbf{r}, \theta)$  violate CS. Since  $\tilde{H}(\mathbf{k}, \mathbf{r})$  is already in the form of an extended Hamiltonian, this further requires that  $H_2$  is anti-diagonal and Hermitian. Finally, the condition  $\tilde{H}^2 = 1$  requires that  $\{\tilde{H}_c, H_2\} = 0$ . Since the CS has the form  $\Gamma H_c(\mathbf{k}, \mathbf{r}, \theta) \Gamma^{-1} = -H_c^\dagger(\mathbf{k}, \mathbf{r}, \theta)$ , we see that by setting  $H_2 = \tilde{\Gamma}$  could satisfy all the conditions mentioned above. We thus define the following mapping

$$\tilde{H}_{nc}(\mathbf{k}, \mathbf{r}, \theta) = \cos \theta \tilde{H}_c(\mathbf{k}, \mathbf{r}) + \sin \theta \tilde{\Gamma}, \quad (\text{A6})$$

where  $\theta \in [0, \pi]$ . Notice that the mapping is defined for the extended Hermitian Hamiltonian (7). Due to the one to one relation between point-gapped Hamiltonian and its Hermitian extension, Eq. (A6) is a valid mapping to send a chiral symmetric point-gapped Hamiltonian to a non-chiral one. Now, by varying types of  $\theta$  between momentum-like or position-like, Eq. (A6) provides

TABLE X: Dimensional Hierarchy maps of AZ and AZ<sup>†</sup> classes.

AZ class	Mapping	Type of $\theta$	Mapped AZ class	TRS	PHS	CS
A	$H_c(\mathbf{k}, \mathbf{r}, \theta) = \cos \theta \tilde{H}_{nc}(\mathbf{k}, \mathbf{r}) \otimes \tau_z + \sin \theta i \Sigma \otimes \tau_x$	$\mathbf{k}/\mathbf{r}$	AIII			$1 \otimes \tau_x$
AIII	$\tilde{H}_{nc}(\mathbf{k}, \mathbf{r}, \theta) = \cos \theta \tilde{H}_c(\mathbf{k}, \mathbf{r}) + \sin \theta \tilde{\Gamma}$	$\mathbf{k}/\mathbf{r}$	A			
AI/AII	$H_c(\mathbf{k}, \mathbf{r}, \theta) = \cos \theta \tilde{H}_{nc}(\mathbf{k}, \mathbf{r}) \otimes \tau_z + \sin \theta i \otimes \tau_0$ $H_c(\mathbf{k}, \mathbf{r}, \theta) = \cos \theta \tilde{H}_{nc}(\mathbf{k}, \mathbf{r}) \otimes \tau_z + \sin \theta i \Sigma \otimes \tau_x$	$\mathbf{k}$ $\mathbf{r}$	BDI/CII CI/DIII	$\tilde{\mathcal{T}}_+ \otimes \tau_0$ $\tilde{\mathcal{T}}_+ \otimes \tau_z$	$\tilde{\mathcal{T}}_+ \otimes \tau_x$ $\tilde{\mathcal{T}}_+ \otimes \tau_y$	$1 \otimes \tau_x$ $1 \otimes \tau_x$
BDI/CII	$\tilde{H}_{nc}(\mathbf{k}, \mathbf{r}, \theta) = \cos \theta \tilde{H}_c(\mathbf{k}, \mathbf{r}) + \sin \theta \tilde{\mathcal{T}}_+ \tilde{\mathcal{C}}_-$	$\mathbf{k}$ $\mathbf{r}$	D/C AI/AII	$\tilde{\mathcal{T}}_+$	$\tilde{\mathcal{C}}_-$	
D/C	$H_c(\mathbf{k}, \mathbf{r}, \theta) = i \cos \theta \tilde{H}_{nc}(\mathbf{k}, \mathbf{r}) \otimes \tau_0 + \sin \theta 1 \otimes \tau_z$	$\mathbf{k}$ $\mathbf{r}$	DIII/CI BDI/CII	$\tilde{\mathcal{C}}_- \otimes \tau_y$ $\tilde{\mathcal{C}}_- \otimes \tau_0$	$\tilde{\mathcal{C}}_- \otimes \tau_z$ $\tilde{\mathcal{C}}_- \otimes \tau_x$	$1 \otimes \tau_x$ $1 \otimes \tau_x$
DIII/CI	$\tilde{H}_{nc}(\mathbf{k}, \mathbf{r}, \theta) = \cos \theta \tilde{H}_c(\mathbf{k}, \mathbf{r}) + \sin \theta i \tilde{\mathcal{T}}_+ \tilde{\mathcal{C}}_-$	$\mathbf{k}$ $\mathbf{r}$	AII/AI D/C	$\tilde{\mathcal{T}}_+$	$\tilde{\mathcal{C}}_-$	
AZ <sup>†</sup> class			Mapped AZ <sup>†</sup> class	TRS <sup>†</sup>	PHS <sup>†</sup>	
AI <sup>†</sup> /AII <sup>†</sup>	$H_c(\mathbf{k}, \mathbf{r}, \theta) = i \cos \theta \tilde{H}_{nc}(\mathbf{k}, \mathbf{r}) \otimes \tau_0 + \sin \theta 1 \otimes \tau_z$	$\mathbf{k}$ $\mathbf{r}$	BDI <sup>†</sup> /CII <sup>†</sup> CI <sup>†</sup> /DIII <sup>†</sup>	$\tilde{\mathcal{C}}_+ \otimes \tau_x$ $\tilde{\mathcal{C}}_+ \otimes \tau_z$	$\tilde{\mathcal{C}}_+ \otimes \tau_0$ $\tilde{\mathcal{C}}_+ \otimes \tau_y$	$1 \otimes \tau_x$ $1 \otimes \tau_x$
BDI <sup>†</sup> /CII <sup>†</sup>	$\tilde{H}_{nc}(\mathbf{k}, \mathbf{r}, \theta) = \cos \theta \tilde{H}_c(\mathbf{k}, \mathbf{r}) + \sin \theta \tilde{\mathcal{C}}_+ \tilde{\mathcal{T}}_-$	$\mathbf{k}$ $\mathbf{r}$	D <sup>†</sup> /C <sup>†</sup> AI <sup>†</sup> /AII <sup>†</sup>	$\tilde{\mathcal{C}}_+$	$\tilde{\mathcal{T}}_-$	
D <sup>†</sup> /C <sup>†</sup>	$H_c(\mathbf{k}, \mathbf{r}, \theta) = \cos \theta \tilde{H}_{nc}(\mathbf{k}, \mathbf{r}) \otimes \tau_z + \sin \theta i \Sigma \otimes \tau_x$ $H_c(\mathbf{k}, \mathbf{r}, \theta) = \cos \theta \tilde{H}_{nc}(\mathbf{k}, \mathbf{r}) \otimes \tau_z + \sin \theta i \otimes \tau_0$	$\mathbf{k}$ $\mathbf{r}$	DIII <sup>†</sup> /CI <sup>†</sup> BDI <sup>†</sup> /CII <sup>†</sup>	$\tilde{\mathcal{T}}_- \otimes \tau_y$ $\tilde{\mathcal{T}}_- \otimes \tau_x$	$\tilde{\mathcal{T}}_- \otimes \tau_z$ $\tilde{\mathcal{T}}_- \otimes \tau_0$	$1 \otimes \tau_x$ $1 \otimes \tau_x$
DIII <sup>†</sup> /CI <sup>†</sup>	$\tilde{H}_{nc}(\mathbf{k}, \mathbf{r}, \theta) = \cos \theta \tilde{H}_c(\mathbf{k}, \mathbf{r}) + \sin \theta i \tilde{\mathcal{C}}_+ \tilde{\mathcal{T}}_-$	$\mathbf{k}$ $\mathbf{r}$	AII <sup>†</sup> /AI <sup>†</sup> D <sup>†</sup> /C <sup>†</sup>	$\tilde{\mathcal{C}}_+$	$\tilde{\mathcal{T}}_-$	

TABLE XI: Homomorphism from  $K_{\mathbb{C}}^U(s, t; d + D, d_{\parallel} + D_{\parallel}, 0, 0)$  to  $K_{\mathbb{C}}^U(s + 1, t; d + D + 1, d_{\parallel} + D_{\parallel}, 0, 0)$  and  $K_{\mathbb{C}}^U(s + 1, t + 1; d + D + 1, d_{\parallel} + D_{\parallel} + 1, 0, 0)$ .

AZ class	$t$	Symmetry	Type of $\theta$	Mapped to	TRS	PHS	CS	Mapped symmetry	Mapped $t$
A	0	${}^c\bar{U}$	$\mathbf{k}_{\perp}/\mathbf{r}_{\perp}$	AIII	$1 \otimes \tau_x$			${}^g\bar{U}_+ = {}^c\tilde{U} \otimes \tau_0$	0
	1	${}^g\bar{U}$	$\mathbf{k}_{\perp}/\mathbf{r}_{\perp}$					${}^g\bar{U}_- = {}^g\tilde{U} \otimes \tau_z$	1
	0	${}^cU$	$\mathbf{k}_{\parallel}/\mathbf{r}_{\parallel}$					${}^c\bar{U}_+ = {}^c\tilde{U} \otimes \tau_x$	1
	1	${}^gU$	$\mathbf{k}_{\parallel}/\mathbf{r}_{\parallel}$					${}^c\bar{U}_- = {}^g\tilde{U} \otimes \tau_y$	0
AIII	0	${}^cU_+$	$\mathbf{k}_{\perp}/\mathbf{r}_{\perp}$	A				${}^cU = {}^cU_+$	0
	1	${}^gU_+$	$\mathbf{k}_{\perp}/\mathbf{r}_{\perp}$					${}^gU = {}^gU_+$	1
	0	${}^cU_+$	$\mathbf{k}_{\parallel}/\mathbf{r}_{\parallel}$					${}^g\bar{U} = \Gamma {}^cU_+$	1
	1	${}^gU_+$	$\mathbf{k}_{\parallel}/\mathbf{r}_{\parallel}$					${}^c\bar{U} = \Gamma {}^gU_+$	0

a mapping between AZ classes with CS and without CS. In the following, we use some examples to illustrate this process.

For complex AZ class, notice that since there is no anti-unitary symmetries, we cannot distinguish momentum-like or position-like  $\theta$ . Therefore, for both types of  $\theta$ , Eq. (A6) would send a Hamiltonian from class AIII ( $s = 0$ ) to class A ( $s = 1$ ).

For real AZ classes with CS, both TRS and PHS symmetries may present. We make the requirement that  $[\mathcal{T}_+, \mathcal{C}_-] = 0$ . We may write the CS operator as

$$\Gamma = i^{(s-2)/2} \mathcal{T}_+ \mathcal{C}_-, \quad (\text{A7})$$

where  $s$  is defined  $s \pmod 4$ .

All the above derivations are also applicable to AZ<sup>†</sup> class. The mapping for AZ<sup>†</sup> class from a CS class to a non-CS one is the same as Eq. (A6). However, the  $\Gamma$  operator is now defined as

$$\Gamma = i^{(s^{\dagger})/2} \mathcal{C}_+ \mathcal{T}_-, \quad (\text{A8})$$

where we used the convention  $[\mathcal{C}_+, \mathcal{T}_-] = 0$  and  $s^{\dagger}$  is defined  $s^{\dagger} \pmod 4$ .

As an example, we consider  $\theta$  is momentum-like. For AZ class, TRS is violated when  $s = 2 \pmod 4$  while PHS is violated when  $s = 0 \pmod 4$ . This corresponds to a clockwise rotation  $s \rightarrow s + 1$ . Similarly, if  $\theta$  is position-like, TRS is violated when  $s = 0 \pmod 4$ . This corresponds to a counter-clockwise rotation  $s \rightarrow s - 1$ . A similar conclusion also apply to AZ<sup>†</sup> class. All the mappings are summarized in Table X.

To sum up this section, the mappings discussed above allow us to establish a one way mapping (homomorphism) from CS classes to non-CS classes i.e.

$$K_{\mathbb{C}}(s; d, D) \rightarrow K_{\mathbb{C}}(s - d + D; 0, 0), \quad s = 0 \quad (\text{A9})$$

for complex AZ classes and

$$K_{\mathbb{R}}(s; d, D) \rightarrow K_{\mathbb{R}}(s - d + D; 0, 0), \quad s = 0, 2, 4, 6 \quad (\text{A10})$$

TABLE XII: Homomorphism from  $K_{\mathbb{R}}^{U/A}(s, t; d, d_{\parallel}, D, D_{\parallel})$  to  $K_{\mathbb{R}}^{U/A}(s + 1, t; d + 1, d_{\parallel}, D, D_{\parallel})$ ,  $K_{\mathbb{R}}^{U/A}(s + 1, t + 1; d + 1, d_{\parallel} + 1, D, D_{\parallel})$ ,  $K_{\mathbb{R}}^{U/A}(s - 1, t; d, d_{\parallel}, D + 1, D_{\parallel})$ , and  $K_{\mathbb{R}}^{U/A}(s - 1, t - 1; d, d_{\parallel}, D + 1, D_{\parallel} + 1)$  for AZ classes without chiral symmetry.

AZ class	$t$	Symmetry	Type of $\theta$	Mapped to	TRS	PHS	CS	Mapped symmetry	Mapped $t$
AI/AII	0	${}^c U_+^+$	$\mathbf{k}_{\perp}$	BDI/CII	$\tilde{\mathcal{T}}_+ \otimes \tau_0$	$\tilde{\mathcal{T}}_+ \otimes \tau_x$		${}^c U_{++}^+ = {}^c \tilde{U}_+^+ \otimes \tau_0$	0
	1	${}^g \bar{U}_-^+$						${}^c U_{+-}^+ = {}^g \tilde{U}_-^+ \otimes \tau_y$	1
	2	${}^c U_+^-$						${}^c U_{++}^- = {}^c \tilde{U}_+^- \otimes \tau_0$	2
	3	${}^g \bar{U}_+^+$						${}^c U_{-+}^+ = {}^g \tilde{U}_+^+ \otimes \tau_y$	3
AI/AII	0	${}^c U_+^+$	$\mathbf{k}_{\parallel}$	BDI/CII	$\tilde{\mathcal{T}}_+ \otimes \tau_0$	$\tilde{\mathcal{T}}_+ \otimes \tau_x$		${}^g U_{++}^+ = {}^c \tilde{U}_+^+ \otimes \tau_0$	1
	1	${}^g \bar{U}_-^+$						${}^g U_{+-}^+ = {}^g \tilde{U}_-^+ \otimes \tau_y$	2
	2	${}^c U_+^-$						${}^g U_{++}^- = {}^c \tilde{U}_+^- \otimes \tau_0$	3
	3	${}^g \bar{U}_+^+$						${}^g U_{-+}^+ = {}^g \tilde{U}_+^+ \otimes \tau_y$	0
AI/AII	0	${}^c U_+^+$	$\mathbf{r}_{\perp}$	CI/DIII	$\tilde{\mathcal{T}}_+ \otimes \tau_z$	$\tilde{\mathcal{T}}_+ \otimes \tau_y$		${}^c U_{++}^+ = {}^c \tilde{U}_+^+ \otimes \tau_0$	0
	1	${}^g \bar{U}_-^+$						${}^c U_{+-}^+ = {}^g \tilde{U}_-^+ \otimes \tau_y$	1
	2	${}^c U_+^-$						${}^c U_{++}^- = {}^c \tilde{U}_+^- \otimes \tau_0$	2
	3	${}^g \bar{U}_+^+$						${}^c U_{-+}^+ = {}^g \tilde{U}_+^+ \otimes \tau_y$	3
AI/AII	0	${}^c U_+^+$	$\mathbf{r}_{\parallel}$	CI/DIII	$\tilde{\mathcal{T}}_+ \otimes \tau_z$	$\tilde{\mathcal{T}}_+ \otimes \tau_y$		${}^g \bar{U}_{-+}^+ = {}^c \tilde{U}_+^+ \otimes \tau_y$	3
	1	${}^g \bar{U}_-^+$						${}^g \bar{U}_{--}^+ = {}^g \tilde{U}_-^+ \otimes \tau_0$	0
	2	${}^c U_+^-$						${}^g \bar{U}_{-+}^- = {}^c \tilde{U}_+^- \otimes \tau_y$	1
	3	${}^g \bar{U}_+^+$						${}^g \bar{U}_{++}^+ = {}^g \tilde{U}_+^+ \otimes \tau_0$	2
D/C	0	${}^c U_+^+$	$\mathbf{k}_{\perp}$	DIII/CI	$\tilde{\mathcal{C}}_- \otimes \tau_y$	$\tilde{\mathcal{C}}_- \otimes \tau_z$		${}^c U_{++}^+ = {}^c \tilde{U}_+^+ \otimes \tau_0$	0
	1	${}^g \bar{U}_-^+$						${}^c \bar{U}_{--}^+ = {}^g \tilde{U}_-^+ \otimes \tau_x$	1
	2	${}^c U_+^-$						${}^c U_{++}^- = {}^c \tilde{U}_+^- \otimes \tau_0$	2
	3	${}^g \bar{U}_+^+$						${}^c \bar{U}_{-+}^+ = {}^g \tilde{U}_+^+ \otimes \tau_x$	3
D/C	0	${}^c U_+^+$	$\mathbf{k}_{\parallel}$	DIII/CI	$\tilde{\mathcal{C}}_- \otimes \tau_y$	$\tilde{\mathcal{C}}_- \otimes \tau_z$		${}^c U_{-+}^+ = {}^c \tilde{U}_+^+ \otimes \tau_y$	1
	1	${}^g \bar{U}_-^+$						${}^c \bar{U}_{-+}^+ = {}^g \tilde{U}_-^+ \otimes \tau_z$	2
	2	${}^c U_+^-$						${}^c U_{-+}^- = {}^c \tilde{U}_+^- \otimes \tau_y$	3
	3	${}^g \bar{U}_+^+$						${}^c \bar{U}_{++}^+ = {}^g \tilde{U}_+^+ \otimes \tau_z$	0
D/C	0	${}^c U_+^+$	$\mathbf{r}_{\perp}$	BDI/CII	$\tilde{\mathcal{C}}_- \otimes \tau_0$	$\tilde{\mathcal{C}}_- \otimes \tau_x$		${}^c U_{++}^+ = {}^c \tilde{U}_+^+ \otimes \tau_0$	0
	1	${}^g \bar{U}_-^+$						${}^c \bar{U}_{++}^+ = {}^g \tilde{U}_+^+ \otimes \tau_x$	1
	2	${}^c U_+^-$						${}^c U_{++}^- = {}^c \tilde{U}_+^- \otimes \tau_0$	2
	3	${}^g \bar{U}_+^+$						${}^c \bar{U}_{-+}^+ = {}^g \tilde{U}_+^+ \otimes \tau_x$	3
D/C	0	${}^c U_+^+$	$\mathbf{r}_{\parallel}$	BDI/CII	$\tilde{\mathcal{C}}_- \otimes \tau_0$	$\tilde{\mathcal{C}}_- \otimes \tau_x$		${}^c U_{-+}^+ = {}^c \tilde{U}_+^+ \otimes \tau_y$	3
	1	${}^g \bar{U}_-^+$						${}^c \bar{U}_{+-}^+ = {}^g \tilde{U}_-^+ \otimes \tau_z$	0
	2	${}^c U_+^-$						${}^c U_{-+}^- = {}^c \tilde{U}_+^- \otimes \tau_y$	1
	3	${}^g \bar{U}_+^+$						${}^c \bar{U}_{-+}^+ = {}^g \tilde{U}_+^+ \otimes \tau_z$	2

for real AZ classes and finally

$$K_{\mathbb{R}}^{\dagger}(s^{\dagger}; d, D) \rightarrow K_{\mathbb{R}}^{\dagger}(s^{\dagger} - d + D; 0, 0),$$

$$s^{\dagger} = 0, 2, 4, 6 \quad (\text{A11})$$

for  $AZ^{\dagger}$  classes. In the next section, we consider one way mappings that would send a non-CS Hamiltonian to CS one such that the equal sign in Eq. (A1) to (A3) is justified.

## 2. Non-CS to CS classes

We focus on the mapping from non-CS to CS classes for AZ classes in this section ( $H_{nc}$  to  $H_c$ ). We first list the process of constructing mappings. Similar to the previous

section, we introduce an extra dimension  $\theta$  to  $\tilde{H}_{nc}(\mathbf{k}, \mathbf{r})$  such that the mapped Hamiltonian obeys CS. We define the mappings

$$H_c(\mathbf{k}, \mathbf{r}, \theta) = \cos \theta H_1(\mathbf{k}, \mathbf{r}) + \sin \theta H_2, \quad (\text{A12})$$

where  $H_1(\mathbf{k}, \mathbf{r})$  is  $\tilde{H}_{nc}(\mathbf{k}, \mathbf{r})$  or  $i\tilde{H}_{nc}(\mathbf{k}, \mathbf{r})$  in a larger Clifford algebra dimension (See Table X);  $H_2$  is an extra term that made  $H_c$  to obeys CS. Notice that unlike Eq. (A6), the mapped Hamiltonian in Eq. (A12) is *not* an extended Hamiltonian. Instead,  $H_c$  is a point-gapped NH Hamiltonian that obeys unitary condition  $H_c^{\dagger} H_c = 1$ . Finally, we need to make sure that PHS and TRS of the mapped Hamiltonian  $H_c$  commute with each other, as this is the convention we use in this paper.

Bear these requirements in mind, we are now ready to discuss specific mappings.

TABLE XIII: Homomorphism from  $K_{\mathbb{R}}^{U/A}(s, t; d, d_{\parallel}, D, D_{\parallel})$  to  $K_{\mathbb{R}}^{U/A}(s+1, t; d+1, d_{\parallel}, D, D_{\parallel})$ ,  $K_{\mathbb{R}}^{U/A}(s+1, t+1; d+1, d_{\parallel}+1, D, D_{\parallel})$ ,  $K_{\mathbb{R}}^{U/A}(s-1, t; d, d_{\parallel}, D+1, D_{\parallel})$ , and  $K_{\mathbb{R}}^{U/A}(s-1, t-1; d, d_{\parallel}, D+1, D_{\parallel}+1)$  for AZ classes with chiral symmetry.

AZ class	$t$	Symmetry	Type of $\theta$	Mapped to	TRS	PHS	CS	Mapped symmetry	Mapped $t$
BDI/CII	0	${}^cU_{++}^+$	$\mathbf{k}_{\perp}$	D/C	$\tilde{c}_{-}$			${}^cU_{++}^+ = {}^cU_{++}^+$	0
	1	${}^g\bar{U}_{++}^+$						${}^g\bar{U}_{++}^+ = {}^g\bar{U}_{++}^+$	1
	2	${}^cU_{--}^+$						${}^cU_{--}^+ = {}^cU_{--}^+$	2
	3	${}^g\bar{U}_{+-}^+$						${}^g\bar{U}_{+-}^+ = {}^g\bar{U}_{+-}^+$	3
BDI/CII	0	${}^cU_{++}^+$	$\mathbf{k}_{\parallel}$	D/C	$\tilde{c}_{-}$			${}^g\bar{U}_{++}^+ = \Gamma {}^cU_{++}^+$	1
	1	${}^g\bar{U}_{-+}^+$						${}^cU_{-+}^+ = i\Gamma {}^g\bar{U}_{-+}^+$	2
	2	${}^cU_{--}^+$						${}^g\bar{U}_{--}^+ = \Gamma {}^cU_{--}^+$	3
	3	${}^g\bar{U}_{+-}^+$						${}^cU_{+-}^+ = i\Gamma {}^g\bar{U}_{+-}^+$	0
BDI/CII	0	${}^cU_{++}^+$	$\mathbf{r}_{\perp}$	AI/AII	$\tilde{\tau}_{+}$			${}^cU_{++}^+ = {}^cU_{++}^+$	0
	1	${}^g\bar{U}_{++}^+$						${}^g\bar{U}_{++}^+ = {}^g\bar{U}_{++}^+$	1
	2	${}^cU_{--}^+$						${}^cU_{--}^+ = {}^cU_{--}^+$	2
	3	${}^g\bar{U}_{+-}^+$						${}^g\bar{U}_{+-}^+ = {}^g\bar{U}_{+-}^+$	3
BDI/CII	0	${}^cU_{++}^+$	$\mathbf{r}_{\parallel}$	AI/AII	$\tilde{\tau}_{+}$			${}^g\bar{U}_{++}^+ = \Gamma {}^cU_{++}^+$	3
	1	${}^g\bar{U}_{-+}^+$						${}^cU_{-+}^+ = i\Gamma {}^g\bar{U}_{-+}^+$	0
	2	${}^cU_{--}^+$						${}^g\bar{U}_{--}^+ = \Gamma {}^cU_{--}^+$	1
	3	${}^g\bar{U}_{+-}^+$						${}^cU_{+-}^+ = i\Gamma {}^g\bar{U}_{+-}^+$	2
DIII/CI	0	${}^cU_{++}^+$	$\mathbf{k}_{\perp}$	AII/AI	$\tilde{\tau}_{+}$			${}^cU_{++}^+ = {}^cU_{++}^+$	0
	1	${}^g\bar{U}_{++}^+$						${}^g\bar{U}_{++}^+ = {}^g\bar{U}_{++}^+$	1
	2	${}^cU_{--}^+$						${}^cU_{--}^+ = {}^cU_{--}^+$	2
	3	${}^g\bar{U}_{+-}^+$						${}^g\bar{U}_{+-}^+ = {}^g\bar{U}_{+-}^+$	3
DIII/CI	0	${}^cU_{++}^+$	$\mathbf{k}_{\parallel}$	AII/AI	$\tilde{\tau}_{+}$			${}^g\bar{U}_{++}^+ = \Gamma {}^cU_{++}^+$	1
	1	${}^g\bar{U}_{-+}^+$						${}^cU_{-+}^+ = i\Gamma {}^g\bar{U}_{-+}^+$	2
	2	${}^cU_{--}^+$						${}^g\bar{U}_{--}^+ = \Gamma {}^cU_{--}^+$	3
	3	${}^g\bar{U}_{+-}^+$						${}^cU_{+-}^+ = i\Gamma {}^g\bar{U}_{+-}^+$	0
DIII/CI	0	${}^cU_{++}^+$	$\mathbf{r}_{\perp}$	D/C	$\tilde{c}_{-}$			${}^cU_{++}^+ = {}^cU_{++}^+$	0
	1	${}^g\bar{U}_{++}^+$						${}^g\bar{U}_{++}^+ = {}^g\bar{U}_{++}^+$	1
	2	${}^cU_{--}^+$						${}^cU_{--}^+ = {}^cU_{--}^+$	2
	3	${}^g\bar{U}_{+-}^+$						${}^g\bar{U}_{+-}^+ = {}^g\bar{U}_{+-}^+$	3
DIII/CI	0	${}^cU_{++}^+$	$\mathbf{r}_{\parallel}$	D/C	$\tilde{c}_{-}$			${}^g\bar{U}_{++}^+ = \Gamma {}^cU_{++}^+$	3
	1	${}^g\bar{U}_{-+}^+$						${}^cU_{-+}^+ = i\Gamma {}^g\bar{U}_{-+}^+$	0
	2	${}^cU_{--}^+$						${}^g\bar{U}_{--}^+ = \Gamma {}^cU_{--}^+$	1
	3	${}^g\bar{U}_{+-}^+$						${}^cU_{+-}^+ = i\Gamma {}^g\bar{U}_{+-}^+$	2

First we consider a mapping from AI/AII to BDI/CII:

$$H_c(\mathbf{k}, \mathbf{r}, \theta) = \cos \theta \tilde{H}_{nc}(\mathbf{k}, \mathbf{r}) \otimes \tau_z + \sin \theta i \otimes \tau_0, \quad (\text{A13})$$

where  $\tilde{H}_{nc}$  obeys TRS with operator  $\tilde{\tau}_{+}$ . If  $\theta$  is a momentum-like parameter, the mapped Hamiltonian  $H_c$  obeys TRS with  $\tilde{\tau}_{+} \otimes \tau_0$ ; PHS with  $\tilde{\tau}_{+} \otimes \tau_x$ . These two symmetries combined,  $H_c$  obeys CS with  $1 \otimes \tau_x$ . Furthermore, since the extended Hamiltonian obeys  $\tilde{H}_{nc}^2 = 1$ , we see that  $H_c^\dagger H_c = 1$ . This corresponds to a shift  $s \rightarrow s+1$  where  $s = 1$  (AI) or  $5$  (AII).

Next, we consider a mapping that would map AI/AII to CI/DIII:

$$H_c(\mathbf{k}, \mathbf{r}, \theta) = \cos \theta \tilde{H}_{nc}(\mathbf{k}, \mathbf{r}) \otimes \tau_z + \sin \theta i \Sigma \otimes \tau_x. \quad (\text{A14})$$

The  $\Sigma$  is the  $\Sigma$  symmetry operator of  $\tilde{H}_{nc}(\mathbf{k}, \mathbf{r})$ . If  $\theta$  is position-like, the mapped Hamiltonian  $H_c$  obeys TRS with  $\tilde{\tau}_{+} \otimes \tau_z$  and PHS with  $\tilde{\tau}_{+} \otimes \tau_y$ . Combining these two

symmetries,  $H_c$  obeys CS with  $1 \otimes \tau_x$ . This corresponds to a shift  $s \rightarrow s-1$  where  $s = 1$  or  $5$ .

By following similar process, we can find a mapping for class D/C and A into adjacent CS classes. For AZ<sup>†</sup> classes, the process of finding mappings into CS classes is essentially the same which we do not repeat here. The mapping and resulting symmetries are summarized in Table X.

Based on the above discussion, we have homomorphisms that map

$$K_{\mathbb{C}}(s; d, D) \rightarrow K_{\mathbb{C}}(s-d+D; 0, 0), \quad s = 1 \quad (\text{A15})$$

for complex AZ classes and

$$K_{\mathbb{R}}(s; d, D) \rightarrow K_{\mathbb{R}}(s-d+D; 0, 0), \quad s = 1, 3, 5, 7 \quad (\text{A16})$$

TABLE XIV: Homomorphism from  $K_{\mathbb{R}}^{\dagger U/A}(s, t; d, d_{\parallel}, D, D_{\parallel})$  to  $K_{\mathbb{R}}^{\dagger U/A}(s+1, t; d+1, d_{\parallel}, D, D_{\parallel})$ ,  $K_{\mathbb{R}}^{\dagger U/A}(s+1, t-1; d+1, d_{\parallel}+1, D, D_{\parallel})$ ,  $K_{\mathbb{R}}^{\dagger U/A}(s-1, t; d, d_{\parallel}, D+1, D_{\parallel})$ , and  $K_{\mathbb{R}}^{\dagger U/A}(s-1, t+1; d, d_{\parallel}, D+1, D_{\parallel}+1)$  for  $AZ^{\dagger}$  classes without chiral symmetry.

$AZ^{\dagger}$ class	$t$	Symmetry	Type of $\theta$	Mapped to	TRS $^{\dagger}$	PHS $^{\dagger}$	CS	Mapped symmetry	Mapped $t$
AI $^{\dagger}$ /AII $^{\dagger}$	0	${}^c\bar{U}_+^+$	$\mathbf{k}_{\perp}$	BDI $^{\dagger}$ /CII $^{\dagger}$	$\tilde{\mathcal{C}}_+ \otimes \tau_x$	$\tilde{\mathcal{C}}_+ \otimes \tau_0$		${}^c\bar{U}_{++}^+ = {}^c\bar{U}_+^+ \otimes \tau_0$	0
	1	${}^g\bar{U}_+^+$						${}^c\bar{U}_{++}^+ = {}^g\tilde{\bar{U}}_+^+ \otimes \tau_x$	1
	2	${}^c\bar{U}_+^-$						${}^c\bar{U}_{+-}^- = {}^c\tilde{\bar{U}}_+^- \otimes \tau_0$	2
	3	${}^g\bar{U}_+^-$						${}^c\bar{U}_{--}^+ = {}^g\tilde{\bar{U}}_+^+ \otimes \tau_x$	3
AI $^{\dagger}$ /AII $^{\dagger}$	0	${}^c\bar{U}_+^+$	$\mathbf{k}_{\parallel}$	BDI $^{\dagger}$ /CII $^{\dagger}$	$\tilde{\mathcal{C}}_+ \otimes \tau_x$	$\tilde{\mathcal{C}}_+ \otimes \tau_0$		${}^c\bar{U}_{+-}^+ = {}^c\tilde{\bar{U}}_+^+ \otimes \tau_y$	3
	1	${}^g\bar{U}_+^+$						${}^c\bar{U}_{-+}^+ = {}^g\tilde{\bar{U}}_+^+ \otimes \tau_z$	0
	2	${}^c\bar{U}_+^-$						${}^c\bar{U}_{+-}^- = {}^c\tilde{\bar{U}}_+^- \otimes \tau_y$	1
	3	${}^g\bar{U}_+^-$						${}^c\bar{U}_{+-}^+ = {}^g\tilde{\bar{U}}_+^+ \otimes \tau_z$	2
AI $^{\dagger}$ /AII $^{\dagger}$	0	${}^c\bar{U}_+^+$	$\mathbf{r}_{\perp}$	CI $^{\dagger}$ /DIII $^{\dagger}$	$\tilde{\mathcal{C}}_+ \otimes \tau_z$	$\tilde{\mathcal{C}}_+ \otimes \tau_y$		${}^c\bar{U}_{++}^+ = {}^c\tilde{\bar{U}}_+^+ \otimes \tau_0$	0
	1	${}^g\bar{U}_+^+$						${}^c\bar{U}_{-+}^+ = {}^g\tilde{\bar{U}}_+^+ \otimes \tau_x$	1
	2	${}^c\bar{U}_+^-$						${}^c\bar{U}_{++}^- = {}^c\tilde{\bar{U}}_+^- \otimes \tau_0$	2
	3	${}^g\bar{U}_+^-$						${}^c\bar{U}_{++}^+ = {}^g\tilde{\bar{U}}_+^+ \otimes \tau_x$	3
AI $^{\dagger}$ /AII $^{\dagger}$	0	${}^c\bar{U}_+^+$	$\mathbf{r}_{\parallel}$	CI $^{\dagger}$ /DIII $^{\dagger}$	$\tilde{\mathcal{C}}_+ \otimes \tau_z$	$\tilde{\mathcal{C}}_+ \otimes \tau_y$		${}^c\bar{U}_{+-}^+ = {}^c\tilde{\bar{U}}_+^+ \otimes \tau_y$	1
	1	${}^g\bar{U}_+^+$						${}^c\bar{U}_{+-}^+ = {}^g\tilde{\bar{U}}_+^+ \otimes \tau_z$	2
	2	${}^c\bar{U}_+^-$						${}^c\bar{U}_{+-}^- = {}^c\tilde{\bar{U}}_+^- \otimes \tau_y$	3
	3	${}^g\bar{U}_+^-$						${}^c\bar{U}_{+-}^+ = {}^g\tilde{\bar{U}}_+^+ \otimes \tau_y$	0
D $^{\dagger}$ /C $^{\dagger}$	0	${}^c\bar{U}_+^+$	$\mathbf{k}_{\perp}$	DIII $^{\dagger}$ /CI $^{\dagger}$	$\tilde{\mathcal{T}}_- \otimes \tau_y$	$\tilde{\mathcal{T}}_- \otimes \tau_z$		${}^c\bar{U}_{++}^+ = {}^c\tilde{\bar{U}}_+^+ \otimes \tau_0$	0
	1	${}^g\bar{U}_+^+$						${}^c\bar{U}_{+-}^+ = {}^g\tilde{\bar{U}}_+^+ \otimes \tau_y$	1
	2	${}^c\bar{U}_+^-$						${}^c\bar{U}_{++}^- = {}^c\tilde{\bar{U}}_+^- \otimes \tau_0$	2
	3	${}^g\bar{U}_+^-$						${}^c\bar{U}_{++}^+ = {}^g\tilde{\bar{U}}_+^+ \otimes \tau_y$	3
D $^{\dagger}$ /C $^{\dagger}$	0	${}^c\bar{U}_+^+$	$\mathbf{k}_{\parallel}$	DIII $^{\dagger}$ /CI $^{\dagger}$	$\tilde{\mathcal{T}}_- \otimes \tau_y$	$\tilde{\mathcal{T}}_- \otimes \tau_z$		${}^g\bar{U}_{-+}^+ = {}^c\tilde{\bar{U}}_+^+ \otimes \tau_y$	3
	1	${}^g\bar{U}_+^+$						${}^g\bar{U}_{-+}^+ = {}^g\tilde{\bar{U}}_+^+ \otimes \tau_0$	0
	2	${}^c\bar{U}_+^-$						${}^g\bar{U}_{-+}^- = {}^c\tilde{\bar{U}}_+^- \otimes \tau_y$	1
	3	${}^g\bar{U}_+^-$						${}^g\bar{U}_{++}^+ = {}^g\tilde{\bar{U}}_+^+ \otimes \tau_0$	2
D $^{\dagger}$ /C $^{\dagger}$	0	${}^c\bar{U}_+^+$	$\mathbf{r}_{\perp}$	BDI $^{\dagger}$ /CII $^{\dagger}$	$\tilde{\mathcal{T}}_- \otimes \tau_x$	$\tilde{\mathcal{T}}_- \otimes \tau_0$		${}^c\bar{U}_{++}^+ = {}^c\tilde{\bar{U}}_+^+ \otimes \tau_0$	0
	1	${}^g\bar{U}_+^+$						${}^c\bar{U}_{-+}^+ = {}^g\tilde{\bar{U}}_+^+ \otimes \tau_y$	1
	2	${}^c\bar{U}_+^-$						${}^c\bar{U}_{++}^- = {}^c\tilde{\bar{U}}_+^- \otimes \tau_0$	2
	3	${}^g\bar{U}_+^-$						${}^c\bar{U}_{++}^+ = {}^g\tilde{\bar{U}}_+^+ \otimes \tau_y$	3
D $^{\dagger}$ /C $^{\dagger}$	0	${}^c\bar{U}_+^+$	$\mathbf{r}_{\parallel}$	BDI $^{\dagger}$ /CII $^{\dagger}$	$\tilde{\mathcal{T}}_- \otimes \tau_x$	$\tilde{\mathcal{T}}_- \otimes \tau_0$		${}^g\bar{U}_{++}^+ = {}^c\tilde{\bar{U}}_+^+ \otimes \tau_0$	1
	1	${}^g\bar{U}_+^+$						${}^g\bar{U}_{-+}^+ = {}^g\tilde{\bar{U}}_+^+ \otimes \tau_y$	2
	2	${}^c\bar{U}_+^-$						${}^g\bar{U}_{++}^- = {}^c\tilde{\bar{U}}_+^- \otimes \tau_0$	3
	3	${}^g\bar{U}_+^-$						${}^g\bar{U}_{++}^+ = {}^g\tilde{\bar{U}}_+^+ \otimes \tau_y$	0

for real AZ classes and finally

$$K_{\mathbb{R}}^{\dagger}(s^{\dagger}; d, D) \rightarrow K_{\mathbb{R}}^{\dagger}(s^{\dagger} - d + D; 0, 0),$$

$$s^{\dagger} = 1, 3, 5, 7. \quad (\text{A17})$$

This allows us to conclude the isomorphism Eq. (A1) to (A3).

## Appendix B: Dimensional Hierarchy of AZ and AZ $^{\dagger}$ with order-two spatial symmetries

In this section, we proof the dimensional hierarchy of AZ and AZ $^{\dagger}$  in the presence of spatial symmetries.

### 1. Complex AZ with order-two unitary symmetries

Consider a Hamiltonian  $H_{nc}$  in class A with an additional symmetry  ${}^c\bar{U}$ . According to Table II, this belongs to class  $(s=0, t=0)$ . We consider the extended version  ${}^c\tilde{\bar{U}}$  on the mapped Hamiltonian in class AIII

$$H_c(\mathbf{k}, \mathbf{r}, \theta) = \cos \theta \tilde{H}_{nc}(\mathbf{k}, \mathbf{r}) \otimes \tau_z + \sin \theta i \Sigma \otimes \tau_x \quad (\text{B1})$$

as listed in Table X. Once again, due to the absence of anti-unitary symmetries, we cannot distinguish whether  $\theta$  is momentum-like or position-like. Therefore, we only need to consider whether  $\theta$  will change under the spatial symmetries. If  $\theta$  is  $\mathbf{k}_{\perp}/\mathbf{r}_{\perp}$  i.e. unchanged under the spatial symmetries, we can define operator  ${}^g\bar{U}_+ = {}^c\tilde{\bar{U}}_+ \otimes$

TABLE XV: Homomorphism from  $K_{\mathbb{R}}^{\dagger U/A}(s, t; d, d_{\parallel}, D, D_{\parallel})$  to  $K_{\mathbb{R}}^{\dagger U/A}(s+1, t; d+1, d_{\parallel}, D, D_{\parallel})$ ,  $K_{\mathbb{R}}^{\dagger U/A}(s+1, t-1; d+1, d_{\parallel}+1, D, D_{\parallel})$ ,  $K_{\mathbb{R}}^{\dagger U/A}(s-1, t; d, d_{\parallel}, D+1, D_{\parallel})$ , and  $K_{\mathbb{R}}^{\dagger U/A}(s-1, t+1; d, d_{\parallel}, D+1, D_{\parallel}+1)$  for  $AZ^{\dagger}$  classes with chiral symmetry.

$AZ^{\dagger}$ class	$t$	Symmetry	Type of $\theta$	Mapped to	TRS $^{\dagger}$	PHS $^{\dagger}$	CS	Mapped symmetry	Mapped $t$
BDI $^{\dagger}$ /CII $^{\dagger}$	0	${}^c U_{++}^+$	$\mathbf{k}_{\perp}$	D $^{\dagger}$ /C $^{\dagger}$	$\tilde{\tau}_{-}$			${}^c U_{++}^+ = {}^c U_{++}^+$	0
	1	${}^g \bar{U}_{++}^+$						${}^g \bar{U}_{++}^+ = {}^g \bar{U}_{++}^+$	1
	2	${}^c U_{+-}^+$						${}^c U_{+-}^+ = {}^c U_{+-}^+$	2
	3	${}^g \bar{U}_{+-}^+$						${}^g \bar{U}_{+-}^+ = {}^g \bar{U}_{+-}^+$	3
BDI $^{\dagger}$ /CII $^{\dagger}$	0	${}^c U_{++}^+$	$\mathbf{k}_{\parallel}$	D $^{\dagger}$ /C $^{\dagger}$	$\tilde{\tau}_{-}$			${}^g \bar{U}_{++}^+ = \Gamma {}^c U_{++}^+$	3
	1	${}^g \bar{U}_{+-}^+$						${}^c U_{+-}^+ = i\Gamma {}^g \bar{U}_{+-}^+$	0
	2	${}^c U_{--}^+$						${}^g \bar{U}_{--}^+ = \Gamma {}^c U_{--}^+$	1
	3	${}^g \bar{U}_{--}^+$						${}^c U_{--}^+ = i\Gamma {}^g \bar{U}_{--}^+$	2
BDI $^{\dagger}$ /CII $^{\dagger}$	0	${}^c U_{++}^+$	$\mathbf{r}_{\perp}$	AI $^{\dagger}$ /AII $^{\dagger}$	$\tilde{c}_{+}$			${}^c U_{++}^+ = {}^c U_{++}^+$	0
	1	${}^g \bar{U}_{++}^+$						${}^g \bar{U}_{++}^+ = {}^g \bar{U}_{++}^+$	1
	2	${}^c U_{+-}^+$						${}^c U_{+-}^+ = {}^c U_{+-}^+$	2
	3	${}^g \bar{U}_{+-}^+$						${}^g \bar{U}_{+-}^+ = {}^g \bar{U}_{+-}^+$	3
BDI $^{\dagger}$ /CII $^{\dagger}$	0	${}^c U_{++}^+$	$\mathbf{r}_{\parallel}$	AI $^{\dagger}$ /AII $^{\dagger}$	$\tilde{c}_{+}$			${}^g \bar{U}_{++}^+ = \Gamma {}^c U_{++}^+$	1
	1	${}^g \bar{U}_{+-}^+$						${}^c U_{+-}^+ = i\Gamma {}^g \bar{U}_{+-}^+$	2
	2	${}^c U_{--}^+$						${}^g \bar{U}_{--}^+ = \Gamma {}^c U_{--}^+$	3
	3	${}^g \bar{U}_{--}^+$						${}^c U_{--}^+ = i\Gamma {}^g \bar{U}_{--}^+$	0
DIII $^{\dagger}$ /CI $^{\dagger}$	0	${}^c U_{++}^+$	$\mathbf{k}_{\perp}$	AII $^{\dagger}$ /AI $^{\dagger}$	$\tilde{c}_{+}$			${}^c U_{++}^+ = {}^c U_{++}^+$	0
	1	${}^g \bar{U}_{++}^+$						${}^g \bar{U}_{++}^+ = {}^g \bar{U}_{++}^+$	1
	2	${}^c U_{+-}^+$						${}^c U_{+-}^+ = {}^c U_{+-}^+$	2
	3	${}^g \bar{U}_{+-}^+$						${}^g \bar{U}_{+-}^+ = {}^g \bar{U}_{+-}^+$	3
DIII $^{\dagger}$ /CI $^{\dagger}$	0	${}^c U_{++}^+$	$\mathbf{k}_{\parallel}$	AII $^{\dagger}$ /AI $^{\dagger}$	$\tilde{c}_{+}$			${}^g \bar{U}_{++}^+ = \Gamma {}^c U_{++}^+$	3
	1	${}^g \bar{U}_{+-}^+$						${}^c U_{+-}^+ = i\Gamma {}^g \bar{U}_{+-}^+$	0
	2	${}^c U_{--}^+$						${}^g \bar{U}_{--}^+ = \Gamma {}^c U_{--}^+$	1
	3	${}^g \bar{U}_{--}^+$						${}^c U_{--}^+ = i\Gamma {}^g \bar{U}_{--}^+$	2
DIII $^{\dagger}$ /CI $^{\dagger}$	0	${}^c U_{++}^+$	$\mathbf{r}_{\perp}$	D $^{\dagger}$ /C $^{\dagger}$	$\tilde{\tau}_{-}$			${}^c U_{++}^+ = {}^c U_{++}^+$	0
	1	${}^g \bar{U}_{++}^+$						${}^g \bar{U}_{++}^+ = {}^g \bar{U}_{++}^+$	1
	2	${}^c U_{+-}^+$						${}^c U_{+-}^+ = {}^c U_{+-}^+$	2
	3	${}^g \bar{U}_{+-}^+$						${}^g \bar{U}_{+-}^+ = {}^g \bar{U}_{+-}^+$	3
DIII $^{\dagger}$ /CI $^{\dagger}$	0	${}^c U_{++}^+$	$\mathbf{r}_{\parallel}$	D $^{\dagger}$ /C $^{\dagger}$	$\tilde{\tau}_{-}$			${}^g \bar{U}_{++}^+ = \Gamma {}^c U_{++}^+$	1
	1	${}^g \bar{U}_{+-}^+$						${}^c U_{+-}^+ = i\Gamma {}^g \bar{U}_{+-}^+$	2
	2	${}^c U_{--}^+$						${}^g \bar{U}_{--}^+ = \Gamma {}^c U_{--}^+$	3
	3	${}^g \bar{U}_{--}^+$						${}^c U_{--}^+ = i\Gamma {}^g \bar{U}_{--}^+$	0

$\tau_0$ , since

$${}^c \tilde{U} \otimes \tau_0 H_c(\mathbf{k}, \mathbf{r}, \theta) {}^c \tilde{U} \otimes \tau_0 = -H^{\dagger}(-\mathbf{k}_{\parallel}, \mathbf{k}_{\perp}, -\mathbf{r}_{\parallel}, \mathbf{r}_{\perp}, \theta). \quad (\text{B2})$$

Then the mapped Hamiltonian is now in  $(s=1, t=0)$ . This process provide a homomorphism  $K_{\mathbb{C}}^U(s=0, t=0; d+D, d_{\parallel}+D_{\parallel}) \rightarrow K_{\mathbb{C}}^U(s=1, t=0; d+D+1, d_{\parallel}+D_{\parallel})$ . Following similar process for other spatial symmetries, we arrive at Table XI, which allows us to conclude

$$\begin{aligned} & K_{\mathbb{C}}^U(s, t; d+D, d_{\parallel}+D_{\parallel}, 0, 0) \\ &= K_{\mathbb{C}}^U(s+1, t; d+D+1, d_{\parallel}+D_{\parallel}, 0, 0) \\ &= K_{\mathbb{C}}^U(s+1, t+1; d+D+1, d_{\parallel}+D_{\parallel}+1, 0, 0). \quad (\text{B3}) \end{aligned}$$

This proof the relationship

$$\begin{aligned} & K_{\mathbb{C}}^U(s, t; d+D, d_{\parallel}+D_{\parallel}, 0, 0) \\ &= K_{\mathbb{C}}^U(s-d+D, t-d_{\parallel}+D_{\parallel}; 0, 0, 0, 0). \quad (\text{B4}) \end{aligned}$$

## 2. Complex AZ with order-two anti-unitary symmetries

As discussed in Sec. IV B, complex AZ classes with anti-unitary spatial symmetries will map the original class into a real AZ or  $AZ^{\dagger}$  class. The dimensional hierarchy is given by Eq.(24).

## 3. Real AZ and $AZ^{\dagger}$ with order-two symmetries

We consider a Hamiltonian in class AI with symmetry  ${}^c U_{+}^+$ . According to Table IV, this place the Hamiltonian in class  $(s=0, t=0)$ . The mapping

$$H_c(\mathbf{k}, \mathbf{r}, \theta) = \cos \theta \tilde{H}_{nc}(\mathbf{k}, \mathbf{r}) \otimes \tau_z + \sin \theta i \otimes \tau_0 \quad (\text{B5})$$

provided in Table X allows to map  $H_{nc}$  to class BDI for a momentum-like  $\theta$ . If the  $\theta$  is *not* flipped under



spatial symmetry i.e it is of the type  $\mathbf{k}_\perp$ , the mapped Hamiltonian  $H_c$  obeys  ${}^cU_{++}^+ = {}^c\tilde{U}_+^+ \otimes \tau_0$ . This place  $H_c$  in the class ( $s = 1, t = 0$ ). Recall that in Sec. IV we showed that all anti-unitary spatial symmetries are equivalent to some of the unitary ones for real AZ classes (See Table IV). The process above then provide a homomorphism  $K_{\mathbb{R}}^{U/A}(s = 0, t = 0; d, d_\parallel, D, D_\parallel) \rightarrow K_{\mathbb{R}}^{U/A}(s = 1, t = 0; d + 1, d_\parallel, D, D_\parallel)$ . Following similar process for other spatial symmetries and AZ classes, we arrive at Table XII and XIII. These two tables allow us to conclude the relationships

$$\begin{aligned}
& K_{\mathbb{R}}^{U/A}(s, t; d, d_\parallel, D, D_\parallel) \\
&= K_{\mathbb{R}}^{U/A}(s + 1, t; d + 1, d_\parallel, D, D_\parallel) \\
&= K_{\mathbb{R}}^{U/A}(s + 1, t + 1; d + 1, d_\parallel + 1, D, D_\parallel) \\
&= K_{\mathbb{R}}^{U/A}(s - 1, t; d, d_\parallel, D + 1, D_\parallel) \\
&= K_{\mathbb{R}}^{U/A}(s - 1, t - 1; d, d_\parallel, D + 1, D_\parallel + 1) \quad (\text{B6})
\end{aligned}$$

which leads to

$$\begin{aligned}
& K_{\mathbb{R}}^{U/A}(s, t; d, d_\parallel, D, D_\parallel) \\
&= K_{\mathbb{R}}^{U/A}(s - d + D, t - d_\parallel + D_\parallel; 0, 0, 0, 0). \quad (\text{B7})
\end{aligned}$$

A similar analysis of  $AZ^\dagger$  classes with spatial symmetries results in Table XIV and XV, which allows us to conclude the relationship

$$\begin{aligned}
& K_{\mathbb{R}}^{\dagger U/A}(s, t; d, d_\parallel, D, D_\parallel) \\
&= K_{\mathbb{R}}^{\dagger U/A}(s + 1, t; d + 1, d_\parallel, D, D_\parallel) \\
&= K_{\mathbb{R}}^{\dagger U/A}(s + 1, t - 1; d + 1, d_\parallel + 1, D, D_\parallel) \\
&= K_{\mathbb{R}}^{\dagger U/A}(s - 1, t; d, d_\parallel, D + 1, D_\parallel) \\
&= K_{\mathbb{R}}^{\dagger U/A}(s - 1, t + 1; d, d_\parallel, D + 1, D_\parallel + 1). \quad (\text{B8})
\end{aligned}$$

Notice that for  $AZ^\dagger$  class, the effect of  $d_\parallel + 1$  on  $t$  is reversed [compare third and fifth row of Eqs. (B6) and (B8)]. Eq. (B8) allows us to conclude

$$\begin{aligned}
& K_{\mathbb{R}}^{\dagger U/A}(s, t; d, d_\parallel, D, D_\parallel) \\
&= K_{\mathbb{R}}^{\dagger U/A}(s - d + D, t + d_\parallel - D_\parallel; 0, 0, 0, 0). \quad (\text{B9})
\end{aligned}$$

### Appendix C: Properties of Clifford Algebra

In this section, we list several useful properties that Clifford Algebra obeys [12, 16].

The complex Clifford algebras obeys

$$Cl_1 \simeq \mathbb{C} \oplus \mathbb{C} \quad (\text{C1})$$

$$Cl_2 \simeq \mathbb{C}(2) \quad (\text{C2})$$

$$Cl_{n+2} \simeq Cl_n \oplus \mathbb{C}(2). \quad (\text{C3})$$

Notably,  $\mathbb{C}(2)$  that represents  $2 \times 2$  complex matrices does not affect the extension problem. This means the

extension problem  $Cl_p \otimes \mathbb{C}(2) \rightarrow Cl_p \otimes \mathbb{C}(2)$  is equivalent to the extension problem  $Cl_p \rightarrow Cl_{p+1}$ .

The real Clifford algebras obeys

$$Cl_{0,1} \simeq \mathbb{R} \oplus \mathbb{R} \quad (\text{C4})$$

$$Cl_{0,2} \simeq \mathbb{R}(2) \quad (\text{C5})$$

$$Cl_{1,0} \simeq \mathbb{C} \quad (\text{C6})$$

$$Cl_{2,0} \simeq \mathbb{H} \quad (\text{C7})$$

$$Cl_{p+1,q+1} \simeq Cl_{p,q} \otimes \mathbb{R} \quad (\text{C8})$$

$$Cl_{p,q} \otimes Cl_{0,1} \simeq Cl_{p,q} \oplus Cl_{p,q} \quad (\text{C9})$$

$$Cl_{p,q} \otimes Cl_{1,0} \simeq Cl_{p+q} \quad (\text{C10})$$

$$Cl_{p,q} \otimes Cl_{0,2} \simeq Cl_{q,p+2} \quad (\text{C11})$$

$$Cl_{p,q} \otimes Cl_{2,0} \simeq Cl_{q+2,p}, \quad (\text{C12})$$

where  $\mathbb{H}$  denotes the set of quaternions,  $\mathbb{R}(2)$  denotes the  $2 \times 2$  real matrices. Similar to the previous case,  $\mathbb{R}(2)$  does not affect the classification. This means extension problem  $Cl_{p,q} \otimes \mathbb{R}(2) \rightarrow Cl_{p,q+1} \otimes \mathbb{R}(2)$  is equivalent to the extension problem  $Cl_{p,q} \rightarrow Cl_{p,q+1}$ , and similar for  $p$  to  $p + 1$ .

### Appendix D: Classifying space of AZ and $AZ^\dagger$ with spatial symmetries from Clifford algebra

In this section, we introduce the process of finding the classifying space of Hamiltonians in AZ and  $AZ^\dagger$  class with additional spatial symmetries. The process is identical to Ref. [12, 16]. Since we have showed in Sec. IV that all antiunitary spatial symmetries can be mapped to unitary one, we only need to consider the addition of unitary symmetries to Hamiltonian.

#### 1. Complex AZ classes

First we consider complex AZ classes. The complex Clifford algebra  $Cl_p$  is generated by a set of generators  $Cl_p = \{e_1, e_2, \dots, e_p\}$ , where all of the generators anti-commute with each other  $\{e_i, e_j\} = \delta_{i,j}$ . Physically, these generators are symmetry operators of the Hamiltonian. The classification space can be found by the addition of extended Hamiltonian to the generators. Since the extended Hamiltonian obeys  $\tilde{H}^2 = 1$ , we can put them into the generators without violating the properties of the set. The addition of Hamiltonian extends the generators by  $Cl_p \rightarrow Cl_{p+1}$ :

$$\{e_1, e_2, \dots, e_p\} \rightarrow \{\tilde{H}, e_1, e_2, \dots, e_p\}. \quad (\text{D1})$$

The mapping from  $Cl_p \rightarrow Cl_{p+1}$  provides us the classification space  $\mathcal{C}_p$ . Furthermore,  $\mathcal{C}_p$  obeys the so-called Bott periodicity  $\mathcal{C}_{p+2} \simeq \mathcal{C}_p$ . The Bott periodicity of complex Clifford algebra is the origin of two complex AZ classes. Hereafter, when referring to generator, we also include Hamiltonian.

TABLE XVI: Classification of 16-fold AZ and AZ<sup>†</sup> classes under additional order-two unitary symmetries. Specific symmetries for each class is given in table IV for AZ classes and table V for AZ<sup>†</sup> classes.

Class	Symmetry	Generators	Extensions	Classifying space
A	$t_0$	$\{\tilde{H}, \Sigma\} \otimes \{^c U\}$	$Cl_1 \otimes Cl_1 \rightarrow Cl_2 \otimes Cl_1$	$\mathcal{C}_1 \times \mathcal{C}_1$
	$t_1$	$\{\tilde{H}, \Sigma, \Sigma^g U\}$	$Cl_2 \rightarrow Cl_3$	$\mathcal{C}_0$
AIII	$t_0$	$\{\tilde{H}, \Sigma, \tilde{\Gamma}\} \otimes \{\Sigma \tilde{\Gamma}^g \tilde{U}_-\}$	$Cl_2 \otimes Cl_1 \rightarrow Cl_3 \otimes Cl_1$	$\mathcal{C}_0 \times \mathcal{C}_0$
	$t_1$	$\{\tilde{H}, \Sigma, \tilde{\Gamma}, \Sigma^g \tilde{U}_+\}$	$Cl_3 \rightarrow Cl_4$	$\mathcal{C}_1$
AI	$t_0$	$\{J\tilde{H}, J\Sigma, \tilde{T}_+, J\tilde{T}_+\} \otimes \{^c U_+\}$	$Cl_{1,2} \otimes Cl_{0,1} \rightarrow Cl_{2,2} \otimes Cl_{0,1}$	$\mathcal{R}_1 \times \mathcal{R}_1$
	$t_1$	$\{J\tilde{H}, J\Sigma, \tilde{T}_+, J\tilde{T}_+, J\Sigma^g \tilde{U}_+\}$	$Cl_{1,3} \rightarrow Cl_{2,3}$	$\mathcal{R}_0$
	$t_2$	$\{J\tilde{H}, J\Sigma, \tilde{T}_+, J\tilde{T}_+\} \otimes \{^c U_-\}$	$Cl_{1,2} \otimes Cl_{1,0} \rightarrow Cl_{2,2} \otimes Cl_{1,0}$	$\mathcal{C}_1$
	$t_3$	$\{J\tilde{H}, J\Sigma, \tilde{T}_+, J\tilde{T}_+, J\Sigma^g \tilde{U}_-\}$	$Cl_{2,2} \rightarrow Cl_{3,2}$	$\mathcal{R}_2$
BDI	$t_0$	$\{\tilde{H}, \tilde{C}_-, J\tilde{C}_-, J\tilde{C}_- \tilde{T}_+, \Sigma\} \otimes \{^c U_{++}\}$	$Cl_{1,3} \otimes Cl_{0,1} \rightarrow Cl_{1,4} \otimes Cl_{0,1}$	$\mathcal{R}_2 \times \mathcal{R}_2$
	$t_1$	$\{\tilde{H}, \tilde{C}_-, J\tilde{C}_-, J\tilde{C}_- \tilde{T}_+, \Sigma, \Sigma^g U_{++}\}$	$Cl_{2,3} \rightarrow Cl_{2,4}$	$\mathcal{R}_1$
	$t_2$	$\{\tilde{H}, \tilde{C}_-, J\tilde{C}_-, J\tilde{C}_- \tilde{T}_+, \Sigma\} \otimes \{^c \tilde{U}_{++}\}$	$Cl_{1,3} \otimes Cl_{1,0} \rightarrow Cl_{1,4} \otimes Cl_{1,0}$	$\mathcal{C}_0$
	$t_3$	$\{\tilde{H}, \tilde{C}_-, J\tilde{C}_-, J\tilde{C}_- \tilde{T}_+, \Sigma, \Sigma^g U_{++}\}$	$Cl_{1,4} \rightarrow Cl_{1,5}$	$\mathcal{R}_3$
D	$t_0$	$\{\tilde{H}, \tilde{C}_-, J\tilde{C}_-, \Sigma\} \otimes \{^c U_+\}$	$Cl_{0,3} \otimes Cl_{0,1} \rightarrow Cl_{0,4} \otimes Cl_{0,1}$	$\mathcal{R}_3 \times \mathcal{R}_3$
	$t_1$	$\{\tilde{H}, \tilde{C}_-, J\tilde{C}_-, \Sigma, \Sigma^g U_+\}$	$Cl_{1,3} \rightarrow Cl_{1,4}$	$\mathcal{R}_2$
	$t_2$	$\{\tilde{H}, \tilde{C}_-, J\tilde{C}_-, \Sigma\} \otimes \{^c \tilde{U}_-\}$	$Cl_{0,3} \otimes Cl_{1,0} \rightarrow Cl_{0,4} \otimes Cl_{0,4} \otimes Cl_{1,0}$	$\mathcal{C}_1$
	$t_3$	$\{\tilde{H}, \tilde{C}_-, J\tilde{C}_-, \Sigma, \Sigma^g U_-\}$	$Cl_{0,4} \rightarrow Cl_{0,5}$	$\mathcal{R}_4$
DIII	$t_0$	$\{\tilde{H}, \tilde{C}_-, J\tilde{C}_-, J\tilde{C}_- \tilde{T}_+, \Sigma\} \otimes \{^c U_{++}\}$	$Cl_{0,4} \otimes Cl_{0,1} \rightarrow Cl_{0,5} \otimes Cl_{0,1}$	$\mathcal{R}_4 \times \mathcal{R}_4$
	$t_1$	$\{\tilde{H}, \tilde{C}_-, J\tilde{C}_-, J\tilde{C}_- \tilde{T}_+, \Sigma, \Sigma^g U_{++}\}$	$Cl_{1,4} \rightarrow Cl_{1,5}$	$\mathcal{R}_3$
	$t_2$	$\{\tilde{H}, \tilde{C}_-, J\tilde{C}_-, J\tilde{C}_- \tilde{T}_+, \Sigma\} \otimes \{^c \tilde{U}_{++}\}$	$Cl_{0,4} \otimes Cl_{1,0} \rightarrow Cl_{0,5} \otimes Cl_{1,0}$	$\mathcal{C}_0$
	$t_3$	$\{\tilde{H}, \tilde{C}_-, J\tilde{C}_-, J\tilde{C}_- \tilde{T}_+, \Sigma, \Sigma^g U_{++}\}$	$Cl_{0,5} \rightarrow Cl_{0,6}$	$\mathcal{R}_5$
AII	$t_0$	$\{J\tilde{H}, J\Sigma, \tilde{T}_+, J\tilde{T}_+\} \otimes \{^c U_+\}$	$Cl_{3,0} \otimes Cl_{0,1} \rightarrow Cl_{4,0} \otimes Cl_{0,1}$	$\mathcal{R}_5 \times \mathcal{R}_5$
	$t_1$	$\{J\tilde{H}, J\Sigma, \tilde{T}_+, J\tilde{T}_+, J\Sigma^g U_+\}$	$Cl_{3,1} \rightarrow Cl_{4,1}$	$\mathcal{R}_4$
	$t_2$	$\{J\tilde{H}, J\Sigma, \tilde{T}_+, J\tilde{T}_+\} \otimes \{^c \tilde{U}_-\}$	$Cl_{3,0} \otimes Cl_{1,0} \rightarrow Cl_{4,0} \otimes Cl_{1,0}$	$\mathcal{C}_1$
	$t_3$	$\{J\tilde{H}, J\Sigma, \tilde{T}_+, J\tilde{T}_+, J\Sigma^g U_-\}$	$Cl_{4,0} \rightarrow Cl_{5,0}$	$\mathcal{R}_6$
CII	$t_0$	$\{\tilde{H}, \tilde{C}_-, J\tilde{C}_-, J\tilde{C}_- \tilde{T}_+, \Sigma\} \otimes \{^c U_{++}\}$	$Cl_{3,1} \otimes Cl_{0,1} \rightarrow Cl_{3,2} \otimes Cl_{0,1}$	$\mathcal{R}_6 \times \mathcal{R}_6$
	$t_1$	$\{\tilde{H}, \tilde{C}_-, J\tilde{C}_-, J\tilde{C}_- \tilde{T}_+, \Sigma, \Sigma^g U_{++}\}$	$Cl_{4,1} \rightarrow Cl_{4,2}$	$\mathcal{R}_5$
	$t_2$	$\{\tilde{H}, \tilde{C}_-, J\tilde{C}_-, J\tilde{C}_- \tilde{T}_+, \Sigma\} \otimes \{^c \tilde{U}_{++}\}$	$Cl_{3,1} \otimes Cl_{1,0} \rightarrow Cl_{3,2} \otimes Cl_{1,0}$	$\mathcal{C}_0$
	$t_3$	$\{\tilde{H}, \tilde{C}_-, J\tilde{C}_-, J\tilde{C}_- \tilde{T}_+, \Sigma, \Sigma^g U_{++}\}$	$Cl_{3,2} \rightarrow Cl_{3,3}$	$\mathcal{R}_7$
C	$t_0$	$\{\tilde{H}, \tilde{C}_-, J\tilde{C}_-, \Sigma\} \otimes \{^c U_+\}$	$Cl_{2,1} \otimes Cl_{0,1} \rightarrow Cl_{2,2} \otimes Cl_{0,1}$	$\mathcal{R}_7 \times \mathcal{R}_7$
	$t_1$	$\{\tilde{H}, \tilde{C}_-, J\tilde{C}_-, \Sigma, \Sigma^g U_+\}$	$Cl_{3,1} \rightarrow Cl_{3,2}$	$\mathcal{R}_6$
	$t_2$	$\{\tilde{H}, \tilde{C}_-, J\tilde{C}_-, \Sigma\} \otimes \{^c \tilde{U}_-\}$	$Cl_{2,1} \otimes Cl_{1,0} \rightarrow Cl_{2,2} \otimes Cl_{0,4} \otimes Cl_{1,0}$	$\mathcal{C}_1$
	$t_3$	$\{\tilde{H}, \tilde{C}_-, J\tilde{C}_-, \Sigma, \Sigma^g U_-\}$	$Cl_{2,2} \rightarrow Cl_{2,3}$	$\mathcal{R}_0$
CI	$t_0$	$\{\tilde{H}, \tilde{C}_-, J\tilde{C}_-, J\tilde{C}_- \tilde{T}_+, \Sigma\} \otimes \{^c U_{++}\}$	$Cl_{2,2} \otimes Cl_{0,1} \rightarrow Cl_{2,3} \otimes Cl_{0,1}$	$\mathcal{R}_0 \times \mathcal{R}_0$
	$t_1$	$\{\tilde{H}, \tilde{C}_-, J\tilde{C}_-, J\tilde{C}_- \tilde{T}_+, \Sigma, \Sigma^g U_{++}\}$	$Cl_{3,2} \rightarrow Cl_{3,3}$	$\mathcal{R}_7$
	$t_2$	$\{\tilde{H}, \tilde{C}_-, J\tilde{C}_-, J\tilde{C}_- \tilde{T}_+, \Sigma\} \otimes \{^c \tilde{U}_{++}\}$	$Cl_{2,2} \otimes Cl_{1,0} \rightarrow Cl_{2,3} \otimes Cl_{1,0}$	$\mathcal{C}_0$
	$t_3$	$\{\tilde{H}, \tilde{C}_-, J\tilde{C}_-, J\tilde{C}_- \tilde{T}_+, \Sigma, \Sigma^g U_{++}\}$	$Cl_{2,3} \rightarrow Cl_{2,4}$	$\mathcal{R}_1$
AI <sup>†</sup>	$t_0$	$\{J\tilde{H}, \Sigma, \tilde{C}_+, J\tilde{C}_+\} \otimes \{^c U_+\}$	$Cl_{0,3} \otimes Cl_{0,1} \rightarrow Cl_{1,3} \otimes Cl_{0,1}$	$\mathcal{R}_7 \times \mathcal{R}_7$
	$t_1$	$\{J\tilde{H}, \Sigma, \tilde{C}_+, J\tilde{C}_+, \Sigma^g U_+\}$	$Cl_{1,3} \rightarrow Cl_{2,3}$	$\mathcal{R}_0$
	$t_2$	$\{J\tilde{H}, \Sigma, \tilde{C}_+, J\tilde{C}_+\} \otimes \{^c \tilde{U}_-\}$	$Cl_{0,3} \otimes Cl_{1,0} \rightarrow Cl_{1,3} \otimes Cl_{1,0}$	$\mathcal{C}_1$
	$t_3$	$\{J\tilde{H}, \Sigma, \tilde{C}_+, J\tilde{C}_+, \Sigma^g U_-\}$	$Cl_{0,4} \rightarrow Cl_{1,4}$	$\mathcal{R}_6$
BDI <sup>†</sup>	$t_0$	$\{J\tilde{H}, \tilde{C}_+, J\tilde{C}_+, J\tilde{C}_+ \tilde{T}_-, \Sigma\} \otimes \{^c U_{++}\}$	$Cl_{1,3} \otimes Cl_{0,1} \rightarrow Cl_{2,3} \otimes Cl_{0,1}$	$\mathcal{R}_0 \times \mathcal{R}_0$
	$t_1$	$\{J\tilde{H}, \tilde{C}_+, J\tilde{C}_+, J\tilde{C}_+ \tilde{T}_-, \Sigma, \Sigma^g U_{++}\}$	$Cl_{2,3} \rightarrow Cl_{3,3}$	$\mathcal{R}_1$
	$t_2$	$\{J\tilde{H}, \tilde{C}_+, J\tilde{C}_+, J\tilde{C}_+ \tilde{T}_-, \Sigma\} \otimes \{^c \tilde{U}_{++}\}$	$Cl_{1,3} \otimes Cl_{1,0} \rightarrow Cl_{2,3} \otimes Cl_{1,0}$	$\mathcal{C}_0$
	$t_3$	$\{J\tilde{H}, \tilde{C}_+, J\tilde{C}_+, J\tilde{C}_+ \tilde{T}_-, \Sigma, \Sigma^g U_{++}\}$	$Cl_{1,4} \rightarrow Cl_{2,4}$	$\mathcal{R}_7$
D <sup>†</sup>	$t_0$	$\{\tilde{H}, J\Sigma, \tilde{T}_-, J\tilde{T}_-\} \otimes \{^c \tilde{U}_+\}$	$Cl_{1,2} \otimes Cl_{0,1} \rightarrow Cl_{1,3} \otimes Cl_{0,1}$	$\mathcal{R}_1 \times \mathcal{R}_1$
	$t_1$	$\{\tilde{H}, J\Sigma, \tilde{T}_-, J\tilde{T}_-, J\Sigma^g \tilde{U}_+\}$	$Cl_{1,3} \otimes Cl_{1,4}$	$\mathcal{R}_2$
	$t_2$	$\{\tilde{H}, J\Sigma, \tilde{T}_-, J\tilde{T}_-\} \otimes \{^c \tilde{U}_-\}$	$Cl_{1,2} \otimes Cl_{1,0} \rightarrow Cl_{1,3} \otimes Cl_{1,0}$	$\mathcal{C}_1$
	$t_3$	$\{\tilde{H}, J\Sigma, \tilde{T}_-, J\tilde{T}_-, J\Sigma^g \tilde{U}_-\}$	$Cl_{2,2} \otimes Cl_{2,3}$	$\mathcal{R}_0$
DIII <sup>†</sup>	$t_0$	$\{J\tilde{H}, \tilde{C}_+, J\tilde{C}_+, J\tilde{C}_+ \tilde{T}_-, \Sigma\} \otimes \{^c U_{++}\}$	$Cl_{2,2} \otimes Cl_{0,1} \rightarrow Cl_{3,2} \otimes Cl_{0,1}$	$\mathcal{R}_2 \times \mathcal{R}_2$
	$t_1$	$\{J\tilde{H}, \tilde{C}_+, J\tilde{C}_+, J\tilde{C}_+ \tilde{T}_-, \Sigma, \Sigma^g U_{++}\}$	$Cl_{3,2} \rightarrow Cl_{4,2}$	$\mathcal{R}_3$
	$t_2$	$\{J\tilde{H}, \tilde{C}_+, J\tilde{C}_+, J\tilde{C}_+ \tilde{T}_-, \Sigma\} \otimes \{^c \tilde{U}_{++}\}$	$Cl_{2,2} \otimes Cl_{1,0} \rightarrow Cl_{3,2} \otimes Cl_{1,0}$	$\mathcal{C}_0$
	$t_3$	$\{J\tilde{H}, \tilde{C}_+, J\tilde{C}_+, J\tilde{C}_+ \tilde{T}_-, \Sigma, \Sigma^g U_{++}\}$	$Cl_{2,3} \rightarrow Cl_{3,3}$	$\mathcal{R}_1$
AII <sup>†</sup>	$t_0$	$\{J\tilde{H}, \Sigma, \tilde{C}_+, J\tilde{C}_+\} \otimes \{^c U_+\}$	$Cl_{2,1} \otimes Cl_{0,1} \rightarrow Cl_{3,1} \otimes Cl_{0,1}$	$\mathcal{R}_3 \times \mathcal{R}_3$
	$t_1$	$\{J\tilde{H}, \Sigma, \tilde{C}_+, J\tilde{C}_+, \Sigma^g U_+\}$	$Cl_{3,1} \rightarrow Cl_{4,1}$	$\mathcal{R}_4$
	$t_2$	$\{J\tilde{H}, \Sigma, \tilde{C}_+, J\tilde{C}_+\} \otimes \{^c \tilde{U}_-\}$	$Cl_{2,1} \otimes Cl_{1,0} \rightarrow Cl_{3,1} \otimes Cl_{1,0}$	$\mathcal{C}_1$
	$t_3$	$\{J\tilde{H}, \Sigma, \tilde{C}_+, J\tilde{C}_+, \Sigma^g U_-\}$	$Cl_{2,2} \rightarrow Cl_{3,2}$	$\mathcal{R}_2$

TABLE VI: (continue)

CIII <sup>†</sup>	$t_0$	$\{J\tilde{H}, \tilde{C}_+, J\tilde{C}_+, J\tilde{C}_+\tilde{T}_-, \Sigma\} \otimes \{^c\tilde{U}_{++}^+\}$	$Cl_{3,1} \otimes Cl_{0,1} \rightarrow Cl_{4,1} \otimes Cl_{0,1}$	$\mathcal{R}_4 \times \mathcal{R}_4$
	$t_1$	$\{J\tilde{H}, \tilde{C}_+, J\tilde{C}_+, J\tilde{C}_+\tilde{T}_-, \Sigma, \Sigma^g\tilde{U}_{++}^+\}$	$Cl_{4,1} \rightarrow Cl_{5,1}$	$\mathcal{R}_5$
	$t_2$	$\{J\tilde{H}, \tilde{C}_+, J\tilde{C}_+, J\tilde{C}_+\tilde{T}_-, \Sigma\} \otimes \{^c\tilde{U}_{++}^-\}$	$Cl_{3,1} \otimes Cl_{1,0} \rightarrow Cl_{4,1} \otimes Cl_{1,0}$	$\mathcal{C}_0$
	$t_3$	$\{J\tilde{H}, \tilde{C}_+, J\tilde{C}_+, J\tilde{C}_+\tilde{T}_-, \Sigma, \Sigma^g\tilde{U}_{++}^+\}$	$Cl_{3,2} \rightarrow Cl_{4,2}$	$\mathcal{R}_3$
C <sup>†</sup>	$t_0$	$\{\tilde{H}, J\Sigma, \tilde{T}_-, J\tilde{T}_-\} \otimes \{^c\tilde{U}_{++}^+\}$	$Cl_{3,0} \otimes Cl_{0,1} \rightarrow Cl_{3,1} \otimes Cl_{0,1}$	$\mathcal{R}_5 \times \mathcal{R}_5$
	$t_1$	$\{\tilde{H}, J\Sigma, \tilde{T}_-, J\tilde{T}_-, J\Sigma^g\tilde{U}_{++}^+\}$	$Cl_{3,1} \rightarrow Cl_{3,2}$	$\mathcal{R}_6$
	$t_2$	$\{\tilde{H}, J\Sigma, \tilde{T}_-, J\tilde{T}_-\} \otimes \{^c\tilde{U}_{++}^-\}$	$Cl_{3,0} \otimes Cl_{1,0} \rightarrow Cl_{3,1} \otimes Cl_{1,0}$	$\mathcal{C}_1$
	$t_3$	$\{\tilde{H}, J\Sigma, \tilde{T}_-, J\tilde{T}_-, J\Sigma^g\tilde{U}_{++}^+\}$	$Cl_{4,0} \otimes Cl_{4,1}$	$\mathcal{R}_4$
CI <sup>†</sup>	$t_0$	$\{J\tilde{H}, \tilde{C}_+, J\tilde{C}_+, J\tilde{C}_+\tilde{T}_-, \Sigma\} \otimes \{^c\tilde{U}_{++}^+\}$	$Cl_{0,4} \otimes Cl_{0,1} \rightarrow Cl_{1,4} \otimes Cl_{0,1}$	$\mathcal{R}_6 \times \mathcal{R}_6$
	$t_1$	$\{J\tilde{H}, \tilde{C}_+, J\tilde{C}_+, J\tilde{C}_+\tilde{T}_-, \Sigma, \Sigma^g\tilde{U}_{++}^+\}$	$Cl_{1,4} \rightarrow Cl_{2,4}$	$\mathcal{R}_7$
	$t_2$	$\{J\tilde{H}, \tilde{C}_+, J\tilde{C}_+, J\tilde{C}_+\tilde{T}_-, \Sigma\} \otimes \{^c\tilde{U}_{++}^-\}$	$Cl_{0,4} \otimes Cl_{1,4} \rightarrow Cl_{4,1} \otimes Cl_{1,0}$	$\mathcal{C}_0$
	$t_3$	$\{J\tilde{H}, \tilde{C}_+, J\tilde{C}_+, J\tilde{C}_+\tilde{T}_-, \Sigma, \Sigma^g\tilde{U}_{++}^+\}$	$Cl_{0,5} \rightarrow Cl_{1,5}$	$\mathcal{R}_5$

The generators for point-gapped Hamiltonian with *only* internal symmetries (5) are provided in Ref. [37]. Notice that Ref. [37] used a different notation systems for symmetry classes from this paper and Kohei [24]. The relationship between these two different notation systems can be found in Ref. [48].

The addition of spatial symmetries would change the classification of original classes. To see this, let's consider a order-two spatial symmetry  $L$  is added to the classification. There are two possible ways in which the addition of  $L$  changes the classification.

(1) Through combination of  $L$  with other generators, the resulting generator  $L'$  might *anti-commute* with all other generators i.e.  $\{L', e_i\} = 0$  for all  $i$  and  $\{L', H\} = 0$ . In such a case, the generators would become  $\{\tilde{H}, e_1, e_2, \dots, e_p, L'\}$ . Correspondingly, the classifying space would shift by  $\mathcal{C}_p \rightarrow \mathcal{C}_{p+1}$ .

(2) It is also possible that  $L'$  *commutes* with all other generators i.e.  $[L', e_i] = 0$  for all  $i$  and  $[L', H] = 0$ . The generators then become  $\{\tilde{H}, e_1, \dots, e_p\} \otimes L'$ . In this case, the Hilbert space splits into two eigenspaces of  $L'$ . Each eigenspace has the same Clifford algebra and hence the same classifying space. The classifying space then becomes  $\mathcal{C}_p \times \mathcal{C}_p$ .

As an example, consider a point-gapped Hamiltonian in class A. The only symmetry  $\tilde{H}$  obeys in this class is the  $\Sigma$  symmetry [Eq. (9)]. Therefore, the Hamiltonian extends the generators as

$$\{\Sigma\} \rightarrow \{\tilde{H}, \Sigma\} \quad (D2)$$

which has classification space  $\mathcal{C}_1$ . This is the classification of class A given in Table I. Next, consider the addition of spatial symmetry  $^g\tilde{U}$  to the system. Recall that  $^g\tilde{U}$  anti-commutes with  $\tilde{H}$ . Then the operator  $\Sigma^g\tilde{U}$  anti-commutes with both  $\tilde{H}$  and  $\Sigma$ . Now, the generators are given by

$$\{\Sigma, \Sigma^g\tilde{U}\} \rightarrow \{\tilde{H}, \Sigma, \Sigma^g\tilde{U}\} \quad (D3)$$

which has classifying space  $\mathcal{C}_2 \simeq \mathcal{C}_0$ .

As another example, we consider a point-gapped Hamiltonian in class A with the addition of  $^c\tilde{U}$ . Recall that the extended operator  $^c\tilde{U}$  that acts on extended Hamiltonian  $\tilde{H}$  commutes with both  $\tilde{H}$  and  $\Sigma$ . Therefore, the generators are now given by

$$\{\Sigma\} \otimes ^c\tilde{U} \rightarrow \{\tilde{H}, \Sigma\} \otimes ^c\tilde{U}, \quad (D4)$$

which has classifying space  $\mathcal{C}_1 \times \mathcal{C}_1$ .

Following a similar process, we summarize the classification of complex AZ classes under spatial symmetries in the first two rows of Table XVI.

## 2. Real AZ and AZ<sup>†</sup> classes

Now consider real AZ and AZ<sup>†</sup> classes. Their classifying space are given by the real Clifford algebra  $Cl_{p,q} = \{e_1, \dots, e_p, e_{p+1}, \dots, e_{p+q}\}$ , where  $\{e_i, e_j\} = \delta_{i,j}$ ,  $e_i^2 = -1$  for  $i = 1, \dots, p$  and  $e_i^2 = 1$  for  $i = p+1, \dots, p+q$ . In this case, the Hamiltonian can extend the generators by

$$\begin{aligned} Cl_{p,q} = \{e_1, \dots, e_{p+q}\} &\rightarrow Cl_{p+1,q} = \{\tilde{H}, e_1, \dots, e_{p+q}\} \\ \tilde{H} &= -1. \end{aligned} \quad (D5)$$

In this case, the classifying space is given by  $\mathcal{R}_{p+2-q}$ . Hamiltonian can also extend the generators by

$$\begin{aligned} Cl_{p,q} = \{e_1, \dots, e_{p+q}\} &\rightarrow Cl_{p,q+1} = \{\tilde{H}, e_1, \dots, e_{p+q}\} \\ \tilde{H} &= 1. \end{aligned} \quad (D6)$$

The classifying space is given by  $\mathcal{R}_{q-p}$ .

Now let's consider the addition of order-two spatial symmetry  $L$ . Similar to complex AZ classes, through the combination of  $L$  and other generators as well as the imaginary unit  $J$ , the resulting generator  $L'$  would commute or anti-commute with the rest of the generators. However, due to the presence of antiunitary symmetries, we need to consider the squared value of  $L'$ . Since  $L'^2 = \pm 1$ , we have four possible situations.

(1)  $L'$  anti-commutes with all generators and  $L'^2 = -1$ . In this case the generators would change by  $p \rightarrow p+1$ .

The new classifying space would be  $\mathcal{R}_{q-p-1}$  ( $\mathcal{R}_{p+3-q}$ ) if  $\tilde{H} = -1$  (1)

(2)  $L'$  anti-commutes with all generators and  $L'^2 = 1$ . In this case the generators would change by  $q \rightarrow q + 1$ . The new classifying space would be  $\mathcal{R}_{q+1-p}$  ( $\mathcal{R}_{p+1-q}$ ) if  $\tilde{H} = -1$  (1)

(3)  $L'$  commutes with all generators and  $L'^2 = -1$ . In this case,  $L'$  would introduce complex structure to real Clifford algebra. The set of generators without Hamiltonian is written as  $Cl_{p,q} \otimes Cl_{1,0}$ . Thus, the classifying space would be the same as complex AZ classes. In fact, we have the relationship  $Cl_{p,q} \otimes Cl_{1,0} \simeq Cl_{p+q}$  (Appendix C). The classifying space is then given by  $\mathcal{C}_{p+q}$ .

(4)  $L'$  commutes with all generators and  $L'^2 = 1$ . In this case, the Hilbert space splits into two eigenspace of  $L'$ . The classifying space is given by  $\mathcal{R}_{q-p} \times \mathcal{R}_{q-p}$  ( $\mathcal{R}_{p+2-q} \times \mathcal{R}_{p+2-q}$ ) if  $\tilde{H} = -1$  (1).

As an example, we consider the classification of class AI in addition to  ${}^gU_+^+$ . The generators for point-gapped

AI class is given by [37]

$$Cl_{2,2} = \{J\tilde{H}, J\Sigma, \tilde{\mathcal{T}}_+, J\tilde{\mathcal{T}}_+\}, \quad (D7)$$

where  $\mathcal{T}_+$  is the TRS operator and  $\Sigma$  is the  $\Sigma$  symmetry (9). Since  $(J\tilde{H})^2 = -1$ , the extension is  $Cl_{1,2} \rightarrow Cl_{2,2}$  which gives classifying space  $\mathcal{R}_1$ . Now we consider the addition of spatial symmetry  ${}^gU_+^+$ . Notice that  $J\Sigma {}^g\tilde{U}_+^+$  anti-commutes with all the generators in Eq. (D7) and it squares to 1 (Recall that  $\Sigma$  and  ${}^g\tilde{U}_+^+$  anti-commute). Therefore, the new set of generators is

$$Cl_{2,3} = \{J\tilde{H}, J\Sigma, \tilde{\mathcal{T}}_+, J\tilde{\mathcal{T}}_+, J\Sigma {}^g\tilde{U}_+^+\}. \quad (D8)$$

The extension is now given by  $Cl_{1,3} \rightarrow Cl_{2,3}$ , which gives classifying space  $\mathcal{R}_0$ .

Following these procedures, we arrive at Table XVI for real AZ and  $AZ^\dagger$  classes.

- 
- [1] X.-L. Qi and S.-C. Zhang, Topological insulators and superconductors, *Rev. Mod. Phys.* **83**, 1057 (2011).
- [2] M. Z. Hasan and C. L. Kane, Colloquium: Topological insulators, *Rev. Mod. Phys.* **82**, 3045 (2010).
- [3] J. E. Moore, The birth of topological insulators, *Nature* **464**, 194–198 (2010).
- [4] M. Sato and Y. Ando, Topological superconductors: a review, *Reports on Progress in Physics* **80**, 076501 (2017).
- [5] A. Kitaev, V. Lebedev, and M. Feigel'man, Periodic table for topological insulators and superconductors, AIP Conference Proceedings [10.1063/1.3149495](https://doi.org/10.1063/1.3149495) (2009).
- [6] A. Altland and M. R. Zirnbauer, Nonstandard symmetry classes in mesoscopic normal-superconducting hybrid structures, *Phys. Rev. B* **55**, 1142 (1997).
- [7] C.-K. Chiu, J. C. Y. Teo, A. P. Schnyder, and S. Ryu, Classification of topological quantum matter with symmetries, *Rev. Mod. Phys.* **88**, 035005 (2016).
- [8] C. L. Kane and E. J. Mele,  $Z_2$  topological order and the quantum spin hall effect, *Phys. Rev. Lett.* **95**, 146802 (2005).
- [9] C. L. Kane and E. J. Mele, Quantum spin hall effect in graphene, *Phys. Rev. Lett.* **95**, 226801 (2005).
- [10] J. C. Y. Teo and C. L. Kane, Topological defects and gapless modes in insulators and superconductors, *Phys. Rev. B* **82**, 115120 (2010).
- [11] J. C. Teo and T. L. Hughes, Topological defects in symmetry-protected topological phases, *Annual Review of Condensed Matter Physics* **8**, 211–237 (2017).
- [12] K. Shiozaki and M. Sato, Topology of crystalline insulators and superconductors, *Phys. Rev. B* **90**, 165114 (2014).
- [13] L. Fu and C. L. Kane, Topological insulators with inversion symmetry, *Phys. Rev. B* **76**, 045302 (2007).
- [14] L. Fu, Topological crystalline insulators, *Phys. Rev. Lett.* **106**, 106802 (2011).
- [15] C.-K. Chiu, H. Yao, and S. Ryu, Classification of topological insulators and superconductors in the presence of reflection symmetry, *Phys. Rev. B* **88**, 075142 (2013).
- [16] T. Morimoto and A. Furusaki, Topological classification with additional symmetries from clifford algebras, *Phys. Rev. B* **88**, 125129 (2013).
- [17] K. Shiozaki, M. Sato, and K. Gomi, Topology of non-symmorphic crystalline insulators and superconductors, *Phys. Rev. B* **93**, 195413 (2016).
- [18] K. Shiozaki, M. Sato, and K. Gomi, Topological crystalline materials: General formulation, module structure, and wallpaper groups, *Phys. Rev. B* **95**, 235425 (2017).
- [19] J. Cano, B. Bradlyn, Z. Wang, L. Elcoro, M. G. Vergniory, C. Felser, M. I. Aroyo, and B. A. Bernevig, Building blocks of topological quantum chemistry: Elementary band representations, *Phys. Rev. B* **97**, 035139 (2018).
- [20] B. Bradlyn, L. Elcoro, J. Cano, M. G. Vergniory, Z. Wang, C. Felser, M. I. Aroyo, and B. A. Bernevig, Topological quantum chemistry, *Nature* **547**, 298–305 (2017).
- [21] S. Yao and Z. Wang, Edge states and topological invariants of non-hermitian systems, *Phys. Rev. Lett.* **121**, 086803 (2018).
- [22] F. Song, S. Yao, and Z. Wang, Non-hermitian skin effect and chiral damping in open quantum systems, *Phys. Rev. Lett.* **123**, 170401 (2019).
- [23] N. Okuma, K. Kawabata, K. Shiozaki, and M. Sato, Topological origin of non-hermitian skin effects, *Phys. Rev. Lett.* **124**, 086801 (2020).
- [24] K. Kawabata, K. Shiozaki, M. Ueda, and M. Sato, Symmetry and topology in non-hermitian physics, *Phys. Rev. X* **9**, 041015 (2019).
- [25] M.-H. L. Xiujuan Zhang, Tian Zhang and Y.-F. Chen, A review on non-hermitian skin effect, *Advances in Physics: X* **7**, 2109431 (2022), <https://doi.org/10.1080/23746149.2022.2109431>.
- [26] K. Zhang, Z. Yang, and C. Fang, Universal non-hermitian skin effect in two and higher dimensions, *Nature Communications* **13**, [10.1038/s41467-022-30161-6](https://doi.org/10.1038/s41467-022-30161-6) (2022).
- [27] R. Lin, T. Tai, L. Li, and C. H. Lee, Topologi-

- cal non-hermitian skin effect, *Frontiers of Physics* **18**, 10.1007/s11467-023-1309-z (2023).
- [28] R. Okugawa, R. Takahashi, and K. Yokomizo, Second-order topological non-hermitian skin effects, *Phys. Rev. B* **102**, 241202 (2020).
- [29] K. Kawabata, M. Sato, and K. Shiozaki, Higher-order non-hermitian skin effect, *Phys. Rev. B* **102**, 205118 (2020).
- [30] T. Liu, Y.-R. Zhang, Q. Ai, Z. Gong, K. Kawabata, M. Ueda, and F. Nori, Second-order topological phases in non-hermitian systems, *Phys. Rev. Lett.* **122**, 076801 (2019).
- [31] K. Zhang, Z. Yang, and C. Fang, Correspondence between winding numbers and skin modes in non-hermitian systems, *Phys. Rev. Lett.* **125**, 126402 (2020).
- [32] Z. Yang, K. Zhang, C. Fang, and J. Hu, Non-hermitian bulk-boundary correspondence and auxiliary generalized brillouin zone theory, *Phys. Rev. Lett.* **125**, 226402 (2020).
- [33] F. Schindler and A. Prem, Dislocation non-hermitian skin effect, *Phys. Rev. B* **104**, L161106 (2021).
- [34] B. A. Bhargava, I. C. Fulga, J. van den Brink, and A. G. Moghaddam, Non-hermitian skin effect of dislocations and its topological origin, *Phys. Rev. B* **104**, L241402 (2021).
- [35] A. Panigrahi, R. Moessner, and B. Roy, Non-hermitian dislocation modes: Stability and melting across exceptional points, *Phys. Rev. B* **106**, L041302 (2022).
- [36] H. Ammari, S. Barandun, J. Cao, B. Davies, and E. O. Hiltunen, Mathematical foundations of the non-hermitian skin effect, *Archive for Rational Mechanics and Analysis* **248**, 10.1007/s00205-024-01976-y (2024).
- [37] H. Zhou and J. Y. Lee, Periodic table for topological bands with non-hermitian symmetries, *Phys. Rev. B* **99**, 235112 (2019).
- [38] J. Ahn, S. Park, and B.-J. Yang, Failure of nielsen-ninomiya theorem and fragile topology in two-dimensional systems with space-time inversion symmetry: Application to twisted bilayer graphene at magic angle, *Phys. Rev. X* **9**, 021013 (2019).
- [39] Y. Hwang, J. Ahn, and B.-J. Yang, Fragile topology protected by inversion symmetry: Diagnosis, bulk-boundary correspondence, and wilson loop, *Phys. Rev. B* **100**, 205126 (2019).
- [40] Z.-D. Song, L. Elcoro, and B. A. Bernevig, Twisted bulk-boundary correspondence of fragile topology, *Science* **367**, 794 (2020), <https://www.science.org/doi/pdf/10.1126/science.aaz7650>.
- [41] H. C. Po, H. Watanabe, and A. Vishwanath, Fragile topology and wannier obstructions, *Phys. Rev. Lett.* **121**, 126402 (2018).
- [42] P. W. Brouwer and V. Dwivedi, Homotopic classification of band structures: Stable, fragile, delicate, and stable representation-protected topology, *Phys. Rev. B* **108**, 155137 (2023).
- [43] J. E. Moore, Y. Ran, and X.-G. Wen, Topological surface states in three-dimensional magnetic insulators, *Phys. Rev. Lett.* **101**, 186805 (2008).
- [44] K. Kawabata, S. Higashikawa, Z. Gong, Y. Ashida, and M. Ueda, Topological unification of time-reversal and particle-hole symmetries in non-hermitian physics, *Nature Communications* **10**, 10.1038/s41467-018-08254-y (2019).
- [45] R. Roy and F. Harper, Periodic table for floquet topological insulators, *Phys. Rev. B* **96**, 155118 (2017).
- [46] T. Yoshida, T. Mizoguchi, and Y. Hatsugai, Mirror skin effect and its electric circuit simulation, *Phys. Rev. Res.* **2**, 022062 (2020).
- [47] C.-H. Liu, H. Jiang, and S. Chen, Topological classification of non-hermitian systems with reflection symmetry, *Phys. Rev. B* **99**, 125103 (2019).
- [48] C.-H. Liu and S. Chen, Topological classification of defects in non-hermitian systems, *Phys. Rev. B* **100**, 144106 (2019).
- [49] K. Shiozaki and S. Ono, Symmetry indicator in non-hermitian systems, *Phys. Rev. B* **104**, 035424 (2021).